The University of Essex

School of Biological Sciences

Dynamics and Drivers: Carbon fluxes from temperate freshwater reservoirs

By Benjamin John Archer

A thesis submitted for the degree of Environmental Biology MSD

Supervised by Dr Thomas Cameron & Dr Etienne Low-Decarie

Date of submission January 2019

Acknowledgments

I would like to thank Dr Thomas Cameron and Dr Etienne Low-Decarie who beyond supervising me throughout this project and developing my scientific skills, have always encouraged and inspired me to pursue a scientific career, for which I am very grateful. I would like to thank John Green and Russell Smart for their wisdom in the lab, as well as the many hours spent with me in the field. I would like to thank Matthew Bond and Amy Sing Wong for their patience and support, as well as Kirralee Baker, my family and anyone else whom I have missed that have helped me throughout this degree.

Abstract

Freshwaters are significant sources of methane (CH_4) and carbon dioxide (CO_2) in the global carbon cycle, influencing the earth's atmospheric energy budget. When considering freshwater reservoirs, these greenhouse gas emissions are anthropogenic, yet have received little research focus or integration into carbon budgets, despite having potential implications for policy makers. This thesis investigates the CH_4 and CO_2 flux dynamics from three reservoir systems in the south east of England, and the physicochemical conditions that influence these flux dynamics, during the summer of 2018. Using the closed dynamic floating chamber method in tandem with physicochemical analysis, an *in-situ* investigation found rates of CH_4 efflux among the highest recorded in the literature from temperate reservoir systems (means up to 48 mg m^{-2} day^{-1}), while CO_2 rates of influx were among the highest (means up to 687 mg m^{-2} day^{-1}). However, these flux rates were heterogeneous between reservoirs and within reservoirs, dependent upon the littoral or limnetic habitats investigated. Most significantly, efflux was correlated with increased phosphorous concentrations within the system (CH_4 and CO_2), pH (CO_2) and the occurrence of physical ebullition events (CH_4), all of which were accentuated by large water drawdowns during the sampling period. This study suggests that system productivity is likely to be the dominant driver of CH_4 and CO_2 production in reservoirs of the south east of England, and highlights the significant role of extreme climate events in potentially driving a positive feedback loop between climate change and Greenhouse Gas (GHG) release. Through water management strategies, the source of GHGs from reservoir systems could be minimised by controlling reservoir water levels and eutrophication, however further research on annual and diel temporal scales are required to incorporate reservoirs into regional carbon budgets accurately.

In addition, water column CH_4 and CO_2 dynamics were investigated on a lab scale through a microcosm experiment. Using headspace analysis, the effect of control, cellobiose, acetate, phosphate and light experimental treatments upon water column CH_4 and CO_2 efflux were investigated. Dark conditions were observed to significantly increase the rate of CO_2 efflux relative to light conditions, emphasising

the need for CO_2 flux dynamics in field investigations to be on a diel scale, to prevent the underestimating of lakes as sources of CO_2. Minimal CH_4 release was observed intermittently throughout the study, however experimental treatments had no statistically significant effect upon the headspace CH_4 concentrations, suggesting that any release resulted from water disturbance rather than biogenic production. As such, this study supports the paradigm that CH_4 production from the sediment, not the water column, drives the CH_4 efflux observed from reservoirs of the south east of England.

Table of Contents

1.0 Introduction

1.1 Climate Change and Greenhouse Gases

Anthropogenic climate change is accepted by the scientific community as an 'unequivocal' process that has, and will continue to have, profound repercussions on human and natural systems across every part of the globe (Houghton et al., 2001; Walther et al., 2005). Although climate change is a naturally occurring phenomenon that has characterised environments on earth for millennia (Crowley, 1983), recent rates of change dramatically surpass those of recent geological eras, and coincide with anthropogenic industrial proliferation since the mid-18th century (Falkowski et al., 2000; IPCC, 2013). Increasing rates of radiatively significant trace gas emission, otherwise known as greenhouse gases (GHG), has culminated in a 'global warming' effect. Heat from incident solar energy is trapped by individual atmospheric GHGs; this amount of heat is termed the radiative efficiency of a molecule. Many molecules together culminate in a radiative forcing value, which increases as the total concentration of GHGs in the atmosphere increase. Increases in radiative forcing result in increasing atmospheric temperatures (Balcombe et al., 2018). Consequently, temperatures have increased by ~1.0^{o}C over the past century, to a peak annual average of 12.99^{o}C in 2016 (NOAA, 2019). These increases are estimated to continue a further 4^{o}C by 2100 if current trends are realised (A1FI scenario IPCC, 2013). Further impacts of climate change include the increasing frequency of extreme weather events, sea level rise as a result of glacial melt, ocean circulation change and extensive changes to global biodiversity (IPCC, 2013; Travis, 2003). Consequently, climate change is frequently referred to as the greatest challenge facing humanity in modern times.

Of the long-lived trace gases contributing to the 'greenhouse effect, carbon dioxide (CO_2) is recognised as the primary driver of global temperature change (Beerling and Royer, 2011). While constituting 0.036% of the atmosphere, its absorption spectrum is such that CO_2 has accounted for ~65% of

atmospheric radiative forcing since the pre-industrial era, and ~82% of the increased radiative forcing over the past 5 years (IPCC, 2013). This ominous acceleration in tropospheric CO_2 concentration has culminated in average atmospheric concentrations of 403.3 ppm in 2016; an increase of 123.3 ppm above pre-industrial levels. In addition, due to arctic ice gas bubble analysis, this current high in global atmospheric CO_2 has been confirmed as the highest concentration for the past 800,000 years (WMO, 2017), dispelling suspicions that trends observed over the past 150 years are merely natural temporal oscillations.

Of the remaining greenhouse gases, methane (CH_4) is the next largest contributor to the global warming phenomenon, acknowledged to cause ~20% of climate forcing since pre-industrial times (Saunois et al., 2016; IPCC, 2013). Despite being lower in total atmospheric concentration (~1853 ppb in 2016 (NOAA, 2016)) and having a lower rate of annual emission relative to CO_2 (3% of CO_2 (Balcombe et al., 2018)), CH_4 has an equivalent global warming potential (GWP) 36 - 87 times that of CO_2, depending on the timescale considered (20 – 100 years) (IPCC, 2013), due to its strong radiative efficiency. Like CO_2, the current atmospheric concentration of CH_4 represents a value much increased relative to pre-industrial times (257% based on the earlier mentioned 2016 value). In contrast, the residence time of CH_4 relative to CO_2 is much lower, having an atmospheric lifetime of 8.4 years (but influencing other atmospheric species for 12.4 years) (IPCC, 2013), while the modelled lifespan of CO_2 shows 50% will dissipate over 37 years, and ~ 22% will persist forever (Neubauer and Megonigal, 2015).

A part of the gaseous CH_4 cycle is its atmospheric oxidation. In the troposphere CH_4 molecules are oxidised by reacting with OH^- radicals to form CO_2 (carbon's lowest oxidation state), H_2O and (when in the presence of NO_x molecules) O_3. In the stratosphere, CH_4 molecules similarly react with OH^- radicals to form CO_2 and H_2O, though here H_2O production results in the loss of O_3. The influence of CH_4 on atmospheric OH^- molecules is detrimental to the oxidising ability of the atmosphere. As a result, higher atmospheric CH_4 concentrations increase the residence time of individual CH_4 molecules, and the overall GWP of CH_4. Additionally, the loss of stratospheric ozone (protecting the earth's inhabitants from cosmic radiation) and the production of tropospheric ozone (which forms the key constituent of smog and

reduced air quality) demonstrate negative global health implications as a result of CH_4 production, beyond that of climate change. (West and Fiore, 2005; De Gruijl et al., 2003). The CO_2 produced by CH_4 oxidation is also considered when calculating CH_4's GWP.

In combination, these features make CH_4 and CO_2 the most important focus of scientific investigation in regard to climate change. Research provides information essential in determining climate mitigation strategies and climate policy, which will halt the proliferation of climate change. However, speculation remains over the sources and relative magnitudes of CH_4 and CO_2.

1.2 The Significance of Freshwater CO_2 and CH_4 Fluxes

Freshwaters are net sources of CO_2 and CH_4 to the atmosphere, playing a disproportionately large role in the global carbon and CH_4 cycles, considering their small global surface area relative to terrestrial and marine biomes. For example, freshwaters are reported to cover ~3% of the global land surface (Downing et al., 2006), yet are cited as one of the factors contributing to the return to increasing atmospheric CH_4 concentrations after the 7 year period with no increases between 1999 and 2006 (Saunois et al., 2016).

For this reason, freshwaters have been coined 'sentinels, integrators and regulators of climate change' (Adrian et al., 2009; Williamson et al., 2009), and are reported to counteract the continental carbon sink (2.6 ± 1.7 Pg C yr^{-1}) by a minimum of 25% (Bastviken et al., 2011). Freshwaters must be included in regional carbon budgeting to prevent the underestimating of global CH_4 and CO_2 concentrations, essential for CO_2 and CH_4 management, budgeting and resulting climate mitigation.

Freshwater systems comprise distinct environmental classifications defined by their physical characteristics, host communities and resultant chemical processes. They each display unique carbon dynamics, having different magnitudes of influence upon the global carbon cycle. Of these distinct environments, lakes and reservoirs cover the largest global surface area; 3,000,000 km^2 (91.3% of this are lakes and 8.7% are reservoirs) (Verpoorter et al., 2014; Raymond et al., 2013). Lakes and reservoirs contribute the largest effluxes of CH_4 to the atmosphere of the freshwater environments (Sanches et al., 2019). Despite an increasing body of literature, calculating the exact global CH_4 budget from freshwater lakes and reservoirs remains difficult, and estimations are vague. For example, there has been little improvement since initial estimations by Ehhalt (1974) (1.25×10^{12} and 25×10^{12} g of CH_4 from lakes per year). Estimates by Bastviken et al. (2004) remain just as wide (8 to 48 Tg CH_4 yr^{-1}), although they are based upon a larger data set and greater understanding of the parameters influencing freshwater GHG fluxes. CO_2 emission rate estimates from lakes are similarly large in range, suggested to be 0.32 ± 0.52 Pg C yr^{-1} by Raymond et al. (2013). Unlike CH_4, lakes do not represent the largest efflux of CO_2 from

freshwater systems, however this contribution is still large when considering the natural ecosystem offset of CO_2 at $\sim$4 Pg C yr^{-1} of anthropogenic emissions (Raymond et al., 2013). Difficulty in estimating freshwater CH_4 and CO_2 fluxes persists due to the difficulties in estimating inland water surface area, as well as the heterogeneity of GHG fluxes from lakes and reservoirs; temporally and spatially (Pavel et al., 2009).

As reservoirs are man-made structures, their contributions of GHGs must be considered as anthropogenic. Their CH_4 flux values are comparable to effluxes from rice paddy fields or biomass burning, and often represent flux values greater that from natural lakes (Harrison et al., 2017). Despite this, reservoir GHG dynamics are currently underrepresented in literature, and more research is required if policy makers are to accurately include them in regional carbon budgets.

1.3 Production of CO_2 and CH_4 in Freshwater Lakes

CH_4 and CO_2 produced in freshwater lakes and reservoirs are the product of oxic and anoxic respiration. The balance between CH_4 and CO_2 source and sink processes determines the final CH_4 and CO_2 flux dynamics of a system.

CO_2 and CH_4 Production Processes

CH_4 efflux rates in lakes and reservoirs are dependent on microbial CH_4 formation rates, and CH_4 oxidation rates. CH_4 formation occurs as a result of the microbial decomposition of organic matter, an obligately anaerobic process called methanogenesis (anaerobic respiration requiring O_2 concentrations < 10 ppm (Borrel et al., 2011)). In lakes and reservoirs, the largest anoxic zone and collection of organic matter occurs in the sediment. As such, the most active site of CH_4 production occurs in these sediments.

Two dominant types of archaeal methanogenesis take place in freshwater sediments; acetoclastic methanogenesis and hydrogenotrophic methanogenesis. Hydrogentrophic methanogenesis utilises CO_2 (or formate) as a terminal electron acceptor, reducing it with hydrogen (H_2) to form CH_4, and theoretically accounts for 30% of all methanogenesis in freshwaters (Conrad., 1999). Acetoclastic methanogenesis splits acetate into CH_4 and CO_2, and is the largest source of CH_4 in freshwaters. A third type of CH_4 production, methylotrophic methanogenesis, although documented to occur in freshwaters, occurs insignificantly due to the rarity of its precursor substrates in freshwaters (Lomans et al., 2001). This process utilises methanol, methylamines, CO, ethanol and secondary alcohol as substrates to convert to CH_4 (Borrel et al., 2011).

The process of methanogenesis is the final step of organic matter decomposition (or mineralisation) and is dependent on preceding steps that provide substrates for methanogenesis. From unprocessed organic

matter, the end product of one metabolism is the substrate for another, until decomposition is complete (Krevš and Kučinskienė, 2018).

These preceding steps are hydrolysis and fermentation. For example, cellulose from a dead algal cell wall is hydrolysed to glucose by cellulolytic bacteria (such as *Fibrobacter* spp. (McDonald et al., 2009)). Primary fermenters (such as *Clostridium papyrosolvens* (Leschine, 1995) then catabolise glucose to acetate and CO_2 for methanogenesis, or to fatty acids and alcohols. Secondary fermenters (such *Syntrophomonas wolfei* (Schmidt et al., 2013)) ferment these primary fermentation products (i.e. fatty acids and alcohols) to H_2, acetate and CO_2; substrates for methanogenesis. In parallel, acetogeneic bacteria can produce acetate from H_2 and CO_2, an alternative route for acetoclastic methanogenisis in freshwater sediments and the release of CH_4 (Zinder, 1984).

Secondary to sediment production, CH_4 production is sometimes recorded to occur in anoxic hypolimnetic and monimolimnetic zones (Fahrner et al., 2008; Franzmann et al., 1991). In addition, CH_4 production has been suggested to occur in the oxic surface mixed layer of lakes (SML). For example, Grossart et al. (2011) have detected methanogenic archaea (such as the acetoclastic genera *Methanosaeta* and *Methanosarcia*) in the SML that bind to the surface of phytoplankton (Figure 1.1), which were suggested to produce CH_4 either through conventional acetoclastic methanogenesis in micro-anoxic zones of the phytoplankton surface, or by performing a symbiotic transfer of substrates to produce CH_4 hydrogenotrophically. While some have suggested that production in the oxic surface mixed layer of lakes can contribute a significant amount of a lakes CH_4 budget (up to 90% (Donis et al., 2017)), others have categorically refuted this, arguing instead that lateral transport of CH_4 to the limnetic SML from the littoral zone (where sediment CH_4 production rates are high) explains CH_4 flux observed from SML/limnetic regions (Peeters et al., 2019).

CH_4 oxidation (methanotrophy) is a process that converts CH_4 to CO_2. In lakes, this is a biological sink of CH_4, and is estimated to catabolise 50 – 95% of CH_4 produced in lakes (Bastviken et al., 2008). CH_4 oxidation is also a source of CO_2, thus increased CH_4 oxidation will increase CO_2 production in a system.

Methanotrophy occurs most dominantly in the oxic water column and oxic surface layers of freshwater sediments via methanotrophic bacteria (such as type 1 methanotrophs; *Methylomonas,* and type 2 methanotrophs; *Methylocystis* (Costello et al., 2002)). However, CH_4 oxidation can also occur in anoxic freshwater sediments (for example in the presence of NO_3^- by *Methylomirabilis oxyfera* (Wu et al., 2011), although comparatively little is currently known about these processes and the extent of their role in freshwater lakes.

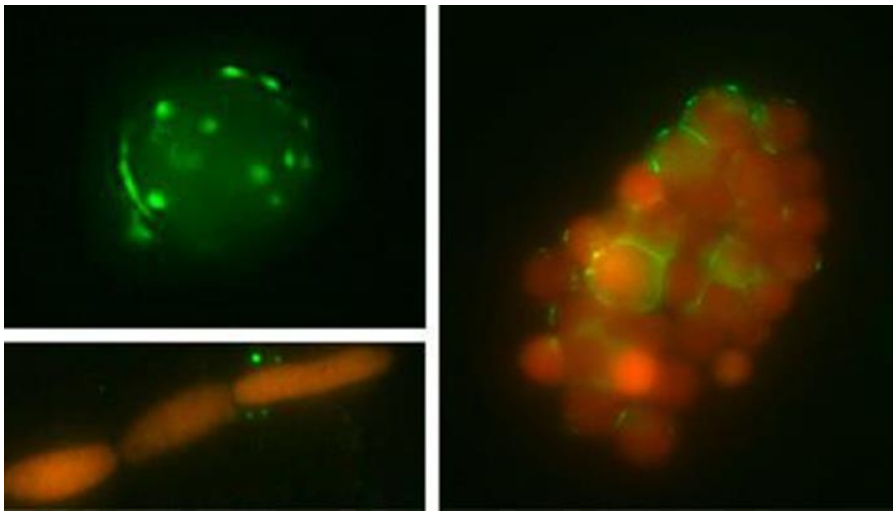

Figure 1.1 Image taken by Grossart et al. (2011), illustrating the attachment of methanogenic Archea (green, FIT C – Labelled oligonucleotide probe) to autotrophic plankton (Red auto-fluorescence) that occupy the pelagic zone, imaged using FISH. (*Upper Left*) A single Chlorella-like algal cell. (*Right*) A colony of Chlorella-like green alga. (*Lower Left*) A filament of the cyanobacterium *Aphanizomenon flos-aquae*".

In addition to CO_2 produced during methanogenesis and methanotrophy, the primary process behind CO_2 production is aerobic respiration. This occurs throughout freshwater sediments and water columns (Pace and Prairie, 2005). The primary sink of CO_2 in freshwater lakes is photosynthesis. Photosynthetic depletion of dissolved CO_2 can lead to lakes behaving as net autotrophic systems and displaying net CO_2 influx dynamics (Casper et al., 2000). However, in most cases, lakes are net heterotrophic systems; aerobic respiration exceeding gross primary production (Del Giorgio and Peters, 1994). The resulting super-saturation of CO_2 in waters causes the majority of lakes to efflux CO_2 to the atmosphere.

Drivers of CO_2 and CH_4 Production Processes

The drivers of CO_2 and CH_4 production in a freshwater lake or reservoir determine the concentration of CO_2 and CH_4 in the system, and the concentration of gas that can potentially be effluxed from a system. Production drives CO_2 and CH_4 flux dynamics from the bottom up. Understanding the factors that affect production are essential if estimating, modelling and creating management strategies for a lake or reservoir's GHG footprint is to be achieved.

CH_4 formation is primarily driven by the productivity of the lake system. Highly productive systems express increased CH_4 production relative to less productive systems (West et al., 2012). Plants and phytoplankton are the most abundant organic carbon sources in ecosystems (Megonigal et al., 2004). As these organisms die, their detritus falls to the sediment, supplying organic matter. As a result, carbon and the substrates for methanogenesis are increasingly available. As methanogens are limited by substrate availability (freshwater substrate concentrations being low for methanogens relative to other methanogen hosting systems (Borrel et al., 2011)), and are outcompeted by iron reducing bacteria, sulphate reducing bacteria and denitrifying bacteria (in the presence of their alternative electron acceptors: Fe^{3+}, SO_4^{2-}, NO_2^-, NO_3^- (Roden and Wetzel, 2003; Stams et al., 2003; Raskin et al., 1996)), this results in higher rates of methanogenesis and consequently higher concentrations of CH_4 in sediments. An additional effect of increased productivity and detritus addition to a system is the increase in aerobic respiration by microorganisms. This increases the production of CO_2, while depleting available concentrations of O_2 in the sediments. This decreased O_2 availability drives further methanogenesis and CH_4 production.

CH_4 production is similarly driven by the trophic state of a system. In lake environments with high concentrations of Nitrogen and Phosphorous, greater concentrations of CH_4 production are expected than from a lake with reduced concentrations of N and P (West et al., 2012). In photoautotrophs, photosynthesis is primarily limited by phosphorous concentrations, followed by nitrogen concentrations, according to the Redfield ratio (Ptacnik et al., 2010). While the productivity of the system remains limited by either N or P availability, their addition will drive sediment CH_4 production.

Similarly, while system productivity is limited by the concentration of N and P, CO_2 intake through photosynthesis and the subsequent oxic respiration of this organic matter litter is limited by the trophic state of the system. In freshwaters with concentrations of N above the threshold needed for methanotrophic growth, NH_4^+ can also behave as an inhibitor of methanotrophy, being complementary with CH_4 binding sites in methane monooxygenase (Bédard and Knowles, 1989). As such, high N concentrations also increase CH_4 concentrations within lake systems by minimising its oxidation.

Another factor driving microbial CH_4 production in freshwater lakes is the temperature of the system. Warmer temperatures are seen to drive increased metabolic activity (and in some cases increased abundance) of methanogens in freshwater lake sediments, leading to increased CH_4 production rates (Fuchs et al., 2016). As temperature drives increased microbial activity, the activity of syntrophs providing the substrates for methanogens similarly increases (optimum growth rate temperatures being higher than those observed in freshwater environments (Chin and Conrad, 1995)). As a result, increased temperatures increase CH_4 production directly and indirectly through increased rates of sediment microbial activity. In contrast, the sensitivity of methanogens to increased temperatures is not matched by methanotrophs, which are relatively insensitive to temperature rises (Duc et al., 2010). Methanotrophic activity is rather explained as a function of CH_4 availability in a system, though the extent of this is likely to depend upon the system investigated.

1.4 Flux Pathways of CO_2 and CH_4 in Freshwater Lakes

Efflux of CH_4 from lakes and reservoirs requires CH_4 to travel from the sediment, its dominant point of production. The pathway taken by CH_4 gas influences the concentration of final efflux to the atmosphere at the water interface, and consists of three main pathways: diffusion, ebullition (bubbling) and plant mediated transport (Casper et al., 2000; Smith and Lewis, 1992) (Figure 1.2), as well as seasonal advection in some cases (Mau et al., 2015).

Ebullition is a product of sediment gas production, to the extent where pore water partial pressures of dissolved gas exceeds ambient pressure and water surface tension, resulting in the formation of free gas (Harrison et al., 2017). Due to the poor solubility of CH_4, ebullition dissolution is minimal; bubbles travelling vertically through the water column to the atmosphere, with minimal opportunity for CH_4 oxidation (McGinnis et al., 2006). When this pathway occurs, it contributes the largest concentrations of CH_4 to the atmosphere of the flux pathways (40–60% (Bastviken et al., 2004)). Similarly, plant mediated transport of CH_4 through plant stems avoids the opportunity for CH_4 oxidation by bypassing the water column (Schutz et al., 1991). As emergent macrophytes often constitute a reduced portion of lake surface area in comparison to the total sediment surface area, this pathway contributes less total lake CH_4 efflux than ebullition. In contrast, sediment diffusion is almost completely oxidised by methanotrophs, as dissolved CH_4 moves from the supersaturated sediments to the water column (Bastviken et al., 2008).

The dominant CO_2 flux pathway in the water column and sediment is diffusion (~90 % of fluxes in Casper et al., 2000). The lack of CO_2 ebullition is primarily due to the solubility of CO_2 in the water column, inhibiting bubble formation and increasing the dissolution rate of bubbles that do form. Additionally, the dominance of CH_4 production in the sediments relative to CO_2 also contributes to the minimal concentrations of CO_2 measured in ebullition bubbles (Tušer et al., 2017).

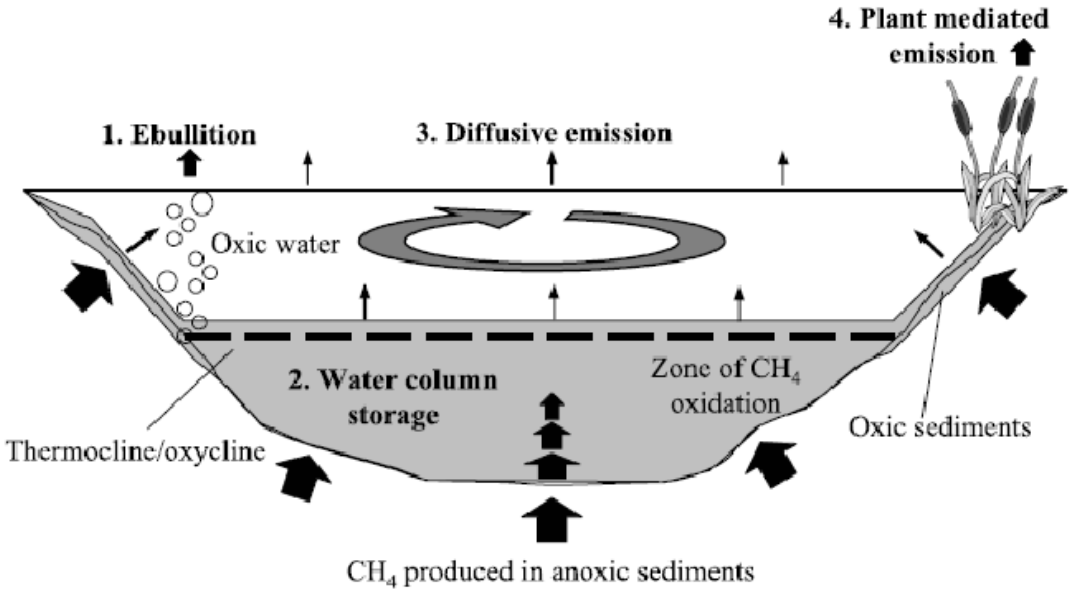

Figure 1.2 CH_4 flux pathways in a freshwater lake or reservoir. CH_4 produced in the sediments travels to the atmosphere via three dominant pathways: Ebullition, diffusion and plant mediated transport. Illustration from Bastviken et al. (2004).

Drivers Affecting Flux Pathways

In addition to the rate of production and removal of GHGs, the rate of gas flux from lakes is driven by factors affecting GHG release from flux pathways.

Trapped free gas release, in the form of ebullition, is driven by hydrostatic pressure events and the cohesive strength of sediments (the sensitivity of sediments to changes in pressure) (Joyce and Jewell, 2003). Factors that affect hydrostatic pressure include changes in water level (decreases in water depth decreasing hydrostatic pressure, increasing ebullition) (Harrison et al., 2017), wind events resulting in bottom sheer (increasing fluxes) (de Vicente et al., 2010) and barometric pressure (drops increasing fluxes) (Casper et al., 2000).

Diffusive efflux from lakes is driven by the difference in CH_4 concentration at the lake water/ atmosphere interface, and the piston velocity (Bastviken et al., 2004). Wind speed drives piston velocity,

therefore high wind speeds result in greater rates of diffusive CH_4 flux. In addition, temperature drives diffusion rates by changing the Henry's Law constant. Higher temperatures decrease the solubility of the dissolved gases, thus higher temperatures increase the rate of diffusive CO_2 and CH_4 efflux from lakes.

In addition, intense rain has been linked to increased CO_2 diffusion (Bartosiewicz and MacIntyre, 2015) and can indirectly effect CH_4 production by increasing water column depth (thus hydrostatic pressure) as well as washing carbon into the lake system, increasing methanogenic activity and CH_4 production in sediments (Hudson et al., 2003).

Lake morphology affects CO_2 and CH_4 flux pathways, and is a key factor in determining lake and reservoir flux dynamics. Lake depth impacts final CH_4 efflux, as the deeper the water column, the greater the opportunity for bubble dissolution and contact time of ebullition with methanotrophs (mentioned previously). Additionally, deeper water columns provide greater time for organic matter breakdown of falling detritus, "lake snow" (Grossart and Simon, 1993), in the water column before reaching anoxic sediments. This reduces the carbon input for methanogens in deep sediments and thus CH_4 production. As such, deeper lakes are expected to release reduced concentrations of CH_4 relative to shallower lakes (Hanson et al., 2007; Smith et al., 2002). Similarly, this process is observed within lakes with shallow areas of lakes (the littoral zone) releasing higher concentrations of CH_4 than deeper areas (the limnetic zone). This habitat flux pattern is also partly driven by higher organic input at littoral zones than limnetic zones, due to plant growth and algal bloom collection on lake shores, and the subsequent detritus/ organic matter deposition in these areas.

Lake shape drives overall lake and reservoir CO_2 and CH_4 flux dynamics. Lakes with larger surface area provide larger littoral and limnetic environments, opportunities for CH_4 and CO_2 production, and water-atmosphere interfaces for gas exchange (Saarnio et al., 2009). Where lake shape causes larger ratios of littoral to limnetic environments, greater total amounts of flux are expected.

Influence of Location and Temporal Scale on Lake Fluxes

Lake CO_2 and CH_4 production rates, release pathways and overall flux dynamics are heavily influenced by the global location (Figure 1.3) or the temporal scale at which they are investigated.

The influence of biome characteristics on lake fluxes is seen when analysing average regional carbon flux data. For example, tropical lakes contribute the largest concentrations of CO_2 and CH_4, despite boreal lakes being greatest by number (Roehm et al., 2009). Lakes and reservoirs in temperate regions experience the greatest levels of anthropogenic stress; morphological change, eutrophication and urbanisation, increasing the potential for CO_2 and CH_4 efflux (Birk et al., 2012) and the sensitivity of these fluxes to climate change (Tranvik et al., 2009). As such, continuing research into temperate regions remains significant.

Temporally rates of CO_2 and CH_4 flux change on annual, between season, within season and within day scales. In regions subject to seasonal change environmental conditions, CO_2 and CH_4 production and flux dynamics change throughout the year (Kankaala et al., 2006). In the most obvious cases, this is observed as greater rates of efflux during the summer season and minimal rates of efflux in the winter season; a result of temperature change and seasonal input of organic material with photoautotrophic growth cycles (Duchemin et al., 2006; Phelps et al., 1998; Maberly, 1996).

Within seasons variations in flux can occur as a result of pressure and weather events (for example rainfall, high winds or temperature, as described in the Flux pathways section). Within days fluxes change with intermittent ebullition events and diel environment change. For instance, variations in flux occur as a result of light intensity (light reported to inhibit methanotrophic processes (Murase and Sugimato (2005), while photosynthesis does not occur under dark conditions thus inhibiting CO_2 influx (Liu et al., 2016)) and temperature (e.g. causing night time mixing and transfer of CH_4 from waters stratified during the daytime (Repo et al., 2007)). For these reasons, it is important to consider temporal variation when planning fieldwork and analysing flux data.

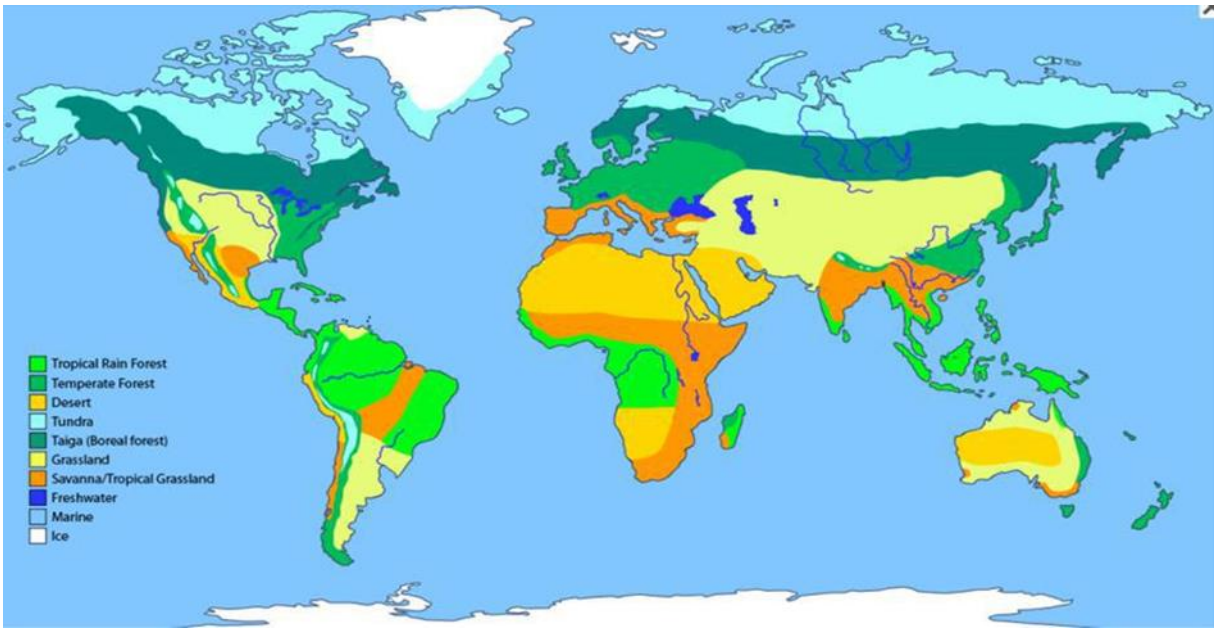

Figure 1.3 Global map of biomes, the environmental characteristics of which result in spatial variation of CO_2 and CH_4 fluxes from freshwater lakes and reservoirs (Illustration taken from askabiologist (2018)).

1.5 Measuring Lake CO_2 and CH_4 Emissions

Freshwater CO_2 and CH_4 emission rates are measured using a variety of techniques. These include flying transects with on-board GHG analysers (on a regional scale) (Kohnert et al., 2014), fixed point eddy covariance towers, tracer techniques (Upstill-Goddard et al., 1990; Wanninkhof et al., 1987), ebullition collection in funnel traps (St. Louis et al., 2000) in combination with diffusion measurement using the thin boundary layer method (TBL) (Lambert and Fréchette, 2005) and the floating flux chamber method (FCM)(Gerardo-Nieto et al., 2009). The FCM and thin boundary layer method are most commonly used in literature.

The FCM uses a chamber of known internal volume, floating upon the surface of a water body being investigated. By measuring the concentration of CO_2 and CH_4 within the chamber headspace for a set amount of time, the rate of CO_2 and CH_4 exchange across the air/water interface, for that time, can be quantified. Three forms of FCM are currently used: non-steady-state non-through-flow chambers (closed static chambers), closed dynamic chambers and steady-state through-flow chambers (open dynamic chambers). Traditionally, the most commonly used chamber method was the closed static chamber. Concentrations of gas within the chamber headspace are measured by taking discrete gas samples from the chamber headspace at set time intervals, for subsequent gas chromatography analyses (Pihlatie et al., 2013). The closed dynamic chamber technique continually measures gas concentrations within the chamber headspace by pumping air from the chamber headspace through a portable GHG analyser, and back into the chamber headspace (Figure 1.4). Technological developments have increased the portability and availability of cavity ring down spectroscopy (CRDS) (Heinemeyer and McNamara, 2011) (a highly sensitive, direct absorption technique based on the absorption of light circulating in an optical cavity (Berden and Engeln, 2009)), for example the Picarro gas scouter G4301 (Picarro Inc) and Los Gatos Ultra-portable Greenhouse Gas Analyzer (UGGA) (Los Gatos Research Inc) which measure both CO_2 and CH_4 accurately. The open dynamic chamber technique continually flows a well-defined carrier gas through the chamber headspace and into a gas analyser, expelling the gas to the

atmosphere (Figure 1.5). As a result, this method avoids the headspace CO_2 and CH_4 build up that occurs in the other two methods, however due to inconvenience of use it is rarely used in freshwaters (Gerardo-Nieto et al., 2019).

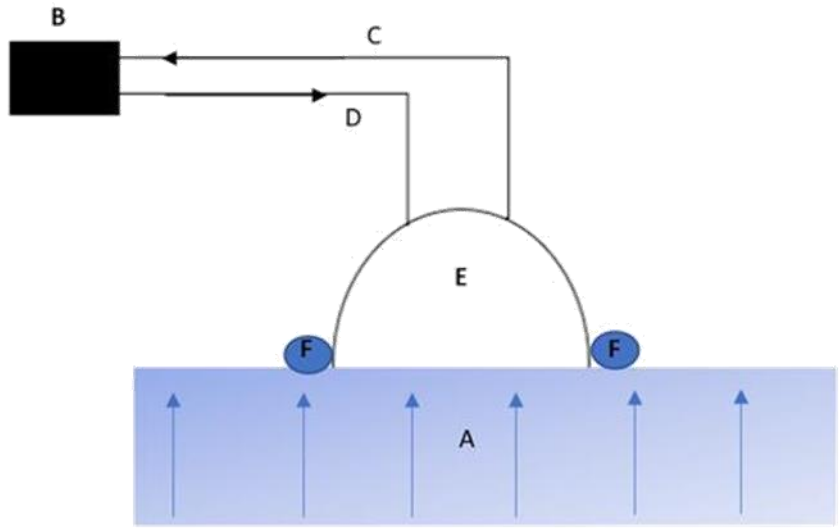

Figure 1.4 Closed dynamic floating chamber method, used to measure the rate of gas flux from water bodies:

A. Water body being measure, arrows represent efflux of gasses into 'E'.
B. The gas analyser connected to the floating chamber measuring the concentration of gas.
C. Inflow gas tight tube, transferring air from the floating chamber into the gas analyser.
D. Outflow gas tight tube, transferring air from the gas analyser back into the floating chamber.
E. Domed gas chamber sitting on the surface of the water.
F. Floatation attached to the dome chamber

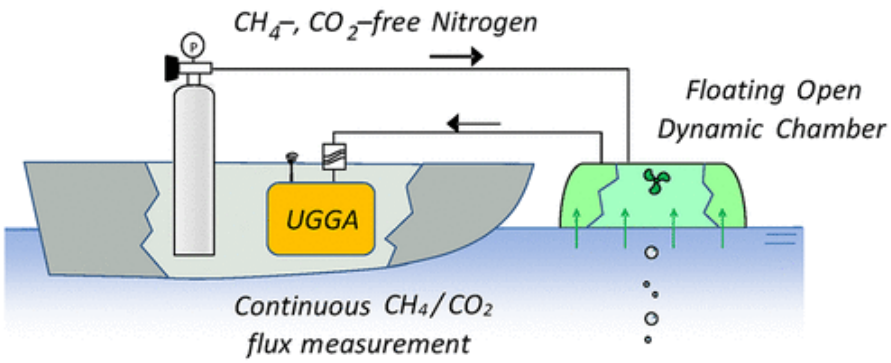

Figure 1.5 - The open dynamic chamber technique: A known carrier gas flows from a gas canister into the floating chamber headspace (Green). From here, headspace gas is mixed and pumped to the GHG analyser (UGGA) and the concentration of gas measured. From this value the flux rate from the air:water interface (green arrows) can be determined. Figure taken from Gerardo-Nieto et al. (2019).

The advantages of FCMs are their extreme portability relative to static methods such as eddy covariance, the simplicity and resulting low cost of the method (Kremer et al., 2003) and the collection of total gas flux (CO_2 and CH_4 flux from diffusion and ebullition pathways). It is also argued that FCMs are the best methods for isolating spatiotemporal variations in CH_4 emission from a water body (Duchemin et al., 1999).

Potential drawbacks of the FCM lie around the potential for disparity of its flux measurements relative to techniques such as eddy covariance (Vachon et al., 2010). However, this disparity in results has been attributed to chamber design, particularly where chambers significantly affect turbulence interference (Kremer et al., 2003; Broecker and Peng, 1984). In chambers where turbulence interference is mitigated, fluxes are found to be representative with other techniques (Soumis et al., 2008; Guérin et al., 2007). An additional drawback to FCM techniques is their limited deployment time, making temporal variation in flux dynamics difficult to quantify. This remains an issue but the ongoing development of automated floating chambers is looking to address this limitation (Duc et al., 2012).

In summary, the method used to measure CO_2 and CH_4 flux dynamics must be considered carefully when designing sampling plans; the most suitable technique for measuring fluxes within and between multiple lakes is the FCM.

1.6 Summary

It is known that lakes and reservoirs, as a whole, behave as significant net sources of CO_2 and CH_4 to the atmosphere. In a warming world understanding their contribution to the atmospheric energy budget is a crucial step in understanding climate change. Despite this estimates of global lake and reservoir CO_2 and CH_4 contributions remain vague, as the mechanisms behind flux production and emission pathways vary substantially between and within lakes. Continued research into lake and reservoir flux dynamics is essential. Research supplies data to the global data set (used in estimating global freshwater GHG contributions to the atmosphere), tracks changes in freshwater flux dynamics that could be occurring as a result of on-going climate change, and provides GHG flux data used in regional carbon budgeting, water management strategies and climate policy. This thesis investigates the dynamics and drivers of CO_2 and CH_4 in reservoirs in the south east of England, and contributes to the global research effort working to solve these issues.

2.0 *In-situ* Dynamics and Drivers of CO_2 and CH_4 Flux in Temperate Freshwater Reservoirs

2.1 Introduction

Freshwater systems have the power to influence continental carbon budgets, despite their relatively small global surface area (Adrian et al., 2009). Considering this disproportionately large contribution to a region's carbon budget, they remain under-investigated relative to other biomes. It is essential, then, that freshwater GHG sources are understood and incorporated into carbon budget calculations. As climate change policy becomes more reliant upon carbon capture techniques (for example tree planting (Nijnik, 2010) and technological capture (Stewart and Hessami, 2005)) to counteract anthropogenic increases in GHGs and meet carbon sequestration targets proposed by IPCC climate models (IPCC, 2018), the accuracy of freshwater CH_4 and CO_2 contribution calculations becomes more important. If freshwater contributions are neglected, regional carbon budget targets will be inaccurate and potentially leave an unmanageable carbon deficit for future generations.

Freshwater lakes and reservoirs are one of the largest components of freshwater systems, whilst providing ecosystem services like drinking water and leisure activities. In addition, reservoirs are some of the most sensitive habitats to climatic stressors. For example, weather events can cause contractions in reservoir surface area and result in dramatic CH_4 efflux events (up to 90% of annual release in some cases (Harrison et al., 2017)). Considering this, by measuring the dynamics of reservoir CH_4 and CO_2 fluxes, the role of temperate freshwaters in the carbon cycle will be understood (a significant step towards understanding the contribution of freshwaters and carbon budgets as a whole) and the scientific data set will be built upon for historical comparison in the future.

The difficulties in measuring and calculating reservoir CH_4 and CO_2 flux dynamics lie in the heterogeneity/variability of their fluxes. This flux heterogeneity is the result of variation in physicochemical conditions, which in turn drive the production rates and flux pathways of CH_4 and CO_2 within a reservoir (discussed in sections 1.3 and 1.4). As physicochemical conditions vary spatially within reservoirs and between reservoirs, as well as temporally (for example as a result of weather, season change and chemical inputs), so to do CH_4 and CO_2 flux rates vary. Although flux dynamics can be speculated upon, based on a water body's physicochemical characteristics, the dynamics are often unique to that lake or reservoir, and must be determined by sampling.

Within a reservoir variation is expected to be observed between the littoral and limnetic environments, which must both be quantified if accurate whole lake CH_4 and CO_2 flux budgets are to be calculated. In general, CH_4 fluxes are expected to be lower in the limnetic region of a lake or reservoir than the littoral region (Bastviken et al., 2008). The physical drivers of this variation are based upon the assumption of deeper water columns in the limnetic zone relative to the littoral zone. Limnetic sediments are on average colder environments than littoral sediments (being less influenced by atmospheric temperature variation) and host lower rates of microbial activity (Glissman et al., 2004). As a result, lower CH_4 production rates are expected in limnetic sediments in comparison to warmer sediments of the littoral zone (Harrison et al., 2017). Limnetic sediments can be denser (due to the increased hydrostatic pressure from the water column) thus allowing less CH_4 ebullition release from sediments relative to soft littoral sediments (Joyce and Jewell, 2003). Greater CH_4 oxidation is expected in the limnetic water column, due to the increased contact time of bubbles with the deeper water column, allowing more time for bubble dissolution and CH_4 oxidation by methanotrophs compared to the littoral region (McGinnis et al., 2006). In addition, CH_4 and CO_2 are degradation products, and are expected to be greater in areas of greater productivity and subsequent organic matter deposition. Littoral zones are often the sites of greatest biological productivity, hosting algal blooms and macrophyte growth. As a result, these zones often receive larger concentrations of organic matter deposition, and greater sediment CH_4 production than limnetic zones (Bastviken et al., 2008).

However, these flux patterns are not always seen. In lakes that are shallow, an opposite pattern of flux can be observed, where CH_4 fluxes are greater from limnetic regions than littoral regions. Sediment focussing into the middle of the lake or reservoir can cause greater concentrations of organic matter in the limnetic region and thus higher rates of CH_4 production in the sediment, which can then be released easily as ebullition (due to the low hydrostatic pressure from the shallow water column), minimally oxidised in the short water column, and released as larger fluxes than in the littoral zone (for example in Lake Balaton (Visnovitz et al., 2015). Alternatively, in lakes that experience water mixing from the littoral areas of the lake into the centre of the lake, dissolved CH_4 produced in littoral sediments can be transported to the limnetic region of the water body via lateral transport (for example, at Lake Stechlin (Tang et al., 2014)). As a result, greater concentrations of CH_4 efflux can occur from the limnetic air/water interface. Therefore, the behaviour of a reservoir's internal flux dynamics must be measured to be determined.

Between reservoirs, variation in mean water column depth, water mixing, and system productivity can result in different limnetic/littoral CH_4 flux dynamics. As water chemistry influences a system's productivity (which drives CH_4 and CO_2 production rates), between-reservoir variation in CH_4 and CO_2 dynamics is also expected to be driven as a result of a system's dissolved organic carbon (DOC), nitrogen and phosphate inputs and resulting dissolved concentrations. As photoautotrophic growth is limited most significantly by phosphorous, then by nitrogen, and finally by DOC (according to the Redfield ratio (Ptacnik et al., 2010)) a reservoir's productivity is in turn expected to be limited by these nutrient concentrations, driving increased organic matter inputs to sediments and resulting in increases of CH_4 production as a degradation product, and total CH_4 efflux (Deemer et al., 2016). However, CO_2 dynamics as a result of production are more variable. In summer seasons increased photoautotrophic growth is expected to result in increased CO_2 influx into reservoirs, as CO_2 is assimilated through photosynthesis. By the autumn, however, this increased photoautotrophic growth will be deposited to the sediments and a delayed increase in CO_2 efflux (as a result of organic matter respiration) can occur (Huotari et al.,

2009). Whether this increased CO_2 influx (as a result of photosynthesis) results in a reservoir behaving as a net CO_2 sink or source is dependent on whether the system is net heterotrophic or autotrophic, which is again reservoir specific.

This investigation studied the CO_2 and CH_4 dynamics of three freshwater reservoirs in the south east of England, that have never previously been the subject of GHG flux measurements. This study aims to understand the role and extent to which reservoirs contribute CO_2 and CH_4 to the region's atmospheric energy balance, by creating CO_2 and CH_4 flux budgets. In doing so, this study aims to understand the spatial variation of fluxes within and between reservoirs of the region, and to understand how CO_2 and CH_4 fluxes are driven by the in-water physicochemical variables and biological communities of freshwater reservoirs.

To test the hypotheses:

1. Within reservoir rates of CH_4 efflux will be greater in limnetic habitats than in littoral habitats, whereas CO_2 efflux will be greater in limnetic habitats than in littoral habitats, in temperate freshwater reservoirs.

2. Rates of per-area CO_2 and CH_4 efflux will vary between freshwater reservoirs of the south east of England.

3. Physicochemical conditions within reservoirs will drive variation in the observed CO_2 and CH_4 flux dynamics, in temperate freshwater reservoirs.

2.2 Methods

2.2.1 Sample Sites

Three freshwater reservoirs located in the south east of England were sampled during the summer of 2018 (May to September): Hanningfield reservoir, Ardleigh reservoir and Alton reservoir. In addition to supplying drinking water to the region, these reservoirs are hubs for leisure activity including fishing, boating and bird watching (see table 2.1 for further information on each reservoir's morphometry).

Ardleigh reservoir is a concrete eutrophic reservoir managed at the time of study by Anglian Water Services Ltd. Created in 1969 by the flooding of arable land, water is supplied directly to the reservoir by the northern and western Salary Brooks (stream catchment areas being 14km^2 cumulatively), in addition to pumping from the river Colne. Mixed conditions are maintained year-round by a bubble curtain and two helixors (Abdul-Hussein and Mason, 1988) (Figure 2.1).

Alton water reservoir is a concrete eutrophic reservoir, with a shallow north-westerly bund, managed at the time of study by Anglian Water Services Ltd. At full capacity since 1986, water is pumped by extraction to the reservoir from the river Gipping. Mixed conditions are maintained year-round by six pneumatic helices (Perkins and Underwood, 2001). Alton water is particularly prone to cyanobacterial blooms, experiencing boating bans in summer 2018 (Figure 2.2).

Hanningfield reservoir is a partial concrete/ mud bottomed highly eutrophic drinking water reservoir (phosphate and nitrate levels rarely reported to fall below 1mg/l (PO_4^{3-}) and 1.5mg/l (NO_3^-) respectively (Simmons, 1998)). Created in 1956 by the flooding of arable land, water is pumped to the reservoir from nearby rivers Chelmer, Ter and Blackwater, in addition to direct small stream discharges (Wootten, 1973). Mixed conditions are maintained year-round by a large bubble curtain installed in 1994. As well as providing water to over half a million people in the Chelmsford area, the site is also an important site of scientific interest (SSSI), managed at the time of study by Essex and Suffolk Water (Figure 2.3).

Limnetic sample sites were taken as transects across the limnetic region and littoral sample sites were taken at a depth of 1m from jetties of each reservoir (Limnetic trajectories and littoral sites are illustrated in section 4.3, figure 4.3.1).

Table 2.1 Morphometric characteristics and annual water budgets of reservoirs investigated in this experiment. Information taken from Abdul-Hussein and Mason, 1988; Redshaw et al., 1990; Simmons, 1998; Perkins and Underwood, 2001.

Reservoir	Hanningfield	Alton	Ardleigh
Co-ordinates	51.6558, 0.50094167	51.9804, 1.1326	51.9165, 0.9530
Date of completion	1957	1987	1971
Surface Area top water level (Km^2)	4.029	1.58	0.49
Mean depth at top water level (m)	7.668768	9	3.9
Maximum depth (m)	17	18	13
Total Volume ($m^3 \times 10^6$)	27.2	9.7	2.19
Trophic state	Hyper-Eutrophic	Eutrophic	Eutrophic
Hydrolic retention time (days)	150	480	210
Mixing	Artificially Mixed	Artificially Mixed	Artificially Mixed

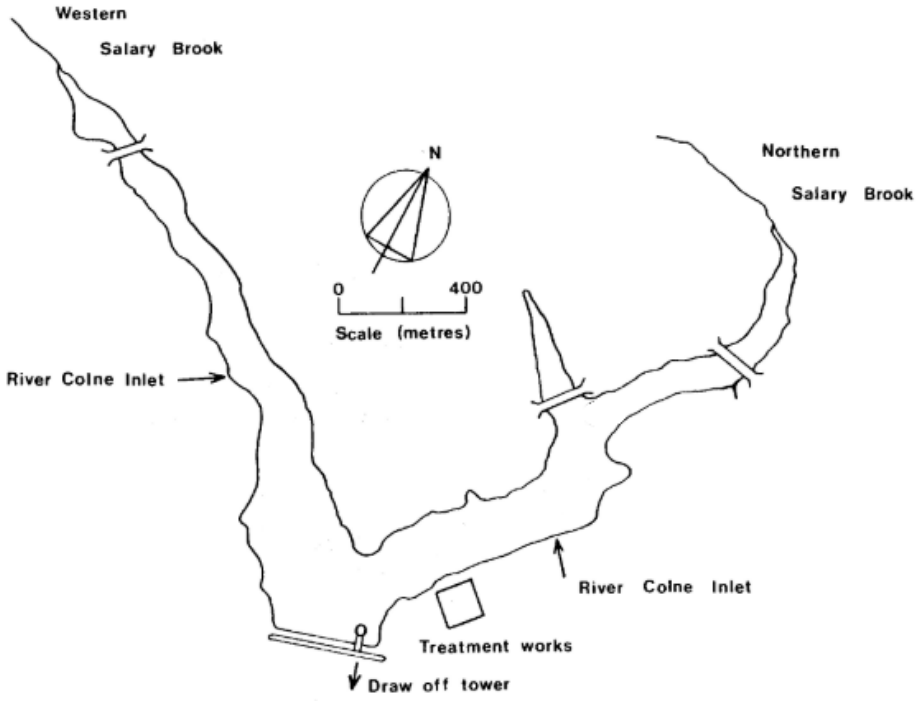

Figure 2.1 Map of Ardleigh reservoir, a eutrophic reservoir created in 1969, managed at the time of study by Anglian Water Services Ltd. CH_4 and CO_2 measurements were made from the limnetic and littoral regions of this reservoir in the summer of 2018. This figure was adapted from Abdul-Hussein and Mason (1988).

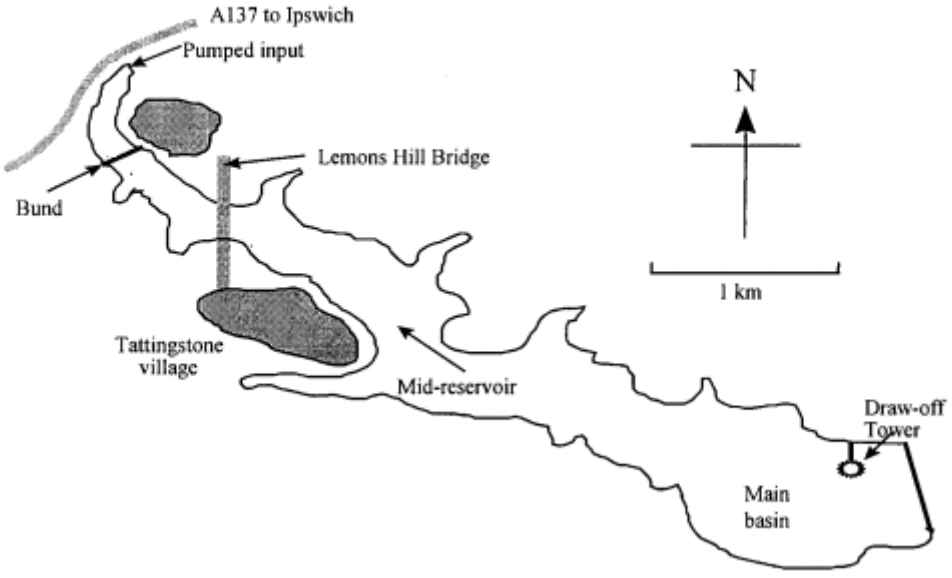

Figure 2.2 Map of Alton reservoir, a hyper-eutrophic reservoir at full capacity since 1956, managed at the time of study by Anglian Water Services Ltd. CH_4 and CO_2 measurements were made from the limnetic and littoral regions of this reservoir in the summer of 2018. This figure was adapted from Perkins and Underwood (2001).

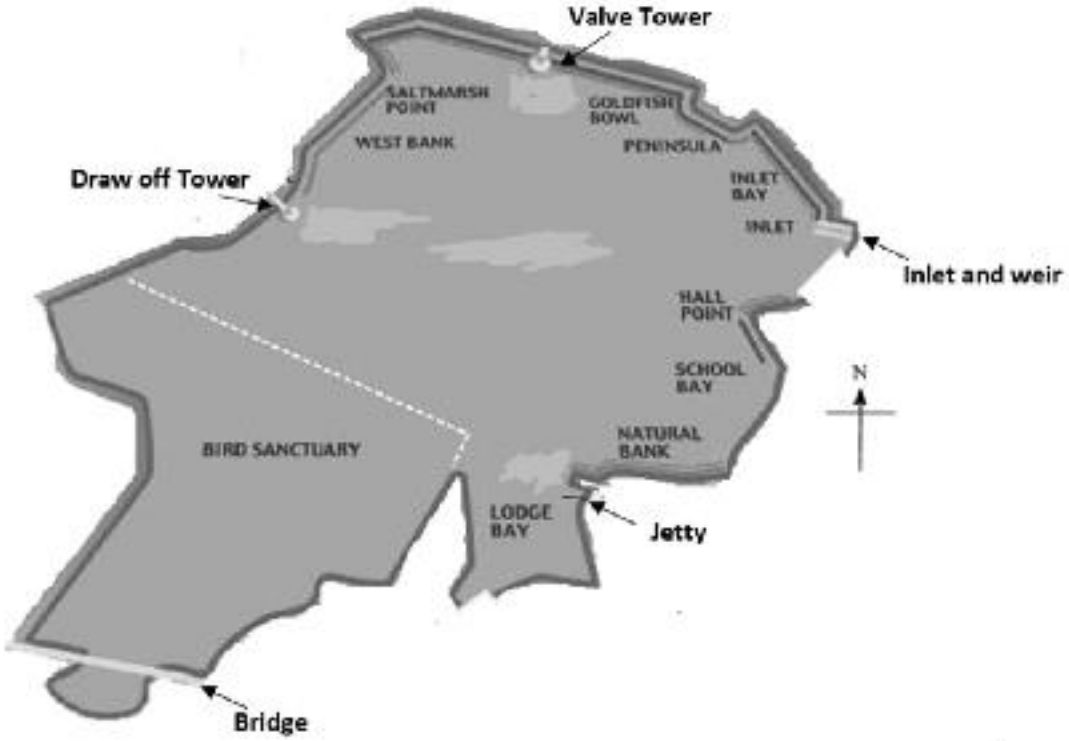

Figure 2.3 Map of Hanningfield reservoir, a eutrophic reservoir at full capacity since 1986, managed at the time of study by Essex and Suffolk Water. CH_4 and CO_2 measurements were made from the limnetic and littoral regions of this reservoir in the summer of 2018. This figure was adapted from Trout Fisherman (2018).

3.2.2 Sample Collection

Flux Sampling

Carbon fluxes were measured using the floating chamber method in a closed loop with Picarro G4301 CRDS GHG analyser (described as the closed dynamic chamber method in section 4.3.2). CO_2 and CH_4 rates of flux were measured from the littoral and limnetic habitats of each reservoir. Limnetic measurements were taken by deploying a floating chamber from the side of a boat, allowed to drift freely across the limnetic zone of the reservoir (as employed by Abril et al., 2005 and Mcginnis et al., 2015). This limited the effects of artificial turbulence (Kremer et al., 2003) and minimised the role of depth as a confounding variable across the habitat. Littoral measurements were taken by deploying the chamber from the side of a reservoir pontoon on a 'loose tether', allowing some free movement of the chamber, again to reduce the effects of artificial turbulence (similar to that employed by Cole et al. (2010)). (Section 4.3 figure 4.3.2 depicts these methods of measurement).

The duration of each flux measurement was 30 minutes (time justification described in section 4.1.3). For each day of sampling, limnetic and littoral habitats were measured twice: 1.5 hours before and 1.5 hours after midday. The second measurement of each habitat was taken three hours after the first, to account for a limited amount of temporal variation that may occur throughout the peak hours of the day. Measurements were structured so that each reservoir was measured at four-week intervals, visiting Ardleigh reservoir in week one, Alton reservoir in week two and Hanningfield reservoir in week three, with no sampling in week 4. This sampling procedure was repeated four times throughout the sampling period of May to September. The total number of flux measurements per habitat was n=24 for all three reservoirs accumulatively, or n=8 for each reservoir individually.

Limnological Sampling

Sampling of reservoir physicochemistry occurred in tandem with each carbon flux measurement (i.e. one water sample was taken for each littoral flux measurement (for a total of two littoral water samples per reservoir visit) and one water sample was taken for each limnetic flux measurement (for a total of two limnetic water samples per reservoir visit)). Two litres of water were taken for each sample in an acid washed 2 litre plastic bottle and rinsed with reservoir water prior to collecting the sample. From these 2 litre samples, 500ml of unfiltered water and 500 ml of water filtered through a 47mm 0.7 µm pore GF/F Whatman filter was frozen for later water chemical analyses. The remaining 1 litre of water was then filtered through a 47mm 0.7 µm pore GF/F Whatman filter for chlorophyll a analysis, the filters being frozen at -80^{o} C for later chlorophyll analyses. Dissolved inorganic nitrogen (DIN) (in the form of nitrate, nitrite and ammonia), dissolved phosphate and dissolved silicates were determined using continuous flow colourimetry (SEAL analytical), after defrosting the previously filtered (through 47mm 0.7 µm pore GF/F Whatman) 500ml water samples. In between chemical analyses, water samples were kept refrigerated.

Total nitrogen (TN) was measured after defrosting the previously frozen unfiltered 500ml water samples, using the ND20 detector of a Formacs^{HT} TOC / TN Analyzer (by Skalar), through chemiluminescence detection (CLD). This catalytically combusted the samples at 850^{o}C, causing chemically bound nitrogen to be converted into NO, which then reacts to form metastable nitrogen dioxide. This emits photons as it decays, which are then detected by a photomultiplier tube. Analyses of TKN concentration was achieved by subtracting the concentrations of NO_3 and NO_2 (measured through colourimetry) from the TN value. Total nitrogen took two runs before results were attained, the first being interrupted by a machine malfunction. Between measurements samples were kept refrigerated. As such, TN and calculated particulate nitrogen could have been affected by the dyssynchronous incubation times.

The formacs^{HT} TOC analyser was additionally used to measure dissolved organic carbon (DOC) and dissolved inorganic carbon (DIC) concentrations from the filtered 500ml water samples. This was repeated using non-filtered 500ml water samples, yielding total organic carbon (TOC), total inorganic carbon (TIC) and total carbon (TOC + TIC). Particulate organic carbon (POC) and particulate inorganic carbon were calculated by taking their dissolved counterpart values from their total measurements (e.g. POC = TOC – DOC). Inorganic carbon measurements were also measured on the formacs^{HT} TOC analyser, which determines inorganic carbon by injecting the sample into an internal reactor containing acid, which converts inorganic carbon into CO_2, which is measured through NDIR (nondispersive infrared spectroscopy). Total phosphorous measurements were made using per-sulphate digestion (Eaton et al., 1995), and the resultant OP concentrations measured using continuous flow colourimetry as used in dissolved phosphate analyses mentioned above.

Chlorophyll a concentration was measured after defrosting the filters, using 100% methanol buffered with $MgCO_3$, and acidified with hydrochloric acid to correct for phaeopigments, following the protocol of Eaton et al. (2005). Absorption was analysed from these samples using photo spectrometry at wavelengths of 750 and at 665 nm.

In-situ water measurements were also made in tandem with each flux measurement. Secchi disk depths were taken using a 30cm diameter Secchi disk for water turbidity measurement. pH and water temperature measurements were taken using a HANNA HI-98130 orb probe. Dissolved oxygen concentrations were recorded using a miniDO2T Logger when the probe was available, at the surface, bottom and middle of the water column at limnetic sites and only at the surface during littoral sampling.

Atmospheric Sampling

Atmospheric data was acquired for each sample from weather stations near to each reservoir (Section 4.3 table 4.3.2), data collected by the open source wunderground.com weather project.

2.2.3 Calculations and Statistics

Rate Extraction

Concentrations of CO_2 and CH_4 measured within the chamber headspace were plotted against time in minutes. For measurements where linear fluxes were observed as a result of diffusion only, a line of best fit was plotted and the slope calculated to determine the rate of concentration change across the time period (section 4.1 figures 4.1.3.2 and 4.1.3.3). In measurements where peaks due to ebullition were detected, a line was plotted from the start concentration to the end concentration of the reading and the slope of the line calculated to determine the rate of concentration change across the time period (section 4.1 figure 4.1.3.4). The value of the slope was corrected for the gas analyser inaccuracies by removing the rate of CO_2 and CH_4 leaks calculated in Section 4.1.2. Rate of concentration change per minute was converted from parts per million (ppm) per minute to molar volume of gas collected per minute, using the combined gas law (which considered the volume of the chamber and the temperature and pressure within the chamber). The rate of CH_4 or CO_2 emission per m^2 per day was then calculated using equation one below:

Equation one:

$$\left(\frac{(moles\ of\ gas\ collected\ per\ minute)}{(surface\ area\ of\ chamber\ in\ m^2)}\right) * 60 * 24$$

Statistical Analyses

Flux of CH_4 and CO_2 were considered separately. To derive models for estimating rates of gas flux, a General Linear Model (GLM) was run to understand gas flux as a function of intra-reservoir habitat, presence of ebullition and physicochemical drivers (CH_4 flux ~ habitat + ebullition + chlorophyll a + particulate phosphate + dissolved phosphate + DIN + DIC +DOC + water temperature + pH +secchi depth). GLM results were tested for significance using an analysis of variance test (ANOVA). Data visualisation for rates of flux and physicochemical drivers were performed using the ggplot 2 package. Other values were tested for significance more specifically using a one-way ANOVA. All the statistical analyses were performed with the statistics software R version 3.4.2 for windows 10 (R Core Team. 2017).

Whole Reservoir Contributions

Whole reservoir contributions of CH_4 and CO_2 were estimated using mean flux values calculated for littoral and limnetic habitats. Littoral habitats were considered to extend 20 metres from the shore (based upon littoral zones extending to a water column depth of 4.5m (Minnesota Department of Natural Resources, 2018)). As bathymetry maps of reservoirs were not available this was an estimate. The littoral surface area of each reservoir was calculated by taking the known reservoir total surface area, calculating this surface area in the shape of a square, then calculating the surface area of the littoral zone as an even 20m from the square perimeter. This littoral surface area was then removed from the total reservoir surface area to determine the total limnetic surface area. The limnetic and littoral habitat rates of flux per m^2 were then multiplied by these surface areas to gather CH_4 and CO_2 daily flux budgets for each habitat and reservoirs as a whole.

2.3 Results

All reservoirs experienced water level drops as a result of evaporation and water extraction throughout the period of study (May to September 2018), resulting in reservoir surface area reductions. In the most extreme cases the littoral zone was pushed back by up to 20 metres, leaving exposed sediment as a result (photographed in section 4.3 figure 4.3.3). During this time ebullition occurred to the extent where it could be obviously observed by eye. The most affected reservoir was Hanningfield, the largest of the three, with CH_4 fluxes from this period reaching a maximum of 204 mmol m^{-2} day $^{-1}$. Additionally, each reservoir experienced periods of algal bloom. A summary of correlation data analysed using general linear models (GLM) is illustrated in table 2.3.1. Mean rates of CH_4 and CO_2 flux from limnetic and littoral regions of individual reservoirs and the three reservoirs combined are presented in table 2.3.2. Estimates of mean CH_4 and CO_2 flux budgets for each reservoir (as a whole) and their limnetic and littoral zones are displayed in table 2.3.3. Mean physicochemical and atmospheric data can be viewed in section 4.3 tables 4.3.1 and 4.3.2.

2.3.1 Flux Dynamics

Intra-Reservoir CH_4 fluxes exhibited statistically significant differences between limnetic (also referred to as pelagic) and littoral habitats within reservoirs. For example, figure 2.3.1 (a.) illustrates larger CH_4 effluxes from littoral habitats (mean= 23.6 mmol m^{-2} day^{-1}, SE= 10.3) relative to pelagic habitats (mean= 1.1 mmol m^{-2} day^{-1}, SE= 0.33). When using a general linear model (GLM), CH_4 fluxes were found to be significantly different between habitats ($t=-2.61$, $P<0.05$). CO_2 fluxes exhibit a less distinct difference between pelagic and littoral habitats within reservoirs. For example, figure 2.3.1 (b.) illustrates influxes of CO_2 in littoral habitats (mean= -5.3 mmol m^{-2} day^{-1}, SE= 2.77) compared to effluxes of CO_2 in pelagic habitats (mean= 7.9 mmol m^{-2} day^{-1}, SE=9.28). However, the large standard error of pelagic habitats extends into influxes, showing great variability. When using a GLM, CO_2 fluxes exhibited a marginal

trend toward significance between pelagic and littoral habitats, though remaining statistically insignificant (t=-2.06, p=0.0515).

Between-Reservoir Fluxes

CO_2 flux displayed statistically significant differences between reservoirs, for both littoral, pelagic and their combined fluxes. Figure 2.3.2 (b.) illustrates the specificity of CO_2 flux patterns to each reservoir. For example, Hanningfield displayed net influxes of CO_2 across both pelagic (mean=-15.7 mmol m^{-2} day^{-1}, SE= 2.73) and littoral (mean= -13.2 mmol m^{-2} day^{-1}, SE= 1.54) habitats, Alton displayed large effluxes of CO_2 in the pelagic (mean= 37.7 mmol m^{-2} day^{-1}, SE= 28.67) but influxes of CO_2 in the littoral (mean= -2.0 mmol m^{-2} day^{-1}, SE= 4.37) and Ardleigh displayed effluxes of CO_2 for the pelagic (mean = 8.4 mmol m^{-2} day^{-1}, SE= 4.73) and marginal patterns of littoral efflux (mean=0.4 mmol m^{-2} day^{-1}, SE= 6.56). When testing with a one-way ANOVA, statistically significant differences in CO_2 flux rates were observed between individual reservoirs. This difference was observed between their pelagic zones ($F= 6.41$, $P< 0.05$, $\eta^2=0.8$), between their littoral zones ($F= 18.66$, $p< 0.05$, $\eta^2=2.7$) and on a whole reservoir scale ($F= 15$, $p< 0.05$, $\eta^2=0.9$).

In contrast, CH_4 fluxes displayed no statistically significant differences between individual reservoirs, but the variability between reservoirs was larger in littoral habitats than in pelagic habitats. For example, figure 2.3.2 (a.) illustrates the differences between reservoirs, Hanningfield having the largest littoral effluxes (mean=49.3 mmol m^{-2} day^{-1}, SE= 24.55) followed by Alton (mean=17.5 mmol m^{-2} day^{-1}, SE=11.81) and Ardleigh the smallest (mean=0.2 mmol m^{-2} day^{-1}, SE= 0.06). However no statistically significant difference in CH_4 flux was found between reservoirs using a one-way ANOVA ($F= 1.615$, $p=0.234$, $\eta^2=0.23$). In contrast, figure 2.3.2 (a.) shows how pelagic rates of efflux remain relatively similar between reservoirs, no statistically significant difference being found when using a one-way ANOVA ($F=0.266$, $P=0.77$, $\eta^2=0.033$), the higher p value and smaller η^2 relative to littoral fluxes showing that between-reservoir variability has comparatively less impact upon pelagic CH_4 flux rates.

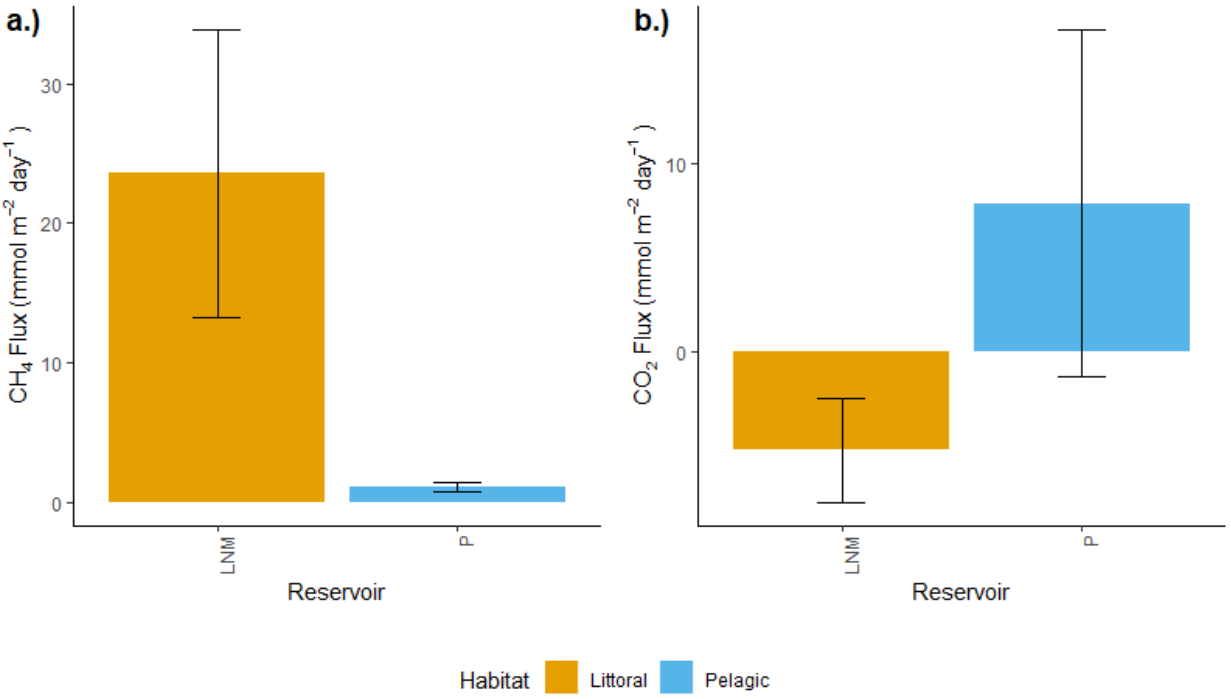

Figure 2.3.1 CH_4 (labelled as "a.") and CO_2 (labelled as "b.") flux rates (mmol m^{-2} day^{-1}) from pelagic and littoral habitats in drinking water reservoirs in the south east of England. Measurements were taken from May to September 2018 using the floating chamber method, headspace concentrations measured with CRDS for 30 minute periods 3 hours around midday. Measurements were combined from three reservoirs in the region: Hanningfield, Ardleigh and Alton. LNM = Littoral zone, P = Pelagic zone. Error bars represent standard error. n=24.

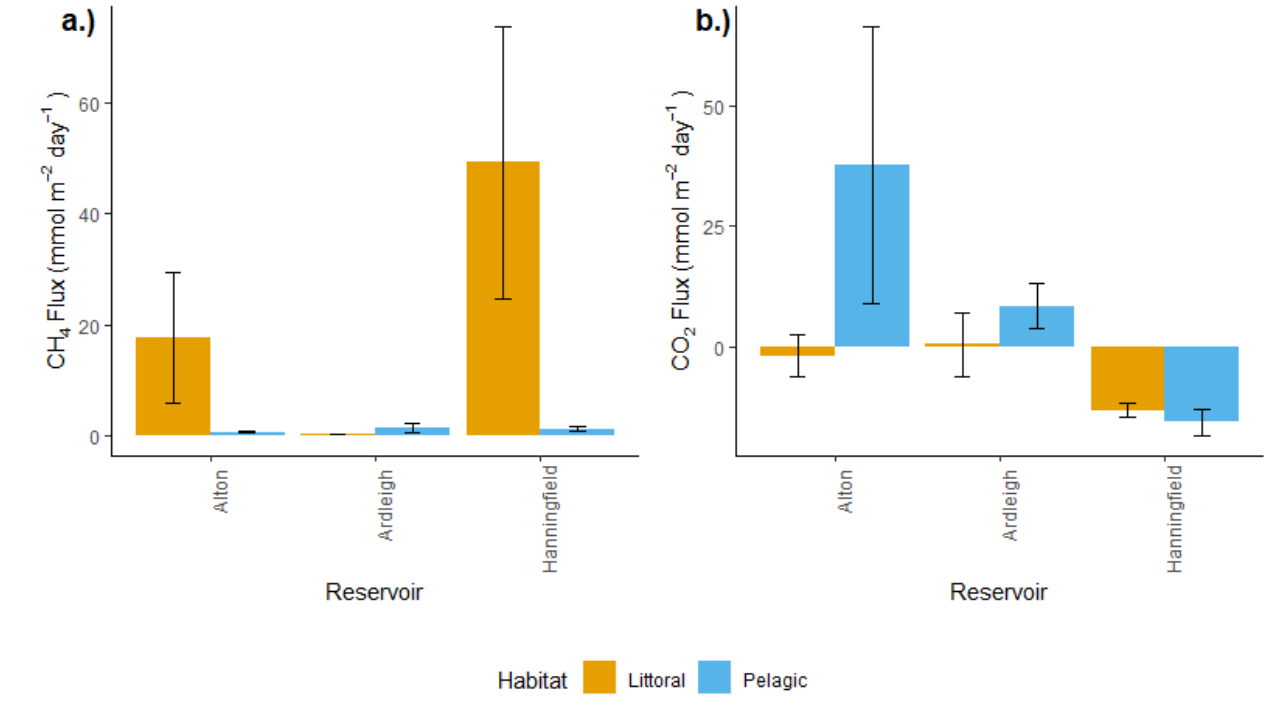

Figure 2.3.2 CH_4 (labelled as "a.") and CO_2 (labelled as "b.") flux rates (mmol m^{-2} day^{-1}) from pelagic and littoral habitats of drinking water reservoirs in the south east of England. Measurements were taken from May to September 2018 using the floating chamber method, headspace concentrations measured with CRDS for 30 minute periods 3 hours around midday. Measurements were taken from three reservoirs in the region: Hanningfield, Ardleigh and Alton. Error bars represent standard error. n=8.

2.3.2 Potential Physicochemical Drivers

Methane

Most significantly, particulate and dissolved phosphates were observed to correlate with increased rates of reservoir methane (CH_4) efflux. Figures 2.3.3 (a.) and 2.3.4 (a.) illustrate positive correlations between CH_4 flux and dissolved/ total phosphate, the rate of CH_4 efflux increasing with increased concentrations of phosphate (for example between total phosphate concentrations of 3000 to 9000 µg/L, CH_4 effluxes increased from 9 to 45 mmol m^{-2} day^{-1}). Analysis using GLMs supported these observations, CH_4 efflux being statistically significantly different between dissolved ($t=-2.63$, $p<0.05$) and particulate ($t=2.81$, $p<0.05$) phosphate.

Similarly, increases in CH_4 effluxes displayed statistically significant correlation with increases in silicate concentration. Figure 2.3.5. (a.) depicts the positive correlation between CH_4 efflux and silicate concentration, silicates increasing from 2500 to 12500 µg/L. When analysed using a GLM, this relationship was found to be statistically significant ($t= 2.286$, $p<0.05$).

Statistically significant differences in CH_4 efflux from reservoirs were observed with increased ebullition from littoral habitats, but no significant difference in CH_4 efflux was observed with increased ebullition from pelagic habitats. For example, figure 2.3.6 (a.) illustrates how the rate of CH_4 efflux is much greater in littoral habitats where ebullition is present (mean= 39.64 mmol m^{-2} day^{-1}, SE= 16.17) than where it is not present (mean= 0.4 mmol m^{-2} day^{-1}, SE= 0.17). In contrast, little difference is observed between pelagic habitats where ebullition is present (mean= 2.6 mmol m^{-2} day^{-1}, SE= 1.66) and where ebullition is not present (mean= 0.8 mmol m^{-2} day^{-1}, SE= 0.22). These observations were supported when investigated using a one-way ANOVA, statistical significance being observed between CH_4 efflux and ebullition in littoral habitats ($F=4.64$, $P<0.05$, $\eta^2=3.09$) but not in pelagic ($p>0.05$). More ebullition observations were recorded for littoral habitats than pelagic ($n= 10$ and $n=2$ respectively).

Table 2.3.1 A summary of correlation analysis results, investigating the correlation between CH_4 emissions and water physico-chemical conditions, as well as results from correlation between CO_2 emissions and water physicochemical conditions. Samples were taken from 3 reservoirs in the south east of England (Ardleigh, Alton and Hanningfield) 3 hours around midday, between May and September 2018. All reservoir data were combined and analysed using a general linear model (GLM). n=48.

	CH_4		CO_2	
Water Physicochemistry	**t value**	**p value**	**t value**	**p value**
Dissolved phosphate	-2.63	0.0153	-2.483	0.0211
Particulate phosphate	2.81	0.0101	0.692	0.4963
Dissolved silicates	2.40	0.022	-3.458	0.0014
pH	1.437	0.1647	-2.79	0.011
Dissolved inorganic carbon	0.983	0.3361	1.981	0.0603
Dissolved organic carbon	-0.232	0.8184	1.431	0.1665
Chlorophyll a	-0.176	0.8618	-0.187	0.853
Dissolved inorganic nitrogen	0.017	0.9864	0.512	0.6137
Water temperature	0.276	0.7854	-1.077	0.293
Turbidity	0.543	0.5926	-0.665	0.5127

Table 2.3.2 Summary of mean rates of CH_4 and CO_2 flux from discrete limnetic and littoral zones of reservoirs in the south east of England (Hanningfield, Alton and Ardleigh). In addition, the mean flux from each habitat is given for all three reservoirs combined, recorded in the "All reservoirs" in the table. Measurements were taken using the floating chamber method, 3 hours around midday from May to September 2018. For each individual reservoir habitat investigated n=8. For all reservoirs combined n= 24.

		CH_4 Flux (mmol m^{-2} day^{-1})		CO_2 Flux (mmol m^{-2} day^{-1})	
Reservoir	**Habitat**	**Mean**	**Standard Deviation**	**Mean**	**Standard Deviation**
Alton	Littoral	17.54	31.24	-2.03	11.55
Alton	Limnetic	0.63	0.45	37.73	75.86
Ardleigh	Littoral	0.16	0.15	0.44	17.36
Ardleigh	Limnetic	1.40	2.50	8.35	13.38
Hanningfield	Littoral	49.32	69.43	-13.22	4.36
Hanningfield	Limnetic	1.11	1.38	-15.70	8.18
All reservoirs	Littoral	23.57	48.30	-5.32	13.00
All reservoirs	Limnetic	1.07	1.65	7.90	45.47

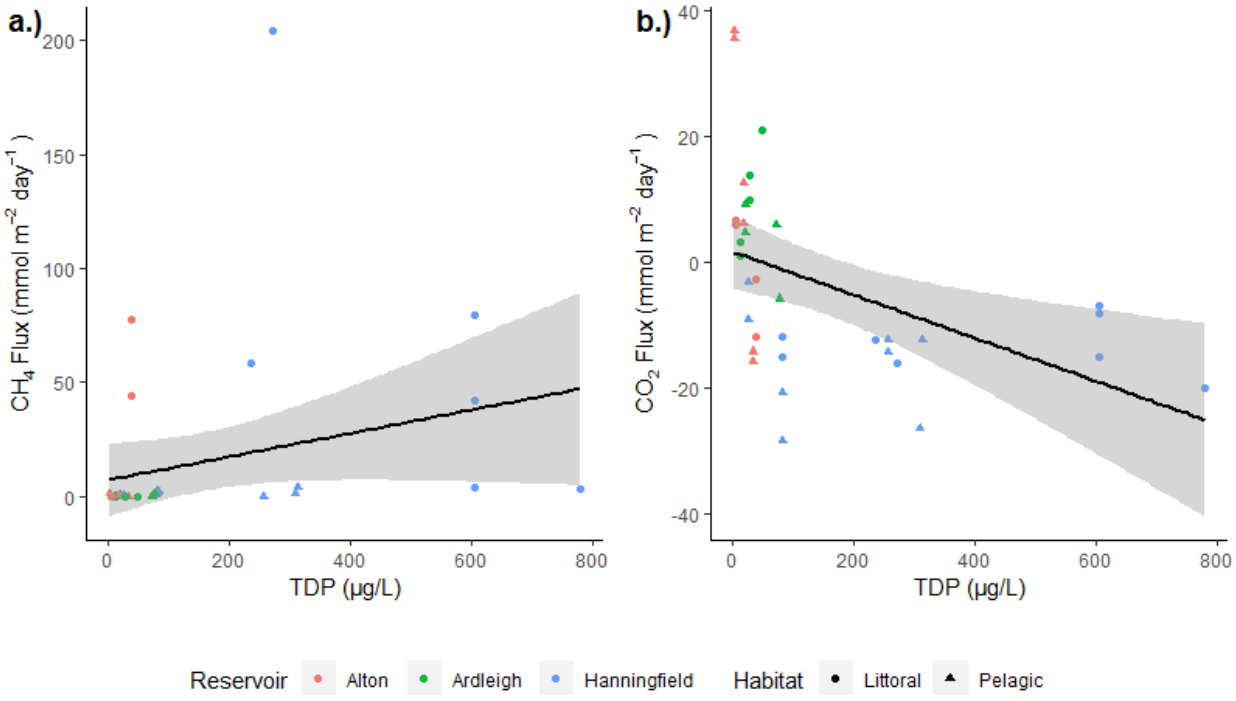

Figure 2.3.3 CH_4 (labelled as "a.") and CO_2 (labelled as "b.") flux rate (mmol m^{-2} day^{-1}) correlations against total dissolved phosphorous (TDP). Point shapes display flux rates from pelagic and littoral habitats, while point colour displays the reservoir from which the measurement was taken. Measurements were taken from May to September 2018 using the floating chamber method, headspace concentrations measured with cavity ring down spectroscopy for 30 minute periods 3 hours around midday. TDP was sampled and analysed using flow through colourimetry. The Line plots the line of best fit, and the grey shaded area is the 95% confidence interval. n= 32.

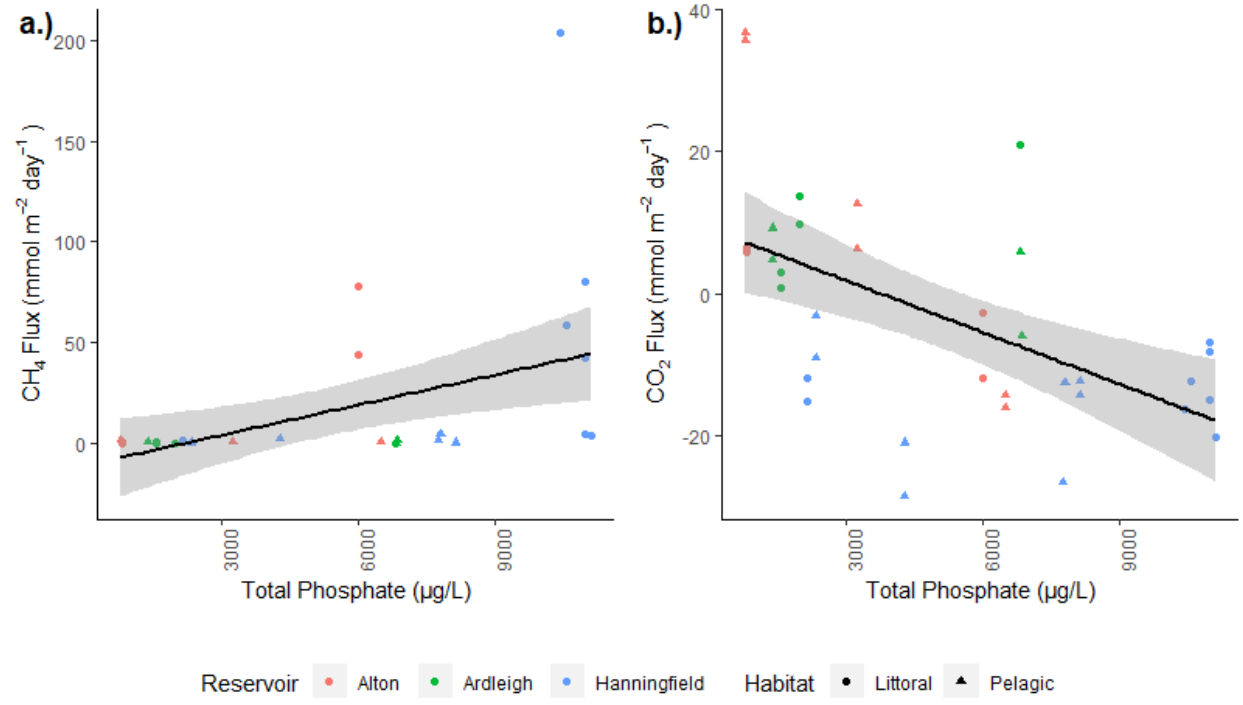

Figure 2.3.4 CH_4 (labelled as "a.") and CO_2 (labelled as "b.") flux rate (mmol m^{-2} day^{-1}) correlations against total phosphate (TP). Point shapes display flux rates from pelagic and littoral habitats, while point colour displays the reservoir the measurement was taken from. Measurements were taken from May to September 2018 using the floating chamber method, headspace concentrations measured with cavity ring down spectroscopy for 30 minute periods 3 hours around midday. TP was measured through per-sulphate digestion followed by flow through colourimetry. The Line plots the line of best fit, and the grey shaded area is the 95% confidence interval. n=32.

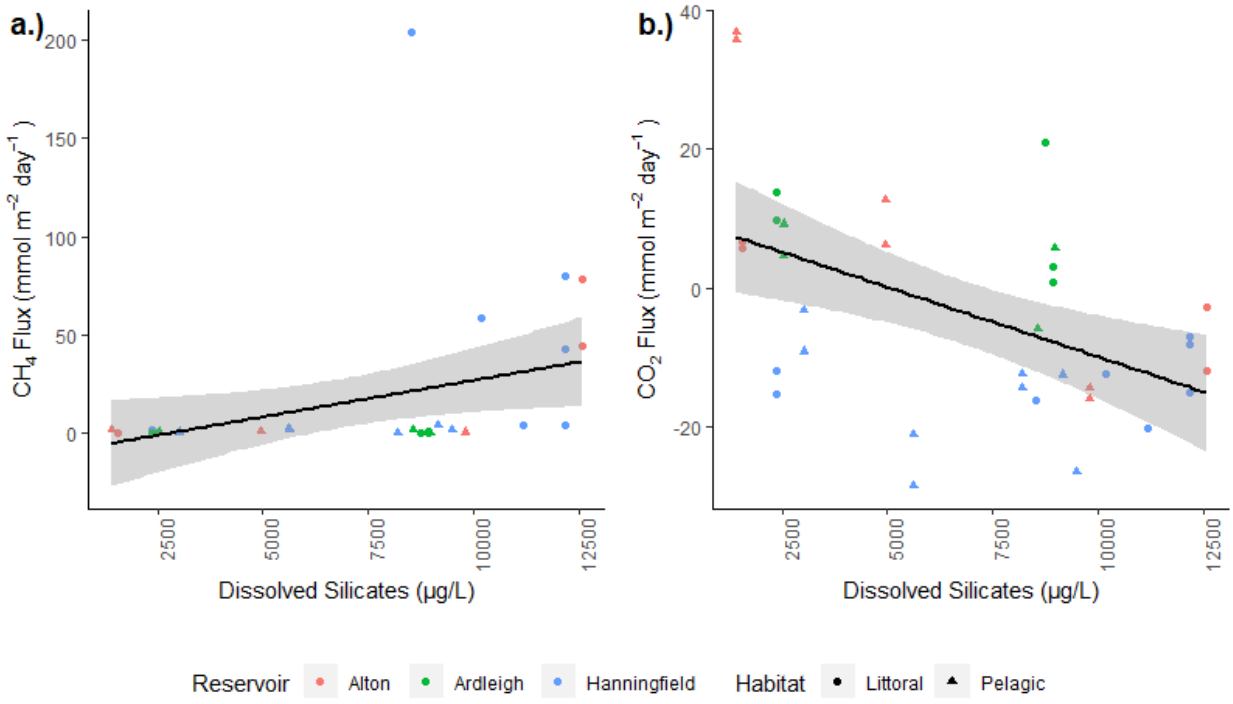

Figure 2.3.5 CH_4 (labelled as "a.") and CO_2 (labelled as "b.") flux rate (mmol m^{-2} day^{-1}) correlations against dissolved silicates. Point shapes display flux rates from pelagic and littoral habitats, while point colour displays the reservoir the measurement was taken from. Measurements were taken from May to September 2018 using the floating chamber method, headspace concentrations measured with cavity ring down spectroscopy for 30 minute periods 3 hours around midday. Dissolved silicate concentration was sampled and analysed using flow through colourimetry. The Line plots the line of best fit, and the grey shaded area is the 95% confidence interval. n=32.

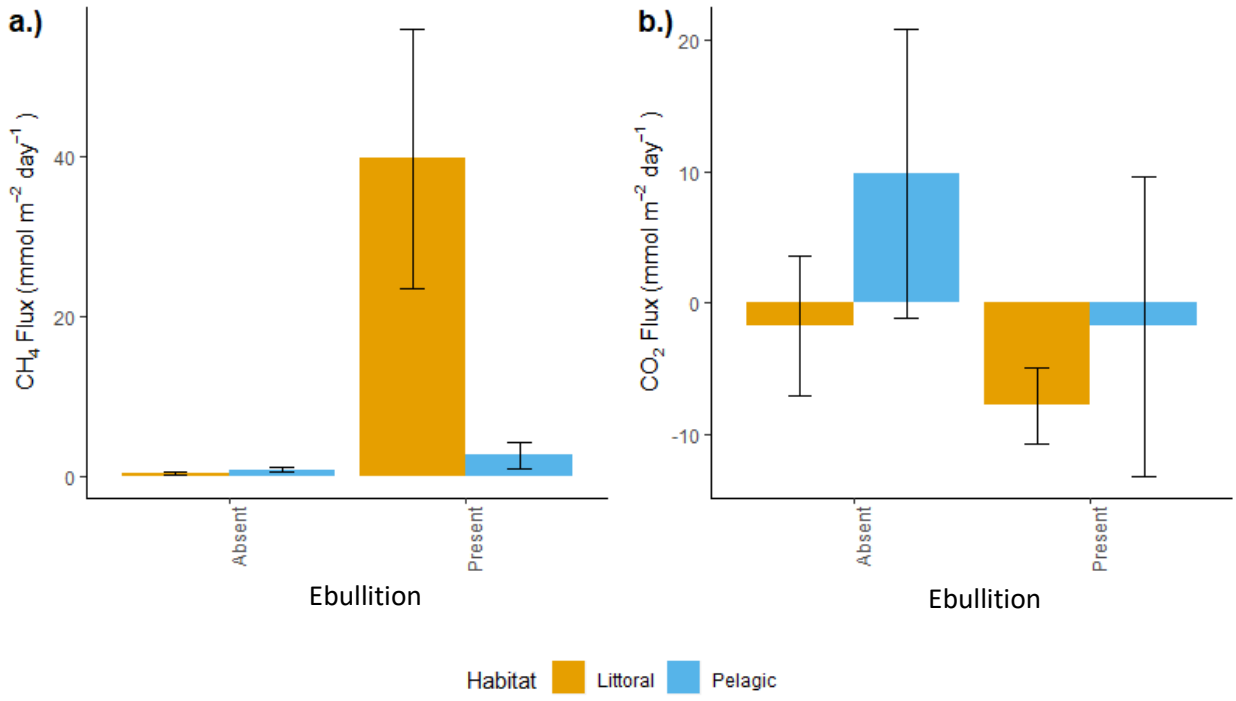

Figure 2.3.6 CH_4 (labelled as "a.") and CO_2 (labelled as "b.") flux rates (mmol m^{-2} day^{-1}) against the presence of ebullition. Measurements were taken from May to September 2018 using the floating chamber method, headspace concentrations measured with cavity ring down spectroscopy for 30 minute periods 3 hours around midday. By plotting the chamber headspace concentrations of CH_4 and CO_2, measured every second, ebullition events were detected as peaks in concentration during the time period. Measurements were combined from three reservoirs in the region: Hanningfield, Ardleigh and Alton. Error bars represent standard error. n=24.

Carbon Dioxide

CO_2 fluxes were significantly correlated with dissolved phosphate concentrations, but not by particulate phosphate. Figure 2.3.3 (b.) illustrates a negative correlation between dissolved phosphorous and CO_2 efflux, rates of efflux decreasing from 3 to -22 mmol m^{-2} day^{-1} with increasing concentrations of dissolved phosphate from 1.8 to 603.5 µg/L. These trends are supported by the results of a GLM, finding phosphorous to have a statistically significant correlation with CO_2 efflux ($t=-2.48$, $p<0.05$).

Increased pH was found to correlate significantly with increased CO_2 efflux. Figure 2.3.7 (b.) shows a clear negative correlation between pH and CO_2 efflux, pH increasing from 7.0 to 9.0 while CO_2 flux decreases from 8 to -17 mmol m^{-2} day^{-1}. After modelling with a GLM this correlation was found to be statistically significant ($t=-2.79$, $p<0.05$).

Similarly, CO_2 fluxes displayed statistically significant differences correlating with silicate concentration. Figure 2.3.5 (b.) depicts the negative correlation between CO_2 efflux and silicate concentration, silicates increasing from 2500 to 12500 µg/L while CO_2 decreased from 8 to -15 mmol m^{-2} day^{-1}. When analysed using a GLM this relationship was found to be statistically significant ($t= -3.4$, $P<0.05$).

Dissolved inorganic carbon (DIC) displayed a marginal trend toward significance in correlations with CO_2 efflux increase, through remained statistically insignificant upon assessment in a GLM ($t=1.98$, $p=0.060$). Figure 2.3.8 (b.) shows a positive correlation between DIC and CO_2 efflux, though the spread of data about the line of best fit is large, explaining the trend towards, but lack of, statistical significance.

Statistically Insignificant Drivers

Physicochemical water qualities including dissolved inorganic nitrogen (DIN), chlorophyll a and water temperature were found to have no statistically significant correlation with CO_2 or CH_4 fluxes, despite plots of CH_4 and CO_2 flux dynamics against these measured variables expressing marginal trends towards correlation (Section 4.3 figures 4.3.5 to 4.3.6). Analysis using GLMs found no statistical significance ($p>0.05$).

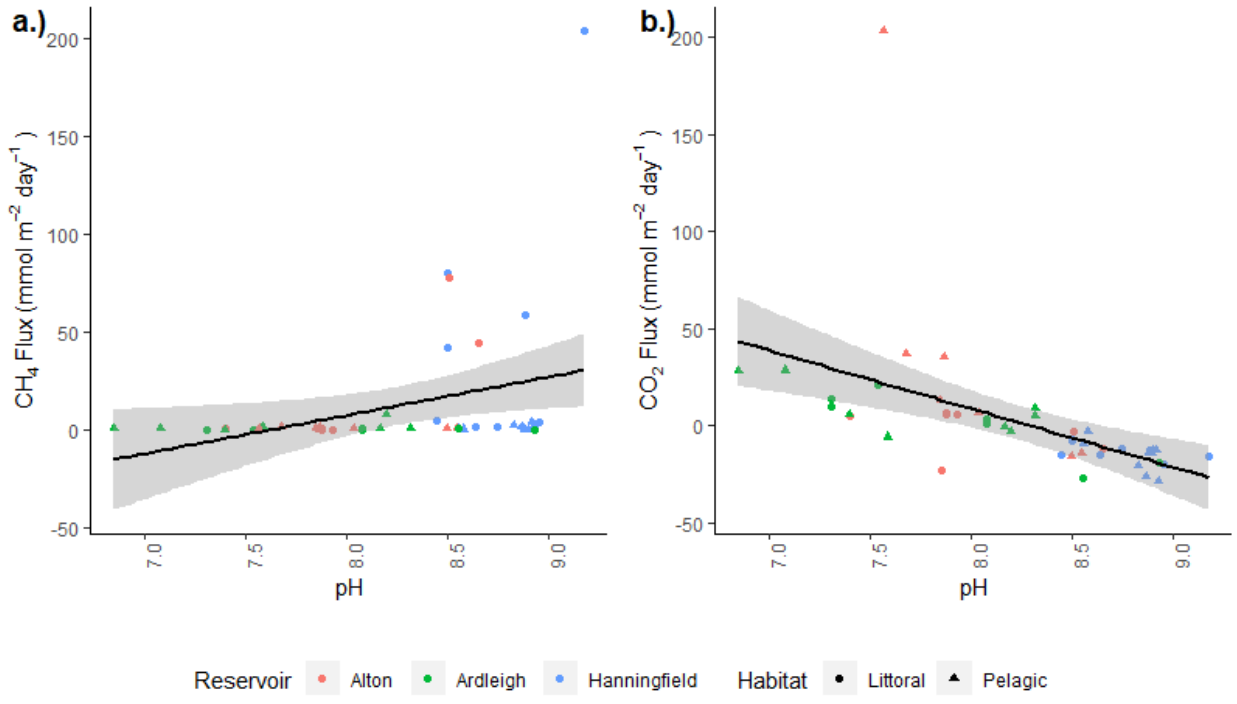

Figure 4.3.7 CH_4 (labelled as "a.") and CO_2 (labelled as "b.") flux rate (mmol m^{-2} day^{-1}) correlations against pH. Point shapes display flux rates from pelagic and littoral habitats, while point colour displays the reservoir the measurement was taken from. Measurements were taken from May to September 2018 using the floating chamber method, headspace concentrations measured with cavity ring down spectroscopy for 30 minute periods 3 hours around midday. pH was measured *in-situ* using a HANNA HI-98130 orb probe. The Line plots the line of best fit, and the grey shaded area is the 95% confidence interval. n=32.

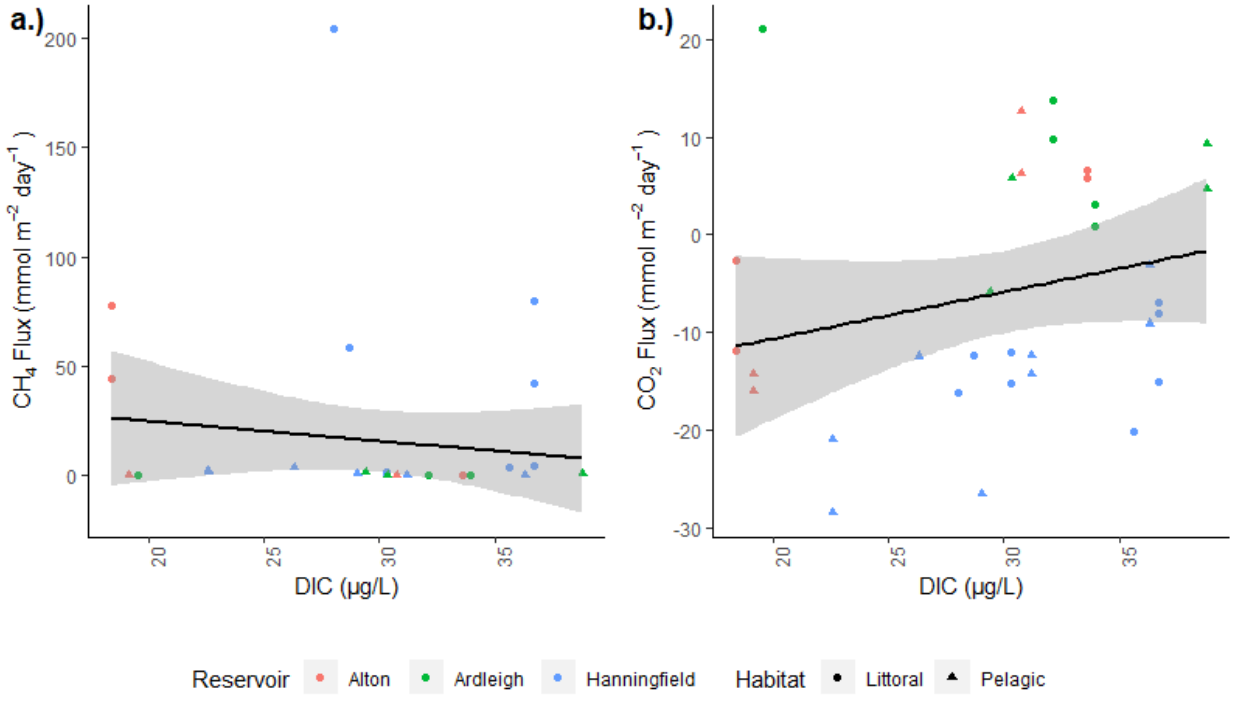

Figure 4.3.8 CH_4 (labelled as "a.") and CO_2 (labelled as "b.") flux rate (mmol m^{-2} day^{-1}) correlations against dissolved inorganic carbon (DIC). Point shapes display flux rates from pelagic and littoral habitats, while point colour displays the reservoir the measurement was taken from. Measurements were taken from May to September 2018 using the floating chamber method, headspace concentrations measured with cavity ring down spectroscopy for 30 minute periods 3 hours around midday. DIC concentration was sampled and analysed using a Formacs^{HT} Analyzer by Skalar with an internal reactor containing acid. The Line plots the line of best fit, and the grey shaded area is the 95% confidence interval. n=32.

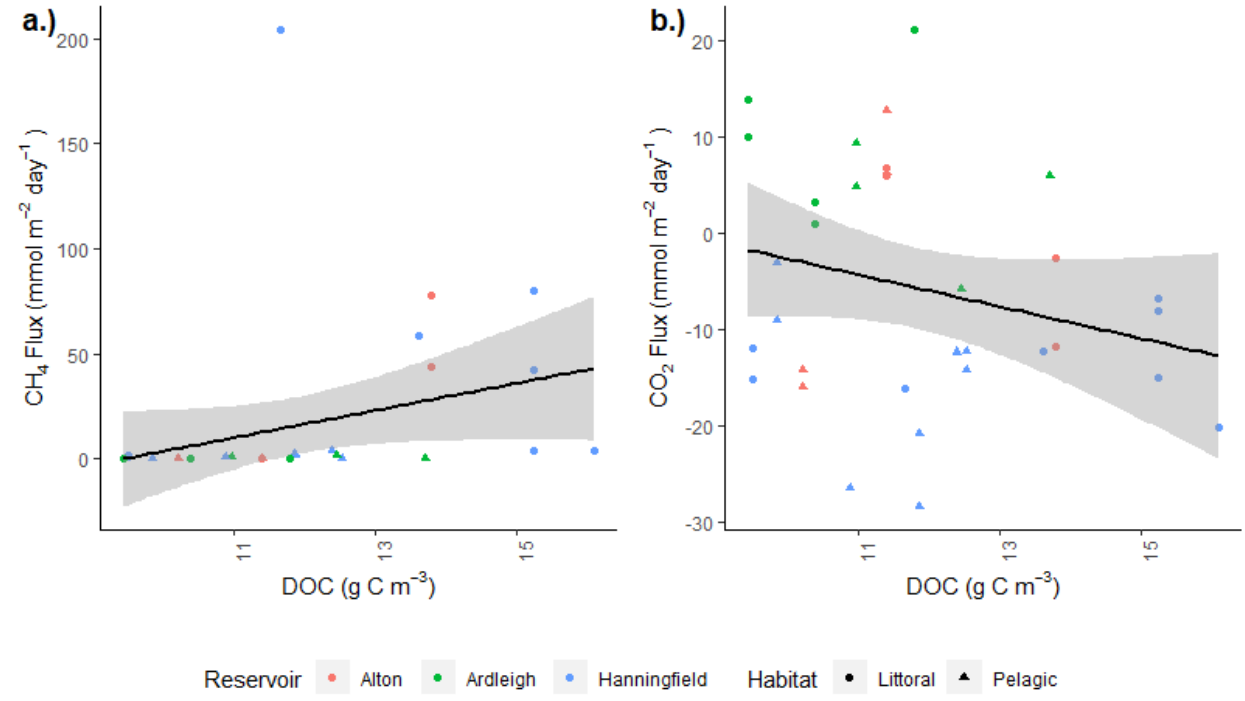

Figure 4.3.9 CH_4 (labelled as "a.") and CO_2 (labelled as "b.") flux rate (mmol m^{-2} day^{-1}) correlations against dissolved organic carbon (DOC). Point shapes display flux rates from pelagic and littoral habitats, while point colour displays the reservoir the measurement was taken from. Measurements were taken from May to September 2018 using the floating chamber method, headspace concentrations measured with cavity ring down spectroscopy for 30 minute periods 3 hours around midday. DOC concentration was sampled and analysed using a Formacs^{HT} TOC Analyzer by Skalar. The Line plots the line of best fit, and the grey shaded area is the 95% confidence interval. n=32.

Table 2.3.3 Estimated mean rates of CH_4 and CO_2 flux from whole reservoirs (c.) and their total littoral (b.) and limnetic zone (a.) contributions. Estimates made from reservoirs in the south east of England (Hanningfield, Alton and Ardleigh) were calculated using the estimated surface area of each habitat type in each reservoir, and the rate of flux of each gas in mmol m^{-2} day^{-1}, collected 3 hours around midday from May to September 2018 using the floating chamber method. Sd represents standard deviation. Regional total is the combined flux from all three reservoirs. For each individual reservoir habitat investigated n=8. For all reservoirs combined n= 24.

(a.)

	Limnetic			
	CH_4 Flux (mol day^{-1})		**CO_2 Flux (mol day^{-1})**	
Resevoir	**Mean**	**Sd**	**Mean**	**Sd**
Hanningfield	4308	5339	-60760	31646
Alton	927	673	55884	112353
Ardleigh	609	1090	3635	5828
Regional total	5844	5491	-1241	116870

(b.)

	Littoral			
	CH_4 Flux (mol day^{-1})		**CO_2 Flux (mol day^{-1})**	
Resevoir	**Mean**	**Sd**	**Mean**	**Sd**
Hanningfield	7840	11038	-2102	693
Alton	1736	3092	-201	1143
Ardleigh	9	8	24	945
Regional total	9585	11463	-2279	1637

(c.)

	Whole Reservoir			
	CH_4 Flux (mol day^{-1})		**CO_2 Flux (mol day^{-1})**	
Resevoir	**Mean**	**Sd**	**Mean**	**Sd**
Hanningfield	12148	12262	-62862	31653
Alton	2663	3164	55683	112359
Ardleigh	618	1090	3659	5904
Regional total	15429	12710	-3520	116882

2.4 Discussion

2.4.1 Dynamics of CO_2 and CH_4 Flux

Between Reservoirs

The rates of CH_4 efflux observed form Ardleigh, Alton and Hanningfield reservoirs are within the rates of CH_4 flux that have been recorded from temperate and boreal reservoirs and lakes in the literature (Table 2.4.1 illustrating a range in mean flux from 1 to 79 mg m^{-2} day^{-1}). However, Hanningfield reservoir is among those with the higher rates of efflux that have been recorded from these regions, expressing a mean rate of flux of 48 mg m^{-2} day^{-1}. This comparatively high rate of efflux from Hanningfield is significant, as being older it would be expected to contribute less significant concentrations of CH_4 relative to its more recent counterparts. For instance, the age of a reservoir is expected to be inversely proportional to its rate of CH_4 efflux. As the large organic matter deposit that occurs through the initial flooding of vegetated land is progressively decomposed, the resulting production and efflux of CH_4 is reduced (St. Louis et al., 2000). In addition, the vegetation that was flooded to form Hanningfield was pastoral, whereas the vegetation that was flooded to form the reservoir with similarly high rates of CH_4 efflux in table 2.4.1 (Lokkaf) was peatland; a habitat of high background CH_4 production relative to pastoral land (Lai et al., 2009). As such, the high rate of CH_4 efflux from Hanningfield relative to its age and formative vegetation must be the result of maintained organic productivity or organic input over time, resulting in maintained sediment organic matter concentrations and CH_4 production through methanogenic decomposition. As Hanningfield is a hypereutrophic reservoir (Section 4.3 table 4.3.1), this process of decomposition driven CH_4 production is likely to be a key factor in its high rates of CH_4 efflux.

An additional factor contributing to why such high rates of CH_4 efflux are observed from Hanningfield reservoir relative to the literature is that sampling took place in the summer season. During summer seasons CH_4 efflux is reported to constitute up to 90% of a reservoir's annual CH_4 budget (Harrison et al.,

2017). This occurs as a result of increased atmospheric temperatures driving increased CH_4 production in reservoir sediments (due to increased methanogenic metabolic activity (Glissman et al., 2004) and decreased oxygen availability in the case of algal blooms), and water level decreases (due to low rates of precipitation in combination with high water draw-out demands). These water level drawdowns result in reduced hydrostatic pressure acting upon the sediment, resulting in the release of trapped CH_4 gas as ebullition release events (Harrison et al., 2017). Of the reservoirs investigated in this field campaign, Hanningfield experienced the largest water level drawdowns (Section 4.3 figure 4.3.3) and highest levels of eutrophication (driving sediment CH_4 production through increased organic matter production (Section 4.3 table 4.3.1)). This is likely to have driven the elevated levels of ebullition measured from the reservoir's littoral zone relative to its limnetic zone (Figure 2.3.2), and caused the high rates of overall CH_4 efflux observed from all three reservoirs. It is likely that if sampling were to occur annually from these reservoirs, their average rates of CH_4 efflux would be reduced relative to this season, thus for accurate CH_4 rate contributions and comparisons with the literature, further research into CH_4 efflux from these reservoirs must occur on an annual scale.

The contributions of CH_4 from these reservoirs during the summer period are significant when considering the role of these reservoirs in the region's CH_4 budget. For example, the rate of CH_4 sequestration from the terrestrial biome is 0.03 to 2.5 mg of $CH_4\,m^{-2}\,day^{-1}$ (Smith et al., 2000), whereas the mean rate of CH_4 efflux from reservoirs in the region based upon these three reservoirs is 31.7 mg of $CH_4\,m^{-2}\,day^{-1}$. As such, the power of reservoirs to 'counteract the continental carbon sink' (Bastviken et al., 2011) despite their reduced surface area relative to the terrestrial biome (Downing et al., 2006) is evident. In relation to cattle, another source of anthropogenic CH_4 which is similarly pressuring the terrestrial CH_4 sink, the combined CH_4 source from the three reservoirs investigated in this study equates to a CH_4 production rate of 904 cattle day^{-1} (considering an individual cow to release 100 kg of $CH_4\,yr^{-1}$ (Johnson and Johnson, 1995)). Considering the number of UK reservoirs, their contribution of anthropogenic CH_4 to the UK's CH_4 cycle is large, adding pressure to a system already stressed by other

anthropogenic sources. This study highlights the need for the inclusion of reservoirs in regional carbon budgets, if climate mitigation strategies focussing on CH_4 efflux limitation are to be realised.

When considering the combined CO_2 dynamics of the reservoirs investigated in this study, they behave as net contributors of CO_2 to the atmosphere (heterotrophic). However, the dynamics of individual reservoirs are varied, Alton and Ardleigh behaving as net heterotrophic systems but Hanningfield behaving as a net autotrophic system. When comparing these rates of CO_2 flux with those observed in the literature, Ardleigh and Hanningfield expressed very low rates of CO_2 efflux, whereas Alton expressed a higher rate of efflux more comparable with that seen in the literature (table 2.4.1). This suggests that the rate of photosynthesis, relative to the rate of respiration, in Ardleigh and Hanningfield was greater than is usual in reservoirs. It is likely, however, that these results are a product of disparity between the time of day that CO_2 flux rates were measured in this study relative to reservoirs investigated in the literature. As such, the values of diel CO_2 flux in this study may underestimate the total diel CO_2 efflux from these reservoirs, night-time emissions estimated to account for up to 40% of a reservoir's CO_2 emissions (Liu et al., 2016). If measurements were taken at different time points in the diel cycle (for example at night when the dominant process is respiration, not photosynthesis) reservoir CO_2 dynamics could be more accurately calculated.

While diel variation does account for some of the discrepancy seen between Ardleigh and Hanningfield with the literature in table 2.4.1, the fluxes from the literature are similarly based upon daytime rates of flux (a subject of criticism towards global lake CO_2 estimates (Liu et al., 2016)). It is more likely that the low rates of CO_2 efflux from Ardleigh and Hanningfield are a result of seasonal variation in CO_2 flux. For instance, during the summer phytoplankton growth is rapid and results in higher rates of carbon assimilation than in other seasons, which are more dominated by respiration processes as phytoplankton biomass from earlier in the season in decomposed (Tranvik et al., 2009). Further research is required to understand the dynamics of CO_2 flux from reservoirs in the south east of England and for accurate comparison with the literature, by extending studies to an annual scale, and incorporating diel light intensity fluctuations into CO_2 flux measurements.

Both CO_2 and CH_4 rates of flux demonstrate heterogeneity between the reservoirs investigated in this study, and between reservoirs investigated in the literature. This illustrates the difficulty in estimating a reservoir or a lake's CO_2 and CH_4 budget without measuring and understanding the individual water body beforehand, and demonstrates the need for research into more reservoirs to improve regional CO_2 and CH_4 budgets, with the perspective of climate mitigation strategies.

Table 2.4.1 Summary of the reservoir CO_2 and CH_4 flux rates measured in this thesis, relative to flux rates observed in other temperate and boreal reservoirs and lakes recorded in the literature. Flux rates from this thesis represent midday rates of efflux in the summer period of 2018. Total flux rates from the literature represent individual ebullition (through funnel traps) and diffusion (through the thin boundary layer method) measurements added together, or collection of both pathways using the floating chamber technique. Rates of flux in the literature represent data taken from inconsistent time points throughout the year, and do not consistently represent both littoral and pelagic habitats.

					CH_4 Flux (mg m^{-2} day^{-1})		CO_2 Flux (mg m^{-2} day^{-1})	
Reference	**Water Body**	**Name**	**Area (km^2)**	**Age (yrs)**	**Mean Flux**	**Range**	**Mean Flux**	**Range**
This thesis	Reservoir	Hanningfield	4	61	48	2 — 191	-687	-1238 — -144
This thesis	Reservoir	Ardleigh	1.6	47	20	0.1 — 108	329	-359 —1220
This thesis	Reservoir	Alton	0.5	31	27	3 — 98	1551	-723 — 8393
Duchemin et al., 1995; Duchemin, 2000	Reservoir	Laforge-1	1000	5	13	1 — 130	2300	200 — 8500
Kelly et al., 1994; Duchemin, 2000	Reservoir	Robert-Bourassa	2500	12 to 19	13	1 — 100	1500	160 — 12,000
Duchemin et al., 1995; Duchemin, 2000	Reservoir	Cabonga	400	68 to 70	18	2 — 260	1400	320 — 4800
Kelly et al., 1997	Reservoir	ELARP[a]	0.2	1 to 2	54	50 — 90	2000	1100 — 3700
Hellsten et al., 1996	Reservoir	Lokkaf[b]	417	28	79	11 — 250	2000	770 — 3400
Hellsten et al., 1996	Reservoir	Porttipahta[b]	214	25	13	12 — 15	2100	1360 — 3300
Bastviken et al., 2004	Lake	Brown	0.3	NA	9	NA	NA	NA
Bastviken et al., 2004	Lake	Crampton	0.3	NA	5	NA	NA	NA
Bastviken et al., 2004	Lake	Morris	0.1	NA	65	NA	NA	NA
Bastviken et al., 2004	Lake	Roach	0.45	NA	1	NA	NA	NA
Huttunen et al.,2003	Lake	Kevätön	4.07	NA	51	16 — 193	616.14	-79 — 1100
Huttunen et al., 2003	Lake	Vehmasjärvi	0.41	NA	4	1 — 6	858	172 — 1400

[a] ELARP is the experimental lakes area reservoir project region in Northern Quebec, Canada. Reservoirs were formed by flooding peatland for the experiment.

[b] LOKKAF is an experimentally flooded area of peatland in Finland.

Within-Reservoir Fluxes

Spatial variation in carbon flux dynamics was observed within reservoirs as well as between them, limnetic and littoral habitats displaying statistically significant differences in CH_4 and CO_2 flux rates. For example, CH_4 effluxes from the littoral zones of Alton and Hanningfield were much larger than in their limnetic zones, whereas in Ardleigh fluxes from the limnetic zone were marginally greater than the littoral zone (Figure 2.3.2). This spatial variability is largely the result of which CH_4 flux pathway dominates in each zone, and is largely decided by the presence of ebullition and its strength as a source of CH_4 efflux relative to diffusive fluxes (Figure 2.3.6). The dynamics viewed in Alton and Hanningfield conform to the traditional paradigm that the ratio of CH_4 to CO_2 is increased in the littoral zones relative to the limnetic zone, as the reduced effects of water column CH_4 oxidation and bubble dissolution in shallow littoral water columns result in larger net CH_4 effluxes relative to deeper limnetic regions (Hanson et al., 2007). When considering intra-reservoir flux dynamics where ebullition is not present, however, there is a trend towards increased CH_4 efflux in the limnetic zone relative to the littoral, as seen in Ardleigh (Figure 2.3.2). This phenomenon, first identified by Scranton and Farrington (1977), is sometimes termed the 'methane paradox' and is generally considered to result from lateral transport of dissolved CH_4 (produced in the littoral zone) to the limnetic region of a lake where it is released to the atmosphere (Murase and Sugimoto, 2017). This was likely to have been the dominant process when sampling Ardleigh reservoir.

As ebullition appears to drive the within-reservoir flux variation in Alton, Ardleigh and Hanningfield reservoirs, and is affected by water level drawdown and temperature in reservoirs (as described previously), so too are within-reservoir flux dynamics likely to be temporally variable. This occurs on a diel scale, as ebullition occurs intermittently throughout the day (Käki et al., 2001), and on a seasonal scale (ebullition is likely to occur more often in summer seasons than winter (Xing et al., 2005; Larmola et al., 2004). This stresses the need for flux data to be of a high temporal resolution if diel and seasonal flux variations within reservoirs are to be quantified and incorporated into carbon budgets accurately.

The within-reservoir flux variation observed in this study additionally emphasises the need for investigations to include sampling of both limnetic and littoral habitats (where different flux pathways prevail) to prevent the under or over estimating of CH_4 flux rates when scaling up full reservoir budgets. For example, by ignoring the littoral fluxes from Hanningfield reservoir, this study would underestimate the reservoirs CH_4 effluxes by ~123kg day^{-1} and overestimate CO_2 effluxes by ~17kg per day, an error climate modellers cannot afford to make. To improve the spatial accuracy in reservoir and lake estimates, bathymetry of lakes should be included in measurements, to allow the depth of an area and the dynamic littoral/limnetic zone boundaries to be tracked.

2.4.2 Drivers of CO_2 and CH_4 Flux

The drivers of between- and within-reservoir CO_2 and CH_4 flux variations stem from the physicochemical and biological heterogeneity of reservoir environments. Regardless of spatial scale, fluxes are the end-product of many individual physical and biological interactions, and as such are highly convoluted systems to try and understand when calculating carbon fluxes.

Chemical Drivers

Results displayed a trend towards increasing dissolved organic carbon (DOC) concentration (and other forms of carbon) with increasing rates of CH_4 efflux and CO_2 influx; though these were not statistically significant. In the literature, DOC is generally observed to correlate significantly with increased effluxes of CH_4 (Yan et al., 2019; Bogard et al., 2014), as the availability of substrates prerequisite to sediment methanogenesis (acetate and CO_2) are increased. Additionally, potential competition of methanogens with other anaerobically respiring organisms that utilise the same source of acetate (such as Sulphur reducing bacteria (SRBs) (Stams et al., 2003)) is reduced. While the trend towards increased DOC concentrations with CH_4 flux indicates some DOC driven methanogenesis, the lack of statistical significance suggests either that the abundance of DOC available exceeds the limiting concentration for

methanogenic growth (e.g. DOC values measured from these reservoirs (Section 4.3. Table 4.3.1) are in the top 50% of lakes globally (Sobek et al., 2007)), or more likely that the increase in carbon directly available to methanogens is not significant enough to cause a visible change in CH_4 efflux, as methanotrophs increase CH_4 oxidation rates in response to any increase in CH_4 production that could occur (Borrel et al., 2011).

The significant correlation between phosphate concentration and increased CH_4 efflux suggests that phosphorous directly or indirectly drives CH_4 production in these environments. The dominant process of phosphorous driving CH_4 production is indirect, its increasing concentrations driving system productivity and subsequent sediment organic matter deposition (Flynn and Clark, 2008). Organic matter degradation using methanogenesis releases CH_4 as a by-product, thus increasing the efflux from the system. An alternative source of biogenic CH_4 that could be driven by phosphorous concentrations is a result of mechanisms proposed by Bogard et al. (2014) whereby Achaea interact symbiotically with cyanobacteria either by providing anoxic habitats or substrates to methanogens (Grossart et al., 2011). In this case, increased phosphorous could drive cyanobacterial growth, and in-turn increase CH_4 efflux directly. Trends in chlorophyll a concentration are often seen to correlate with increasing CH_4 efflux and increasing CO_2 influx (Yan et al., 2019), in line with the phosphate pathways discussed. However, although these trends were observed in this investigation (figure 4.3.5), the statistical insignificance of chlorophyll a suggests other factors may be at play.

A potential direct effect of phosphate concentration on methanogenesis and subsequent CH_4 flux is the role of cyclic 2,3-diphosphoglycerate (cDPG) in methanogen carbohydrate metabolism (Musti et al., 1992), which is suggested to limit methanogen growth. It is possible that in phosphorous limited environments methanogen populations will be smaller and result in lower net rates of CH_4 production. However, it is likely that the role of phosphate in this process is not as significant as its indirect role in system productivity, and would need further study focussing on this process to make conclusions beyond speculation.

Another process that would perhaps result in the correlation of phosphate concentrations with CH_4 release from a system is bacterial demethylation of methyl-phosphonate, as observed by Yao, Henny and Maresca (2016) in Lake Matano. If bacterial activity using this process increased, more CH_4 efflux could be observed while phosphate concentrations increased as a product of the process of demethylation, rather than as a driver of the process. Again, more study focussed on this topic would be required to determine whether this process was occurring in the reservoirs investigated, and if so the contribution this process makes towards the correlation trend observed.

The absence of statistical significance in trends between dissolved nitrogen and increasing CH_4 flux may be the result of reservoir hyper-eutrophication. The expected correlation with increased nitrogen concentrations is increased CH_4 efflux and increased CO_2 influx (Yan et al., 2019; Bogard et al., 2014; Huttunen et al., 2003). Nitrogen drives phytoplankton growth which can lead to algal blooms and increased rates of CO_2 influx as carbon is assimilated into biomass. This not only provides increased organic matter concentrations available in the sediment for CH_4 production, but also increases the anoxia area in the water column, as greater concentrations of oxygen are required for respiration of the large organic matter input that occurs with algal blooms (Barica et al., 1980). As methanogenesis requires anoxia, a greater portion of the upper sediment and water column can be inhabited by methanogens, resulting in increased rates of CH_4 production and efflux as an indirect product of nitrogen concentration increase. It is likely that due to the hyper-eutrophication observed in these reservoirs (Section 4.1 table 4.3.1), phytoplankton growth is not limited by nitrogen concentrations but rather by phosphorous (following the Redfield ratio; phosphorous limiting algal growth at the lowest concentrations (They et al., 2017)), thus explaining the lack of statistical significance between N or DOC on CH_4 and CO_2 efflux, but the statistical significance of phosphorous concentrations. In addition, the statistically significant correlations of dissolved silicates with CH_4 efflux and CO_2 influx (Figure 2.3.5), strengthen the suggestion that overall fluxes are a product of phytoplankton productivity pathways, as dissolved silicates are a proxy for phytoplankton abundance (Admiraal et al., 1990).

Decreased CO_2 effluxes correlated significantly with higher pH levels from reservoirs throughout the investigation. This relationship between pH and dissolved CO_2 concentration is expected, as high concentrations of dissolved CO_2 form the weak acid carbonic acid, suppressing the pH of the system. As such, pH in a system is an indicator of the biological activity occurring in it, higher pH often being a result of photosynthetic CO_2 depletion, and lower pH of increased CO_2 production through respiration (Talling, 2010). As high pH correlated with increased CO_2 influx in this investigation, it is further evidence to suggest that productivity is driving CO_2 dynamics in the reservoirs investigated. In addition, the very high pHs recorded in some reservoirs are likely to be due to the combined effect of increased productivity driving CO_2 depletion and evaporative concentration of bicarbonate in the reservoirs (Talling, 2010). As the atmospheric temperatures throughout the summer of 2018 were very high (joint hottest on record for the UK (Met Office, 2018)), the large depletions in reservoir water level (for example observed at Hanningfield reservoir figure 4.3.3) were likely to be due in part to evaporation (in addition to water draw off), thus the concentration of basic bicarbonate increased and high pHs were observed.

The relationship between eutrophication and increased CH_4 efflux indicates a shared interest between carbon budget policy makers and water companies. Reducing eutrophication will improve water quality and reduce processing costs for water companies, while reducing the regions GHG effluxes. Together the economic and environmental benefits provide a shared impetus to reduce freshwater reservoir eutrophication.

Physical Drivers

The large rates of CH_4 efflux observed in the results are likely to have been due to the combined effect of increased biogenic CH_4 production (discussed in the last section) and increased release of CH_4 from its site of production, driven by physical conditions. Most significantly, the unusually hot summer that took place during sampling is likely to have driven the high rates of CH_4 efflux observed by increasing methanogenic activity and water level drawdowns (as mentioned previously). These, in turn, stimulate ebullition release events (Harrison et al., 2017), as well as increasing the rates of dissolved GHG flux physically through the Henry's law coefficient (Nicholson et al., 1984) and Fickian transport, increasing molecule entropy and resulting GHG piston velocities. In addition, the shallow average depths of the reservoirs investigated in this study (Table 2.1), suggest that these reservoirs are likely to be high sources of CH_4 regardless of the effects of water-level drawdown. The average contact time between CH_4 ebullition and methanotrophs is minimal (Del Sontro et al., 2016; Davidson et al., 2018), and the sediments are on average more sensitive to changes in temperature than deeper reservoirs (Bergstroem et al., 2010). As temperature extreme events are likely to increase in frequency as a result of climate change, and reservoir water-level drawdowns like those seen at Hanningfield are similarly observed across the temperate region (Section 4.3 figure 4.3.4), evidence from this study suggests that increased reservoir CO_2 and CH_4 effluxes can be expected, in turn contributing further towards climate change in an accumulating feedback loop. This highlights the need for continued inter-annual study into reservoirs to track their changes in CO_2 and CH_4 flux dynamics.

2.4.3 Issues and Further Research

Most significantly, results from this study emphasise the need for inter-seasonal and inter-annual sampling efforts in order to fully understand reservoir CO_2 and CH_4 flux dynamics and drivers. For example, this investigation only represents 3 hours either side of midday, and does not take diel fluxes into account, which in other lakes are observed to vary between night and day (Cole et al., 2010). Temporal considerations are important if these kinds of investigation are to be used in accurate carbon budgeting. Similarly, between and within reservoir variation indicates the importance of increasing the sample size in future investigations to prevent reservoir sampling, and the resulting conclusions, from being unrepresentative.

Secondly, results show the dynamic nature of habitat area and the need for investigations to record entire reservoir footprints, rather than just assuming that one measured habitat is representative of the entire water body. As mentioned previously, bathymetry mapping and frequent depth measurement would allow the accurate determination of littoral and limnetic habitats in reservoirs, and improve the accuracy of carbon flux modelling. Likewise, all the pathways of CH_4 flux should ideally be investigated, as this study neglected CH_4 transport through emergent macrophytes (one of the largest sources of CH_4 flux across reservoir habitats on a m^{-2} basis (Larmola et al., 2004)).

Thirdly, although the physicochemical drivers of carbon flux were investigated, the biological drivers of carbon flux (which physicochemical factors influence) were not directly investigated. In order to determine whether the physicochemical conditions that correlated significantly with CH_4 and CO_2 flux dynamics in this study were driving the fluxes beyond speculation, further research is required in a controlled setting, isolating the CH_4 and CO_2 responses to potential drivers.

Other pathways/sources of CH_4 and CO_2 that were not investigated in this project, include the age of CH_4 (was it new or old CH_4 being released (Garnett et al., 2013)), geological venting (Etiope, 2009) and invertebrate transfer of CH_4 from sediments (for instance *Chaorborous* spp., which consumes sediment CH_4 as a vertical motility strategy, releasing it at the surface (Carey et al., 2018)). For an in-depth

understanding of all the possible sources and pathways of CH_4 influencing efflux dynamics in these systems, these factors should be addressed in future investigations.

2.4.4 Conclusion

In summary, drinking water reservoirs in the south east of England display some of the largest freshwater reservoir CH_4 effluxes recorded, acting as a net source of CH_4 and CO_2. Spatial heterogeneity in flux dynamics was observed between reservoirs (confirming hypothesis 2) and within reservoirs; however, the habitat responsible for the greater rate of CH_4 and CO_2 efflux per m^{-2} within a reservoir was not consistent between reservoirs, thus hypothesis one can only be accepted for Alton reservoir. The study highlights the significant role of extreme weather events in driving increased reservoir CH_4 efflux, by changing reservoir morphology, and acknowledges the significant influence of reservoir habitat upon CH_4 and CO_2 dynamics. Investigations must measure all the pathways of GHG flux and cover more water bodies if carbon budgets are to be accurately determined.

Physicochemical results highlight the significance of phosphorous concentrations, correlating with increased CH_4 efflux and increased CO_2 influx, as a result of photoautotrophic growth/reservoir productivity. However, these results more importantly highlight the combined effects of many individual conditions influencing CO_2 and CH_4 dynamics where individually their trends may lack statistical significance, emphasising that CO_2 and CH_4 flux is the end product of many interactions. Though correlation results support hypothesis 3 in principle, further research is required to quantitatively determine the role of physicochemical conditions as drivers of flux in these systems. The findings point towards a shared interest between water companies and climate biologists in improving reservoir water quality, as eutrophication driving poor water quality similarly drives increased CH_4 efflux.

3.0 Ex-situ Microcosm Treatment Investigation

3.1 Introduction

Freshwaters are important areas of biogeochemical research in light of their potent contributions of GHGs to the atmosphere. As such they have the potential to influence continental carbon sinks and significantly affect atmospheric energy balances. In order to understand freshwater GHG contributions properly, the physical and chemical composition of a water body must be understood in the context of biogenic CH_4 and CO_2 production. With this knowledge their response to changing physical conditions or chemical pollution could be predicted in the context of GHG emissions.

Section 2 illustrated the difficulty in directly attributing changes in reservoir physicochemical characteristics to individual drivers of biogenic CH_4 or CO_2 production, due to the complexity of microbial communities and the convoluted pathways of gaseous flux. The investigations did, however, find significance in correlations between increased CO_2 influx and increased phosphate concentration, as well as trends towards significance in dissolved organic carbon (DOC) increase and increased CO_2 influx. It is expected that in phosphorous and DOC limited systems, the rate of phytoplankton growth will increase when the concentration of bioavailable phosphorus or DOC in the system is increased (Sterner et al., 1997). As a result, the net rate of CO_2 influx would be expected to increase as carbon is assimilated into phytoplankton biomass. As phytoplankton growth is more significantly limited by phosphorous availability than DOC availability (based on the Redfield ratio (Ptacnik et al., 2010)) CO_2 influx is expected to increase more prominently with phosphorous concentration increase.

Additionally, during daylight hours decreased CO_2 effluxes are expected from reservoir water columns, as a result of photosynthetic processes assimilating CO_2 into phytoplankton biomass (Liu et al., 2016). Under dark conditions however, CO_2 assimilation as a result of photosynthesis is expected to stop, respiration replacing it as the dominant process in phytoplankton communities. As a result, reservoirs and lakes are expected to be greater sources of CO_2 efflux during the night than during the day (Eugster et al., 2003). As night time constitutes a significant portion of the diel cycle, a reservoir's diel CO_2 budget is expected to be greatly influenced by this time. Despite this, many studies do not include diel variation of CO_2 into lake and reservoir diel CO_2 budgets, and risk underestimating their average contributions of CO_2 to the atmosphere (Raymond et al., 2013). Similarly, section 2 did not investigate CO_2 dynamics from reservoirs in dark conditions, due to difficulties in night time sampling.

By removing samples of a reservoir's water column to investigate on a laboratory scale, the effects of individual chemicals (such as phosphorous and DOC) or physical conditions (such as the intensity of light), as drivers of CO_2 production or assimilation in a system, can be determined. In turn, this can form a proxy for estimating the effects of nutrient change or physical change in that system on its CO_2 flux dynamics. This information is useful for carbon budgeters who are attempting to accurately incorporate reservoirs into their regional estimates, and to policy makers who are justifying reservoir water quality management by including the role of reservoirs in the perspective of climate change.

Furthermore, section 2 found significance in correlations between increased CH_4 effluxes and increased phosphate concentration, as well as trends towards significance with increased DOC and increased CH_4 efflux. These observed trends agree with the paradigm that biogenic reservoir CH_4 fluxes are mediated by the productivity of a system (Peeters et al., 2019). Increased system productivity is acknowledged to drive CH_4 production in sediments indirectly through increased sediment organic matter deposition (and resulting sediment methanogenic activity) observed in

lab and system scale investigations (Fuchs et al., 2016; Duc et al., 2010). However, the recent suggestion of water column CH_4 production (Donis et al., 2017), has stimulated fierce debate over claims of water column CH_4 production, its very existence, and its contribution to a lake's overall CH_4 budget. In the case that near surface water column CH_4 production occurs and, if so, is mediated directly by a water column's phytoplankton community (for example behaving as hosts for methanogens or as symbiotic sources of substrate for methanogenesis (Grossart et al., 2011)) rather than indirectly fuelling sediment CH_4 production, rates of CH_4 production and efflux would be expected to be influenced by the drivers of phytoplankton growth. For example, if phytoplankton form a symbiotic relationship with methanogenic archaea, or are a direct source of CH_4 through an unknown metabolic process, the physical effects of light and dark conditions, and the chemical effects of phosphorous and nitrate concentrations, would be expected to affect water column CH_4 production and final emission rates (in addition to their effects on phytoplankton mediated CO_2 dynamics). Likewise, in the case that acetoclastic methanogens are harboured in micro-anoxic zones on phytoplankton cell walls, the addition of acetate (or other forms of DOC that subsequently provide substrates for methanogenesis) would be expected to elicit increases in water column CH_4 production and efflux rates, considering the very low concentrations of acetate in freshwater systems relative to other methanogenically viable systems (Borrel et al., 2011).

This study aims to quantify the effect of light conditions on water column CO_2 flux dynamics in freshwater reservoirs of the south east of England, and the implications of not including dark conditions in their daily CO_2 budgets. It aims to understand the effects of increasing water column phosphorous and DOC concentrations on CO_2 flux dynamics in reservoirs of the south east of England. It also aims to determine the dominance of sediment CH_4 production in freshwater reservoirs in the south of England by measuring any CH_4 production that can be detected or stimulated in the near surface water column, using physicochemical treatments.

By testing the hypotheses:

1. Increasing the concentration of DOC and phosphate in reservoir water column samples will increase the rate of CO_2 influx under light conditions, while increasing the rate of CO_2 efflux under dark conditions.

2. Increasing the concentration of phosphate in water samples will drive more significant increases in CO_2 influx rate than increases in DOC concentration, under light conditions.

3. Applying dark conditions to water column samples will result in increased rates of CO_2 efflux relative to fluxes when light conditions are applied.

4. DOC, phosphorous and light treatments will have no effect upon the rate of CH_4 efflux in samples taken from reservoir water columns.

4.2 Methods

3.2.1 Reservoir Sampling

Samples were collected from three drinking water reservoirs (0.49 to 4.03 km^2) in the south east of England: Hanningfield reservoir, Alton water Reservoir and Ardleigh reservoir. Detailed information on these sites is available in section 2.1, as the reservoirs were chosen to correspond with the investigation of section 2. Reservoirs were sampled in the summer period (May to September) of 2018. For each treatment investigated three samples were collected - one from each reservoir. Samples were taken from the water surface, where littoral habitats were 1m in depth, at each lake. Water samples were collected using a 20-litre carboy, which was rinsed with water from the site prior to taking 10 litres of sample water (section 4.4, Figure 4.4.1 (a.)). The water samples were taken at the same time as *in-situ* greenhouse gas flux and water chemistry sampling described in section 2.2. Care was taken to leave headspace in the carboy, allowing gas transfer with the water thus maintaining the sample's integrity for the ensuing experiment. Once in the lab, samples were immediately divided into four autoclaved 5-litre glass conical flasks with foam bungs, 2.5 litres of sample in each flask, and placed into a 16^{O}C walk in lab to incubate (Section 4.4, Figure 4.4.1 (b.)). These flasks formed the microcosms.

3.2.2 Treatments

Two types of treatment were investigated in this experiment: physical and chemical treatments. Three chemical treatments were investigated separately: two forms of dissolved organic carbon (DOC) and one form of phosphorous. The first DOC treatment was cellobiose ($C_{12}H_{22}O_{11}$), derived from cellulose, lichenan and laminaran. Cellobiose is a less rapidly metabolised form of DOC than glucose (Ng and Zeikus, 1982), so was chosen for its longevity in order to last the duration of the experiment. The second DOC treatment was acetate in the form of sodium acetate ($C_2H_3NaO_2$). Being the precursor to acetoclastic methanogenesis, it was chosen to directly supply

methanogenic CH_4 mineralisation without requiring bacterial acetogenesis to digest DOC beforehand (Drake et al., 2008), as could be required in the cellobiose treatment. The third treatment was phosphorous in the form of disodium phosphate (Na_2HPO_4), a standard for phosphate treatment investigations (for example Schindler et al. (1971)).

After trial investigations (Section 4.2), 300 mg of $C_{12}H_{22}O_{11}$ (120 mg L^{-1}) was determined as the cellobiose treatment for microcosms, added directly to flasks in powdered form and swirled for 1 minute. This concentration was within the bounds of DOC observed in global lakes by Sobek et al. (2007). For acetate treatments, 300 mg of $C_2H_3NaO_2$ (120 mg L^{-1}) was added to each treatment microcosm directly in powdered form and swirled for 1 minute. This concentration was used to match that of cellobiose treatments, a high concentration in order to ensure that potential methanogen growth would not be acetate limited. For phosphate treatments, 200µg L^{-1} of Na_2HPO_4 was added to each treatment microcosm and swirled for 1 minute. This treatment matched the full lake additions of Schindler et al. (1971), and was above the 100 µg L^{-1} concentration proposed by Filstrup and Downing (2017) as a critical threshold concentration for increasing chlorophyll a. The starting concentration of DOC and phosphate in microcosms was measured as a part of the reservoir water chemistry sampling in section 2, as the samples were both taken in the 20L carboy mentioned previously (the mean water chemistry values of which can be observed in Section 4.3 table 4.3.1). 500ml water samples were collected from microcosms at the end of the investigation to determine the final concentrations of DOC and phosphate to compare nutrient uptake; unfortunately due to a refrigeration malfunction in the lab these samples were lost before analysis could commence.

Two light treatments were applied: light and dark. Light conditions were maintained at daylight conditions (~10000 lux) artificially using fluorescent tube lamps 10cm above the 5L flasks. Dark conditions were applied using aluminium foil jackets, completely excluding light for the duration of the treatment. In addition to investigating the effects of light treatments and their joint effect with chemical treatments on carbon fluxes, light treatments acted as a proxy to check the experimental set-up against known CO_2 and predicted CH_4 interactions.

3.2.3 Flask Analysis

Samples remained at 16^{o}C for 20 hours before sampling ensued. Circadian lighting matching that of the environment was maintained during this incubation period. Incubation at 16^{o}C removed the effect of temperature as a confounding variable, which is known to be a primary physical driver of gas concentration gradients, or piston velocities, resulting in increased rates of flux across the water/ atmosphere interface. 16^{o}C was chosen to be representative of the average atmospheric summer temperature in England from 2015 to 2017 (Statista, 2018). The rates of CH_4 and CO_2 fluxes were calculated by measuring their concentration in the head space of the conical flasks over the period of 1 hour. Concentration measurements were made using a Picarro Gas Scouter G4301 cavity ring down spectroscope (CRDS). CRDS inlet and outlet ports were connected to the headspace of each flask in a closed loop, using gas-tight tubing through a silicone bung, precautionarily wrapped in parafilm at the neck of the flask. The outlet tube continued down into the sample ending with a diffuser, bubbling the headspace through the sample to increase the speed of gaseous equilibrium and maintain oxic-conditions (Methods developed in section 4.2).

Sampling Regime

Three chemical treatment experiments were investigated, for cellobiose, DOC and phosphate. These experiments are considered separately, the sampling regime being repeated for each distinct experiment.

In each experiment a total of 6 microcosms received chemical treatment (n=6), and a total of 6 microcosms received no chemical treatment, behaving as control treatments (n=6). 2 chemical treatment microcosms were paired with 2 control treatment microcosms in each experimental block. These microcosm water samples were taken from the same reservoirs at the same time, and were investigated in the lab at the same time. As three reservoirs were sampled, and 2 samples were taken from each reservoir for each type of treatment (2 chemical treatment microcosms and 2 control treatment microcosms), a total of n=6 samples were investigated for each treatment. This block experiment considered the sample set as reservoirs from the south east of England, rather than individual reservoirs.

Figure 1 illustrates the workflow for measuring CO_2 and CH_4 flux dynamics from each microcosm. Fluxes were measured at the beginning (1 hour after treatment addition) and at the end (24 hours after addition) of each run. Firstly, a chemical treatment was added to the 'treated' microcosm (for example, cellobiose in the cellobiose experiment) (illustrated as "t." in figure 3.2.1) and allowed to incubate for 1 hour in light conditions (illustrated as "1.t." in figure 3.2.1). In parallel, whilst the treatment microcosm incubated, the gas analyser set-up (described in section 4.2.2) was applied to the control microcosm headspace, and CO_2 / CH_4 free gas concentrations were measured for a period of 1 hour under light conditions (illustrated in figure 3.2.1 as "1.c."). After a period of 1 hour, the gas analyser set-up was removed from the control treatment microcosm, rinsed with deionised water to prevent contamination between microcosms, and transferred to the chemically treated microcosm. Here the headspace CO_2 and CH_4 concentrations were measured for a period of 1 hour under light conditions (illustrated as "2.t." in figure 3.2.1). In parallel, dark conditions were applied to the control microcosm for 1 hour, in the form of an aluminium foil jacket (illustrated in figure 3.2.1 as "2.c."). After this hour, the gas

analyser set-up was removed from the chemically treated microcosm, rinsed in deionised water, and placed into the dark control microcosm. Here the control microcosm headspace CO_2 and CH_4 concentrations were measured under dark conditions for 1 hour (illustrated as “3.c.” in figure 3.2.1). In parallel, dark conditions were applied to the chemically treated microcosm for 1 hour, by applying an aluminium foil jacket (illustrated as “3.t.” in figure 3.2.1). After 1 hour had elapsed, the gas analyser was removed from the dark control microcosm, rinsed in deionised water, and applied to the dark chemically treated microcosm for 1 hour of headspace gas analyses (illustrated as “4.t.” in figure 3.2.1). In parallel the foil jacket was removed from the control treatment microcosm, which was then in light conditions again (illustrated as “4.c” in figure 3.2.1). After 1 hour had elapsed, the gas analyser equipment was removed from the dark chemically treated microcosm, and the foil jacket removed to expose the microcosm to light conditions (illustrated as “5.t” in figure 3.2.1). From this point, both the control and chemically treated microcosms were left to the regular diel cycle for 20 hours (illustrated as “5.c.” and “5.t.” in figure 3.2.1). After 20 hours of incubation, the cycle of headspace measurement described above was repeated once more (illustrated as the yellow arrows in figure 3.2.1) to measure the “end of time period” gas measurements. This measurement process was repeated for the second control and chemical treatment microcosm pair of each block, beginning at the start of the 20 hour incubation time of the first pair of microcosms (“5.c.” and “5.t.” figure 3.2.1).

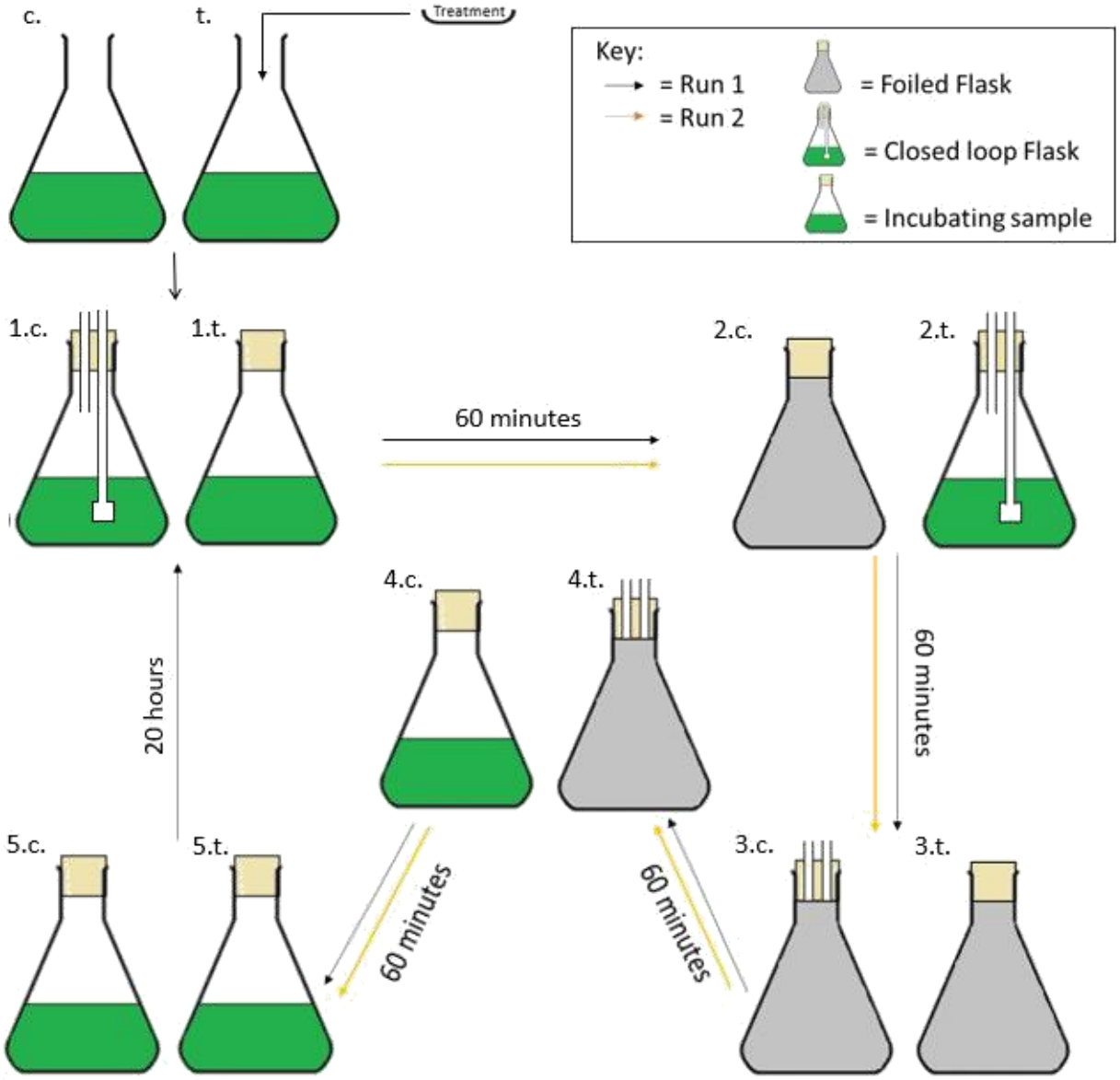

Figure 3.2.1 Workflow for measuring CO_2 and CH_4 flux dynamics from each microcosm treatment pair. Firstly, a chemical treatment was added to the 'treated' microcosm "t." and allowed to incubate for 1 hour in light conditions "1.t.". In parallel, whilst the treatment microcosm incubated, the gas analyser was applied to the control microcosm headspace, and CO_2 / CH_4 free gas concentrations measured for a period of 1 hour under light conditions "1.c.". After a period of 1 hour, the gas analyser set-up was removed from the control treatment microcosm, rinsed with deionised water to prevent contamination between microcosms, and transferred to the chemically treated microcosm. Here the headspace CO_2 and CH_4 concentrations were measured for a period of 1 hour under light conditions "2.t.". In parallel, dark conditions were applied to the control microcosm for 1 hour, in the form of an aluminium foil jacket "2.c.". After this hour, the gas analyser set-up was removed from the chemically treated microcosm, rinsed in deionised water, and placed into the dark control microcosm. Here the control microcosm headspace CO_2 and CH_4 concentrations were measured under dark conditions for 1 hour "3.c.". In parallel, dark conditions were applied to the chemically treated microcosm for 1 hour, by applying an aluminium foil jacket "3.t.". After 1 hour had elapsed, the gas analyser was removed from the dark control microcosm, rinsed in deionised water, and applied to the dark chemically treated microcosm for 1 hour of headspace gas analyses "4.t.". In parallel, the foil jacket was removed from the control treatment microcosm, which was then in light conditions again "4.c". After 1 hour had elapsed, the gas analyser equipment was removed from the dark chemically treated microcosm, and the foil jacket removed to expose the microcosm to light conditions "5.t". From this point, both the control and chemically treated microcosms were left to the regular diel cycle for 20 hours "5.c." and "5.t". After 20 hours of incubation, the cycle of headspace measurement described above was repeated once more (illustrated as the yellow arrows), measuring the "end of time period" gas measurement.

Rate Extraction

To quantify the rate of gas flux, the concentration of each gas was plotted against time in minutes. The first 45 minutes were ignored (justified in section 4.2.2), and from the last 15 minutes of the hour, a linear model / line of best fit was plotted through the data points. From this slope, gradients were calculated (results of which are illustrated in section 4.5 figures 4.4.1.1 to 4.4.3.6). Values were corrected against negative controls (section 4.2.2) and converted from ppm $minute^{-1}$ to mmol day^{-1} in accordance with units used by the *in-situ* reservoir flux investigations (section 2), as well as helping to distinguish rate variance.

Statistical Analysis

For each chemical treatment, CH_4 and CO_2 fluxes from the microcosms were investigated individually. In addition, the relationship between the control and treated microcosms was investigated as a ratio of treated fluxes to control fluxes. General linear models were applied, modelling the rate of either CH_4 or CO_2 as a product of the variables: chemical treatment applied, light treatment and hours after the addition of the treatment. Next the results of these models were summarised and submitted to an analysis of variance test (ANOVA). All statistical analyses were performed using R version 3.4.2 for windows 10 (R Core Team, 2017).

3.3 Results

3.3.1 Control Microcosms

Control microcosms (receiving no chemical treatments) displayed opposite trends in CO_2 and CH_4 flux dynamics in light and dark conditions, however the direction of flux was specific to the gas and time into the experiment. For example, figure 3.3.1 (a.) illustrates that at the beginning of the experiment (1 hour in) mean CO_2 fluxes are negative during light conditions (-683.27 mmol day^{-1}) but positive during dark conditions (175.05 mmol day^{-1}). In contrast figure 3.3.1 (b.) illustrates that at the beginning of the experiment mean CH_4 fluxes increase under light conditions (0.139 mmol day^{-1}) but decrease under dark conditions (-0.0437 mmol day^{-1}). Standard error bars suggest that variation around the mean for these trends are low, supported by investigation using a one-way ANOVA which found statistical significance in CO_2 trends for controls investigated during the acetate and phosphate experiments, but no statistical significance for controls investigated during the cellobiose experiment. However, when investigating these trends in CH_4, only marginal trends towards statistical significance were observed in controls microcosms, across all experiments ($p>0.05$). These results illustrate larger variation in CO_2 flux patterns than CH_4 across controls at the beginning of the experiment. In contrast, at the end of the experiment (after 24 hours), mean trends in both CO_2 and CH_4 appear to be reversed relative to their trends after 1 hour. For example, figure 3.3.1 illustrates increased CO_2 efflux during light conditions (1290.67 mmol day^{-1}) relative to dark influx (-762.83 mmol day^{-1}), and increased CH_4 effluxes during dark conditions (0.0489 mmol day^{-1}) relative to light (-0.120 mmol day^{-1}). Figure 3.3.1 also illustrates the large spread of data around the mean at the end of the experiment, as standard error bars overlap. There is, therefore, no statistically significant difference between light or dark conditions for either gas at the end of the experiment (confirmed by the results of one-way ANOVAs finding $p>0.05$).

In addition, variation of CH_4 efflux in control microcosms occurred between the different treatments. For example, figure 3.3.2 illustrates variation of between +0.15 mmol day^{-1} in control microcosms

measured during phosphate treatment experiments in light conditions, and -0.5 mmol day^{-1} in control microcosms measured during cellobiose treatment experiments in light conditions.

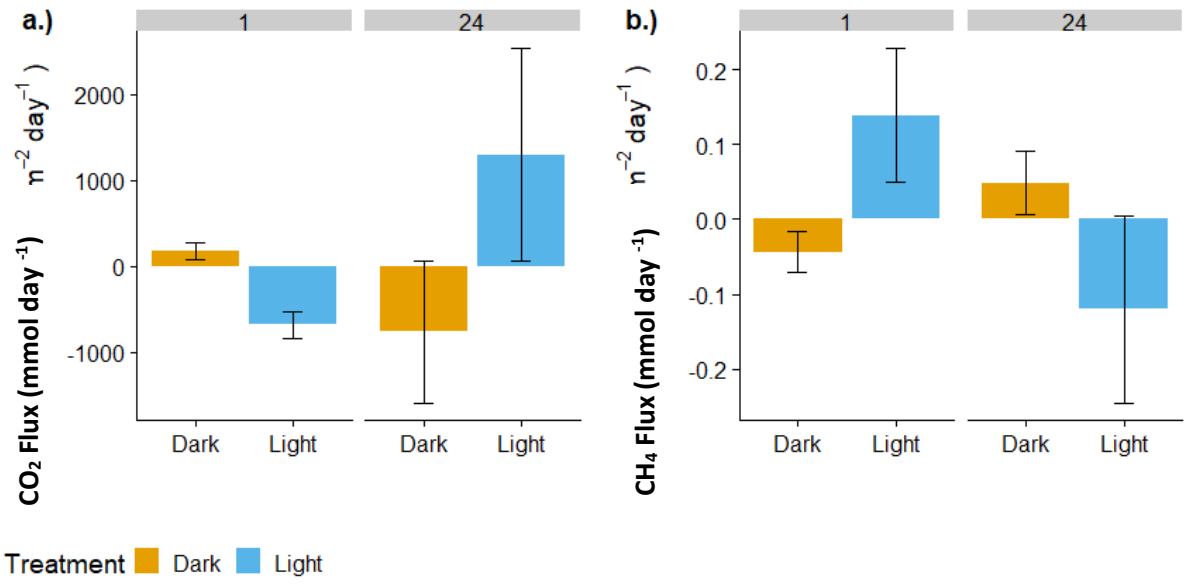

Figure 3.3.1 Illustration of CO_2 and CH_4 gaseous flux from control microcosm flasks at the beginning (1 hour into the experiment, shown as "1" on the top axis) and the end (24 hours into the experiment, shown as "24" on the top axis) of the experiment. Samples taken from Alton, Ardleigh and Hanningfield reservoirs in the south east of England. Control microcosms of each individual chemical treatment experiment (n=6) considered together, for a total of n=18, for each light and dark treatment.

3.3.2 Phosphate Treatment

Phosphate treated microcosms displayed trends of increased mean effluxes of CH_4 relative to control microcosms in light conditions, 1 and 24 hours into the experiment (ratio of treated to control being positive in figure 3.3.3). For example, figure 3.3.2 illustrates increases in efflux from -0.0399 to 0.334 mmol day $^{-1}$ after 1 hour, and increases from 0.124 to 0.259 mmol day $^{-1}$ after 24 hours. Also evident, however, is the wide spread of variation between samples in the standard error bars, with 24 hour bars overlapping. Results of statistical analyses using a GLM displayed no statistically significant difference between treated and control microcosm CH_4 fluxes ($p>0.05$).

In contrast, under dark conditions phosphate treated microcosms displayed trends of increased mean influxes of CH_4 relative to control microcosms 1 hour into the experiment, while displaying increased efflux relative to control microcosms 24 hours into the experiment. For example, figure 3.3.2 illustrates these trends as 0.0319 to -0.132 mmol day $^{-1}$ after 1 hour, and 0.099 to 0.207 mmol day $^{-1}$ after 24 hours. Similarly, larger variations in standard error were observed, again resulting in statistically insignificant differences between treated and control microcosms when using a GLM ($p>0.05$).

The results of phosphate treatment had no effect upon trends in CO_2 flux during light or dark conditions, across either 1 or 24 hours. For example, figure 3.3.2 illustrates increases in mean efflux of -46.25 to 147.95 mmol day $^{-1}$ in the dark after 1 hour and decreases of 181.15 to 124.98 mmol day $^{-1}$ after 24 hours, while potentially increasing influx of CO_2 with phosphate addition during the dark 1 hour after addition (-910.78 to -1074.14 mmol day $^{-1}$) being nullified by the large spread of data about the mean (standard error bars overlapping between control and treatment). Analyses with GLMs supported these results by finding no statistical significance between control and treatment microcosm across any time or light variable ($p>0.05$).

3.3.3 Cellobiose Treatment

Cellobiose treated microcosms demonstrated trends of mean decreases in CH_4 efflux 24 hours into the experiments but no difference 1 hour into the experiment, relative to control microcosms under dark conditions (figure 3.3.3 ratios). For example, figure 3.3.2 illustrates the 24 hour mean decrease in efflux of 0.0838 to 0.0336 mmol day $^{-1}$, but also illustrates the overlapping of standard error bars. Upon analyses using a GLM, cellobiose treatment was observed to have no statistically significant difference compared with controls ($p>0.05$).

In contrast, under light conditions trends in mean CH_4 efflux decreased after 1 hour, whilst after 24 hours a net influx of CH_4 in control microcosms changed to a net zero flux with cellobiose addition. For example, figure 3.3.2 illustrates this pattern with changes from 0.0761 to 0.0188 mmol day $^{-1}$ after 1 hour, and -0.481 to 0.003 mmol day $^{-1}$ after 24 hours, error bars overlapping for hour 1 but not hour 24. Upon statistical analysis with a GLM, trends in treatment, light condition and time into experiment were again found to be insignificant ($p>0.05$).

No effect of cellobiose treatment upon CO_2 was observed under dark conditions for either sampling time, however in light conditions after 24 hours net control efflux in CO_2 changed to a net influx. For example, figure 3.3.2 illustrates this through a change in mean flux of 4874.06 to -2579.48 mmol day $^{-1}$. Upon statistical analyses with a GLM no significant difference was found across any treatment ($p>0.05$).

3.3.4 Acetate Treatment

Acetate treatment had little effect upon CH_4 efflux under dark conditions after 1 hour, but displayed a reduced rate of influx after 24 hours relative to control treatments. Figure 3.3.2 illustrates the mean decrease in influx from 0.0365 to 0.0043 mmol day $^{-1}$ after 24 hours. This decrease was found to be statistically insignificant upon investigation with GLMs, ($p>0.05$). Under light conditions acetate treatment changed mean microcosm effluxes to influxes after 1 hour, whilst having minimal effect after 24 hours. Figure 3.3.2 illustrates mean changes of 0.381 to -0.0971 mmol day $^{-1}$ in light conditions after 1 hour, but also the large standard error for both control and treated results. Statistical analyses with a GLM displayed no statistical significance in these mean differences ($p>0.05$).

Acetate treatment appeared to have no effect upon CO_2 fluxes across either light or time treatments, relative to the control. However marginal mean reductions in the rate of influx 1 hour into the experiment under light conditions and mean reduction in efflux 1 hour into the experiment under dark conditions can be perceived (figure 3.3.2). The overlapping error bars and lack of statistical significance after testing with a GLM again find these mean flux patterns to be insignificant.

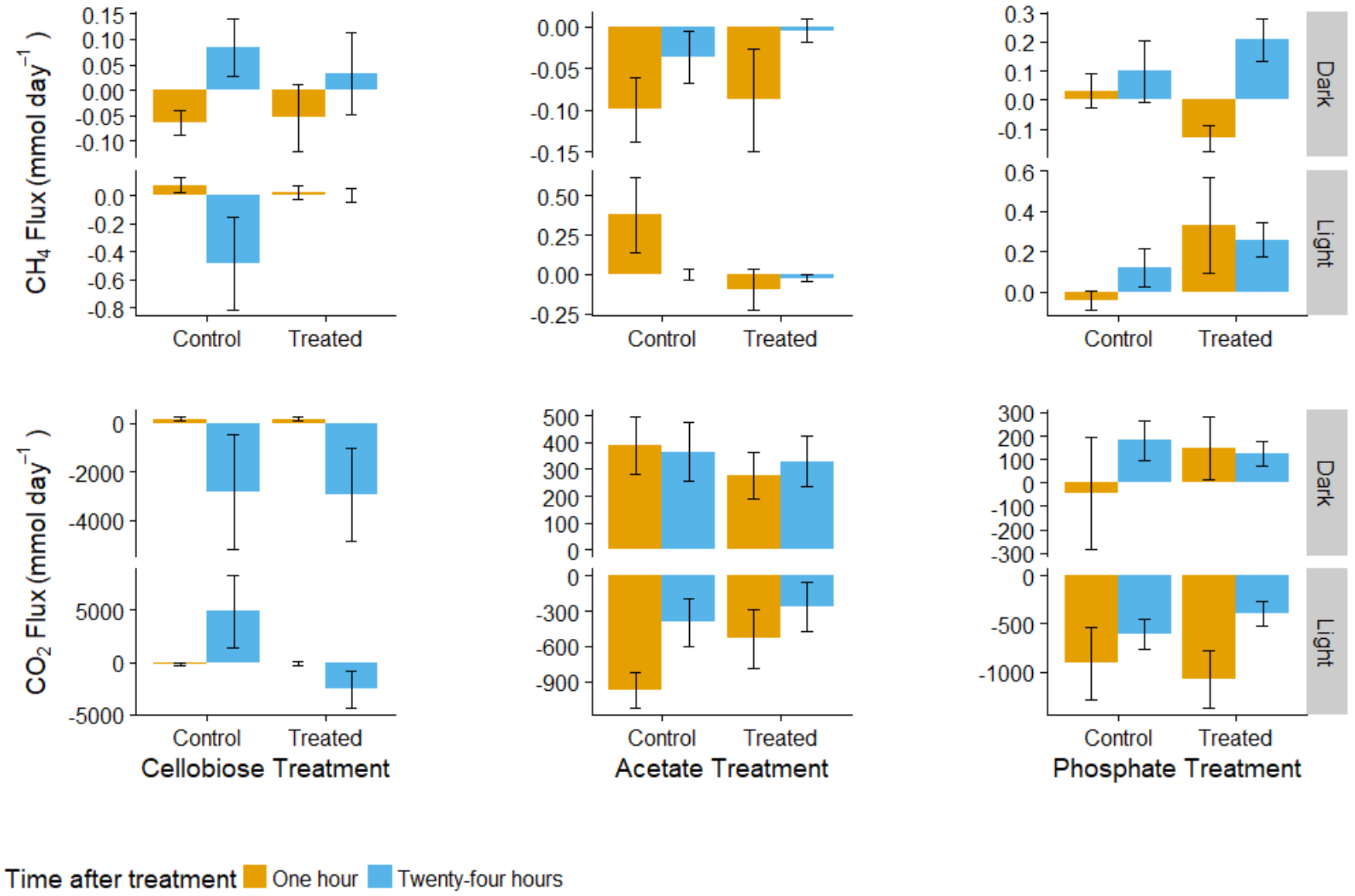

Figure 3.3.2 Bar plots displaying the mean rate of CO_2 and CH_4 flux (mmol day^{-1}) for cellobiose, acetate and phosphate treatment experiments. Water samples were taken from water columns in the
tion

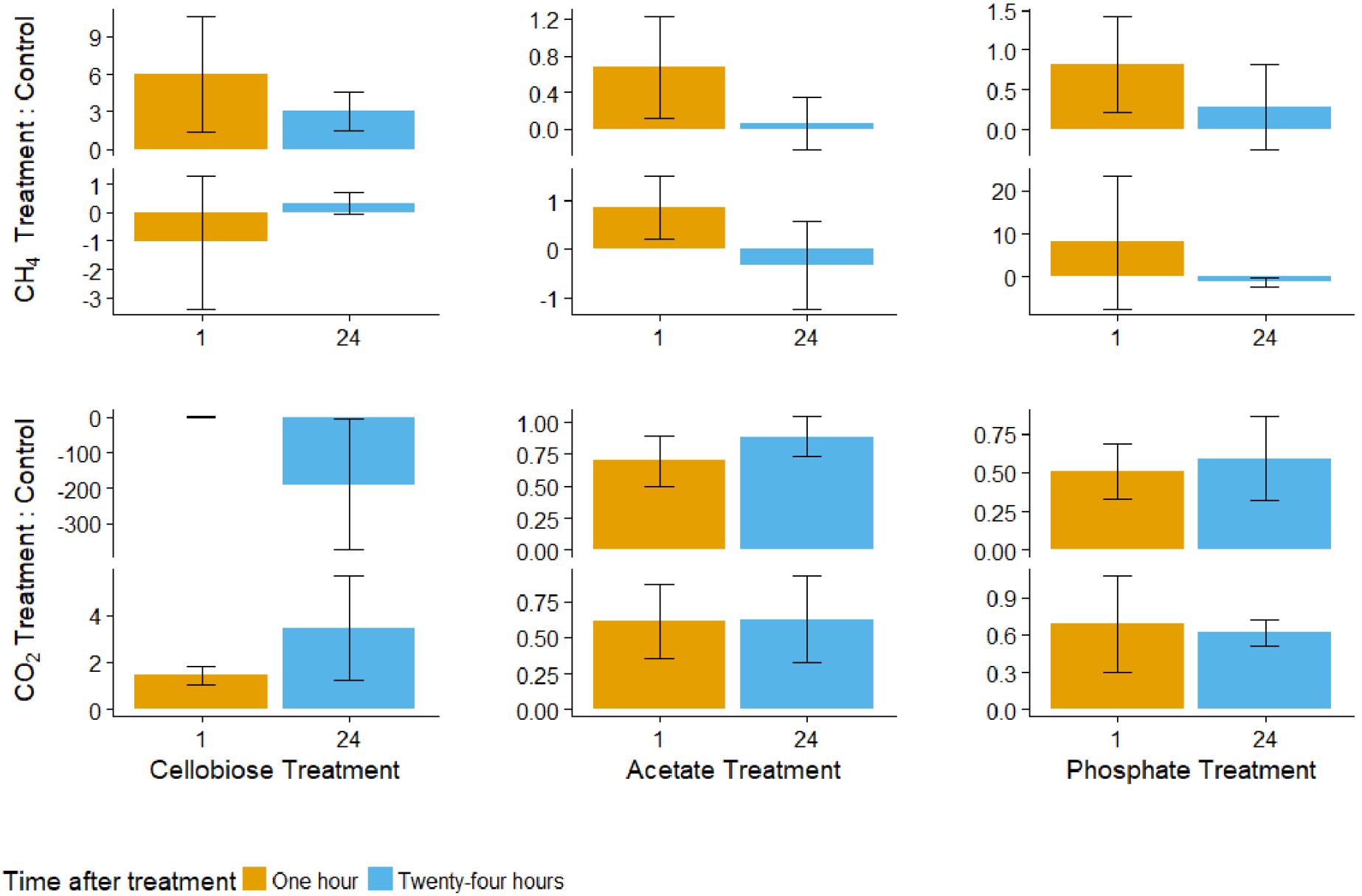

Figure 3.3.3 Bar plots displaying the mean log respective ratios of treatment to control samples for the rate of CH_4 and CO_2 flux (mmol day^{-1}) . cellobiose, acetate and phosphate treatment experiments are displayed. Water samples taken throughout the summer of 2018, from the water column of 3 drinking water reservoirs in the south east of England. Measurements taken one hour and 24 hours after treatment. Error bars represent standard error n=6.

3.4 Discussion

3.4.1 Control Microcosm Responses: CH_4 and CO_2 Flux Dynamics

Throughout the experiments microcosms were shown to release CH_4 from the water phase into the headspace, after equilibrium between free CH_4 gas in the headspace and dissolved CH_4 in the water column had been reached (equilibration method explained in section 4.2.2). As oxic conditions were maintained in the water column of the microcosms (evidenced in section 4.2.2), the finding of any increase in CH_4 concentration was counterintuitive, archaeal methanogenesis being an obligatory anaerobic process (Borrel et al., 2011). As these concentrations of CH_4 efflux were very low and not seen consistently, the increases cannot on their own be directly attributed to biogenic CH_4 production. The CH_4 concentration increase observed could alternatively be the result of the bubbling treatment breaking up flocks of phytoplankton in the microcosm water, resulting in the release of trapped CH_4 into the water column and its subsequent diffusive release into the microcosm headspace. This would also explain the inconsistent CH_4 efflux rates observed in the control microcosm treatments between the different chemical treatment experiments, as the concentrations were the result of random release events rather than consistent production.

Despite this possibility, there are theoretically suggested oxic water column CH_4 production processes that could explain these rates of CH_4 production. For example the symbiotic methanogenic archaea/ cyanobacteria relationships mentioned in section 3.1 (Grossart et al., 2011), bacterial demethylation of methylphosphonates (Yao et al., 2016), direct CH_4 release from cyanobacterial metabolism (Bizic-Ionescu et al., 2018) and oxic release of CH_4 from methanethiol have been suggested to be energetically feasible (Damm et al., 2010). If the marginal CH_4 release observed in these microcosm experiments could be stimulated through chemical dosing, designed to target the potential pathways for CH_4 production in this oxic environment (acetoclastic methanogenesis and phytoplankton productivity) then maybe some evidence of water column CH_4 production in reservoirs could be provided. Based on the

control microcosms alone, however, the evidence supports the paradigm that the dominant source of CH_4 production in freshwater reservoirs is the anoxic sediment and not the oxic water column, supporting the argument of Peeters et al. (2019), not Donis et al. (2017).

The response of control microcosm CO_2 dynamics to light and dark conditions, 1 hour into the experiment, shows that the biological CO_2 production and assimilation rates in reservoirs of the south east of England are significantly affected by the diel light cycle, and will have substantial effects upon the CO_2 flux dynamics of these systems. As expected, dark conditions yielded greater rates of net CO_2 efflux than under light conditions, following increased rates of photosynthetic carbon assimilation into phytoplankton biomass (in the form of CO_2) in the light, and increased rates of respiration processes (releasing CO_2) in the dark. What is significant is the extent of this variation, rates of efflux being up to 3 times greater under dark conditions than under light conditions. As a result, daily CO_2 efflux budgets based upon CO_2 flux data collected only during the daytime (light) conditions risk underestimating reservoirs as a source of CO_2 to the atmosphere. This has substantial connotations for carbon budgeters incorporating reservoir CO_2 fluxes, who must consider this diel variation when calculating daily or annual contributions of CO_2 from reservoir environments, as many investigations used by carbon budgeters base their daily flux rates upon measurements taken in the daytime only.

Light and dark treatments were also used to investigate the functionality of the experimental set-up throughout the period of the study. For example, the CO_2 flux dynamics of control microcosms after 24 hours, did not display the expected light/dark dynamics, whereas experiments after 1 hour did. After 24 hours, the rates of CO_2 flux between light and dark conditions were statistically insignificantly different, but increases in CO_2 influx were expected in light conditions relative to dark. This suggested that the integrity of the samples changed throughout the sampling period. The increase in observed CO_2 effluxes during light conditions, in comparison to the net CO_2 influx in the 1hour portion of the experiment,

suggest a biological community change shifting towards a heterotrophic system as phytoplankton in the samples become no longer viable. However, when analysing the individual treatment experiments, this pattern was only observed for controls of the cellobiose treatment, and not for phosphate or acetate controls which respond to light as expected (figure 3.3.2).This has implications for the functionality of the experimental set-up, validity of the data collected after 24 hours and the conclusions made with this data for the cellobiose treatment only. Time affected the fitness of communities within the microcosm flasks, which were therefore no longer comparable to *in-situ* reservoir biological communities. As a result, CO_2 flux data after 24 hours does not represent reservoir flux data in the cellobiose treatment. These changes in CO_2 flux dynamics as a result of time could be a result of chemical limitation within the cellobiose control treatment samples, as key nutrients such as phosphate and DOC are assimilated into the organisms over time.

3.4.2 Treatment Microcosm Responses

DOC Treatments

Results showed that cellobiose treatments elicited no significant effect upon CH_4 or CO_2 flux. If CH_4 production in the samples had been the result of acetoclastic methanogenesis in microanoxic zones of the sample, the addition of a precursor to acetate (i.e. cellobiose) would be expected to result in increased CH_4 production and resulting CH_4 efflux from the microcosm water phase. As no response was observed, this in itself would suggest that acetoclastic methanogenesis was not responsible for any observed CH_4 release, and that the water column is not a driver of CH_4 production in the reservoirs investigated.

However, there are alternative possibilities that could explain these results. Firstly, cellobiose is not directly bioavailable to acetoclastic methanogens that could theoretically have been active in the

microcosm sample. For example, metabolising the cellobiose into acetate (the prerequisite form of carbon for acetoclactic methanogens) would require acetogenic bacteria. As acetogenesis requires anoxia, the oxic conditions within the microcosm water would not allow for this process, resulting in cellobiose treatments having no observed effect upon CH_4 flux. Secondly, it could suggest that methanogenesis was not driving CH_4 production, but rather another CH_4 releasing process not driven by DOC concentrations, for example demethylation of methylphosphonates. These possibilities were explored through further chemical treatments.

The results of acetate treatment similarly yielded no significant effect upon CH_4 flux. As acetate is the direct prerequisite substrate for acetoclastic methanogenesis, its failure to stimulate CH_4 production in the microcosm conclusively eliminates acetoclastic methanogenesis as a potential source of CH_4 production in these water columns. The results of this investigation concluded that based upon this experimental procedure, DOC addition has no statistically significant effect on water column CH_4 release.

In addition, neither acetate nor cellobiose concentration had any significant impact upon CO_2 flux rates in either light or dark conditions. This suggests that in the reservoirs investigated, respiration and photosynthetic processes are not limited by the concentration of dissolved DOC, which was available in excess at the time of study. As such, organic carbon inputs into reservoirs are not expected to significantly drive the rate of CO_2 efflux as a result of water column processes.

Phosphate Treatment

Phosphate treatments did not show any statistically significant effect on CH_4 flux rates in microcosms. However, trends in CH_4 efflux were observed to increase under light conditions. These trends correlate with the *in-situ* results of section 2, which found statistically significant correlation between increased dissolved phosphate concentrations and increased rates of CH_4 efflux. However, the role of dissolved phosphorous could not be conclusively discerned from section 2 alone; fluxes could have been driven through increased phytoplankton productivity (and resulting organic matter deposition driving sediment CH_4 production), correlations between increasing phosphate concentrations and CH_4 release being a by-product of bacterial demethylation of methylphosphonates, or potentially the result of a metabolic process or symbiotic relationship of cyanobacteria with methanogenic archaea. The results of this investigation suggest no significant causative relationship between phosphate concentration in the water column and CH_4 production in the water column. As such, the theoretical CH_4 production pathways suggested in oxic water columns, either directly through phytoplankton processes or symbiotic relationships, cannot be causing the minimal rates of CH_4 release seen from microcosms, and do not constitute any significant source of CH_4 in freshwater reservoirs of the south east of England. Although the bacterial demethylation of methylphosphonates in the water column could have caused the small production of CH_4 sometimes observed from microcosms, as the lack of response after phosphate addition correlates with them being a source, there is no way to credit this beyond speculation. Either way, as the release of CH_4 from these water columns is so small, the dominant driver of CH_4 in these reservoir systems is sediment CH_4 production.

The marginal trends of increased CH_4 influx observed in dark conditions could be a result of increased CH_4 oxidisation in dark conditions. For example, light inhibition of CH_4 oxidation processes has been observed in some systems (Murase and Sugimoto, 2005), with light suggested to behave as a bacteriostatic agent. If this was driving increased CH_4 oxidation in the dark, the process was not statistically significant so cannot be considered a significant process that might be affecting diel CH_4

dynamics in the reservoirs investigated. The extent of insignificance observed in this investigation could, however, be due to the experimental design, between-reservoir variation in samples explaining the wide spread of data, and the small number of repeats not representing the environments accurately. For conclusions to be made beyond speculation, further research investigating a greater number of replicates, and investigating reservoirs individually would increase the statistical reliability of conclusions made from microcosm treatment experiments.

The results illustrated minimal and statistically insignificant increases in CO_2 influx under light conditions after phosphate addition. This was unexpected, as the literature suggests influxes of CO_2 should significantly increase as a result of phosphate addition (Ptacnik et al., 2010). It could be that these increased concentrations of phosphate did not affect the photosynthetic processes of phytoplankton significantly because concentrations of phosphate present in the reservoir waters (section 2.3) already exceeded the concentrations required for significant phosphorous limitation in the water column. This has implications for policy makers responsible for the reservoirs investigated. Productivity of the systems exceeds nutrient limitation and as such, to reduce phytoplankton blooms and resulting increases in CH_4 production as a result of sediment production, focus should be placed upon reducing the concentrations of phosphate in these systems. Alternatively, the lack of statistical significance in CO_2 influxes after phosphate addition, despite a marginal mean increase in influx, could be the result of experimental design. This could be addressed by considering the reservoirs of the system individually rather than regionally as the individual CO_2 dynamics of reservoirs may be different, for example some behaving as net heterotrophic systems (Ardleigh and Alton) and others as autotrophic systems (Hanningfield) (section 2.4, table 2.4.1). As a result, the effect of dosing phosphate will be unique to the system, and CO_2 flux responses from microcosms will be insignificant due to the large variation. Further research is needed to understand the effects of phosphate in individual systems, and how this may impact the CO_2 flux results observed in this investigation.

3.4.3 Issues and Further Research

The results of this investigation highlight potential issues in experimental design and the need for future research to address these. To confidently interpret the flux dynamics from these investigations, more test repeats need to be undertaken. If results are to be analysed as an umbrella study for all reservoirs across the region, more reservoirs need to be investigated to ensure the samples are representative; section 2 highlights the inter-reservoir variability and the power this has in influencing resultant fluxes and interpretations. An alternative solution would be to collect samples from a single reservoir, thereby negating inter-reservoir variation as an influence upon microcosm results. Similarly, by carrying out the investigation on an inter-annual basis, any temporal variation in community assemblage or pre-existing water chemistry that may affect the response of microcosms to chemical treatment will be accounted for.

As mentioned throughout the discussion, investigating the effects of chemical addition upon reservoirs already hypereutrophic and loaded with DOC may have supressed the response of potential biological drivers. If future investigations aim to understand all the potential effects of chemical drivers on CO_2 and CH_4 fluxes, then more appropriate waters to investigate would be nutrient limited systems, for example mesotrophic reservoirs. As such the results of this experiment only represent the effects of DOC and phosphate addition in already nutrient polluted environments, and cannot be used to estimate the response of DOC and phosphate pollution on GHG flux from other systems.

To understand the results of these chemical additions beyond speculation, the dominant biological processes by which fluxes occur could be investigated on a microbial level. By identifying the species present in water columns and their relative abundances, their contribution to CO_2 and CH_4 flux dynamics could be understood more clearly. Finally, further trialling of the experimental protocol is required to

investigate the trends in 24 hour fluxes and CH_4 emission as a product of the experimental set-up. For example, trialling the way in which samples reach equilibration as a result of bubbling (section 4.2), increasing the volumes of microcosms or incubating them in their respective reservoirs to be more representative of reservoir environments, could be manipulated in the future.

3.4.4 Conclusions

In conclusion, chemical treatments had insignificant effects upon the CO_2 and CH_4 flux from oxic-water microcosms established from reservoirs in the south east of England (therefore hypothesis 4 is accepted while hypotheses 1 and 2 are rejected). The largest trend towards significance for CH_4 fluxes was observed with phosphate treatment, which correlated with the findings of *in-situ* investigation in section 2 (increased CH_4 effluxes occurring in the presence of increased phosphate concentrations). This highlighted the need for water companies and climate scientists to collaborate in reducing phosphate concentration in reservoirs, thus improving water quality and reducing regional GHG emissions. The effects of both acetate and cellobiose on GHG dynamics were negligible. Physical variables of light and time had the largest effects upon fluxes, highlighting the need to consider these factors when creating daily or annual lake flux budgets, especially when considering the diel variability in CO_2 flux rates, effluxes increasing significantly in dark conditions (therefore hypothesis 3 is accepted). Speculation around the biological drivers of observed CH_4 fluxes highlights the need for further research to investigate biological drives in tandem with physicochemical conditions, although this investigation finds no evidence to support claims of oxic water CH_4 production pathways, or that these habitats provide a release of CH_4 relative to sediment CH_4 production. This experiment also highlights the need for future

investigations of this kind to include more reservoirs, temporal scales and test repeats if investigations are to reliably understand the effects of chemical drivers upon carbon fluxes.

This project has emphasised the importance of freshwaters in carbon budgeting and taken a step towards understanding their drivers in English reservoir systems, whilst providing direction for future research into these systems. Understanding what drives the disproportionately large sources of GHG from freshwaters is complicated, but through continued research the convolution of these systems will be resolved.

4.0 Appendices

4.1 Methods Development

4.1.1 Detection of a False Positive

In testing the Picarro G4301 greenhouse gas analyser ("the Picarro") before use in the field, negative control testing was undertaken to ensure correct functioning and calibration of the machine. For the first negative control investigation, 5 litre flasks were filled with 2.5 litres of milliQ water and autoclaved to stop microbial activity (a potential source of greenhouse gasses (GHGs)). Gaseous fluxes from these negative controls were then measured by attaching the GHG analyser inlet and outlet to the flask headspace using a silicone bung. The results of these measurements were an almost linear increase in CO_2 of 30ppm (965ppm to 995ppm (figure 4.1.1.2)) and an increase in CH_4 of 0.35 ppm (2.05ppm to 2.4ppm (figure 4.1.1.3)) over the hour, with no sign of equilibration. The expected rates of efflux from a negative control in this configuration are 0 ppm $minute^{-1}$ of CO_2 and CH_4. The detection of CO_2 and CH_4 efflux suggested either a problem with the experimental set-up (the short measurement period resulting in measurements of water equilibration with the lab atmosphere instead of CO_2 and CH_4 - production rates, or a leak in the flask seal causing diffusion from the lab atmosphere into the flask headspace) or a problem with the Picarro GHG analyser (e.g. a calibration or internal leak issue within the instrument).

A second negative control experiment was undertaken to determine if the detected increase in headspace CO_2 and CH_4 concentrations was a result of the experimental set-up, or a problem with the Picarro GHG analyser. Again, 5 litre flasks were filled with 2.5 litres of milliQ water and autoclaved, to form the negative control samples. To increase the rate of equilibration between the dissolved gas in the sample water and the free gas of the flask headspace, the headspace air was cycled through the sample water as bubbling. Using the Picarro gas analyser, headspace gas was pumped into the gas analyser, CO_2 and CH_4 concentrations measured, and pumped back into the water phase of the negative

control sample in a closed loop (figure 4.1.1.1) (similarly used in section 4.2.2). CO_2 and CH_4 concentrations were measured for 24 hours in this configuration. The result of this negative control experiment was a continual increase in CH_4 concentrations throughout the time period (for example, figure 4.1.1.5 shows a concentration increase from 3.8 ppm to 8.8ppm over the time period), and a more variable net increase in CO_2 concentrations throughout the time period (for example figure 4.1.1.4 showing an increase from 530ppm to 600ppm over the time period, despite a plateau and marginal decrease in concentration from 500 to 1150 minutes). As these results displayed continued CO_2 and CH_4 production in the headspace (despite having addressed potential problems in the experimental design) the problem was isolated to the Picarro GHG analyser.

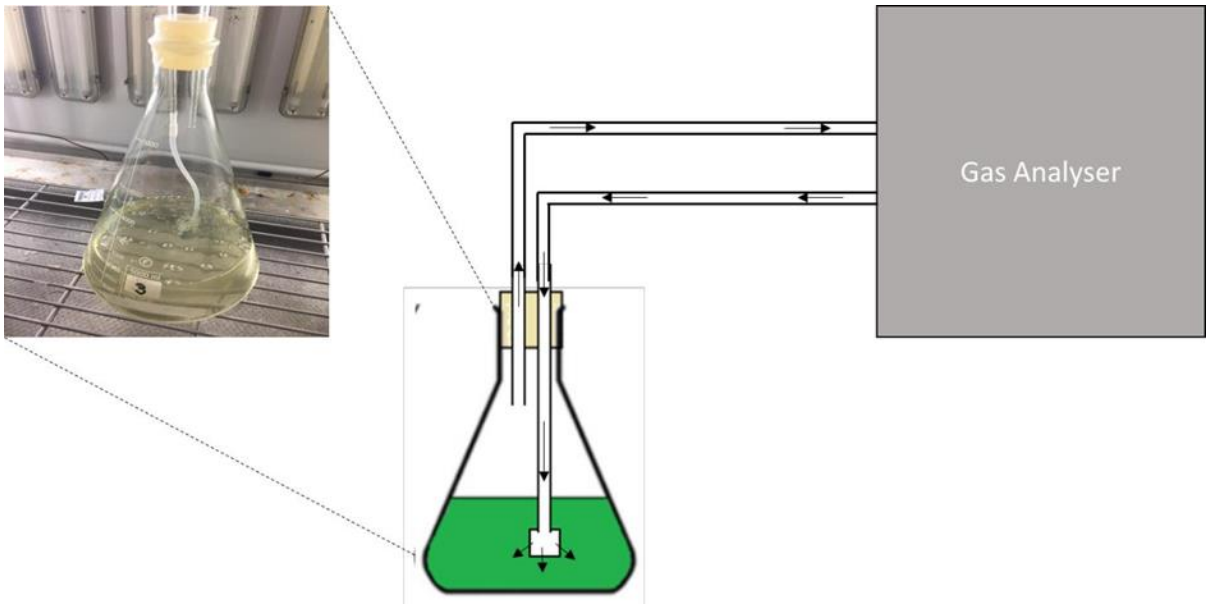

Figure 4.1.1.1 Set-up of the second negative control experiment investigating false positives detected in the first negative control experimental set-up. Rate of equilibration is increased by circulating the flask headspace through the negative the water sample (green). Air is pumped in a closed loop using the Picarro GHG analyser (Gas Analyser).

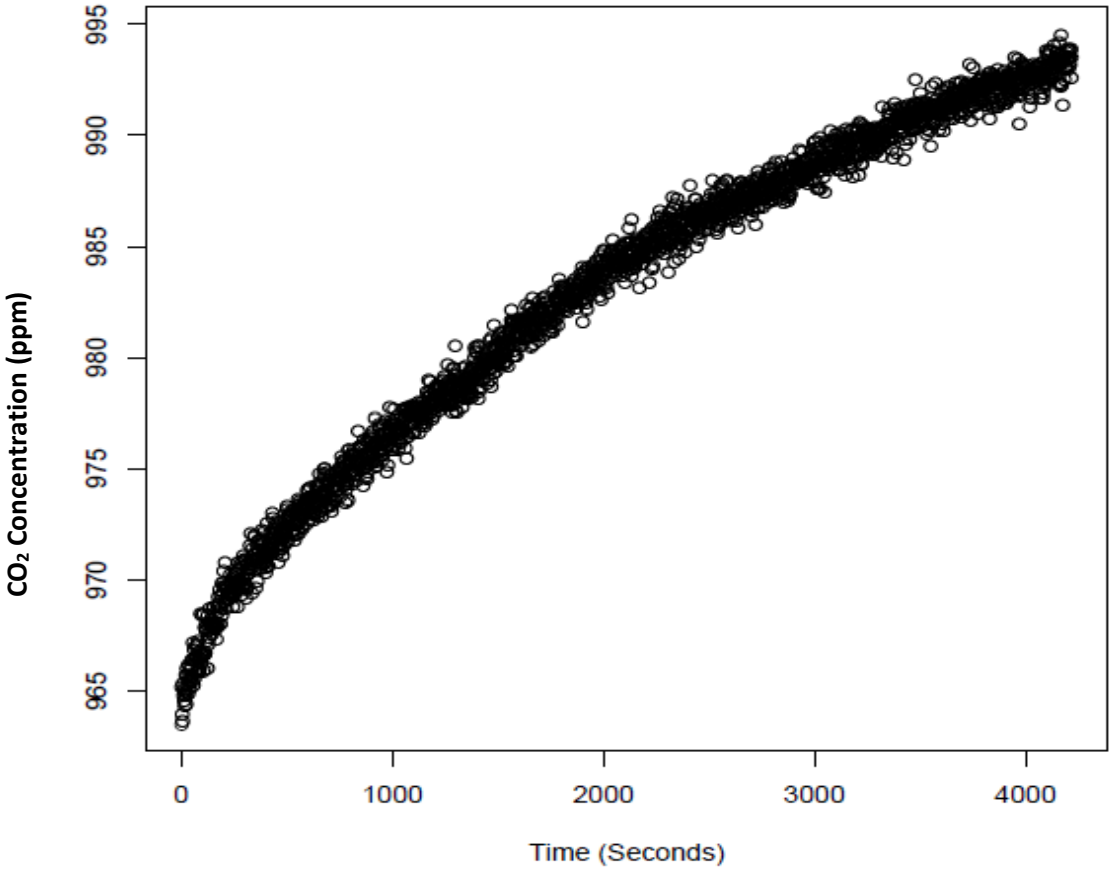

Figure 4.1.1.2 Negative control experiment 1. CO_2 measured from a negative control flask headspace (a 5 litre flask filled with 2.5L of sterile water) for a period of 1 hour. Measurements were made using the Picarro gas scout GHG analyser connected in a closed loop with the flask headspace. Flasks were incubated at 16°C for 24 hours prior to taking the measurement. n=1.

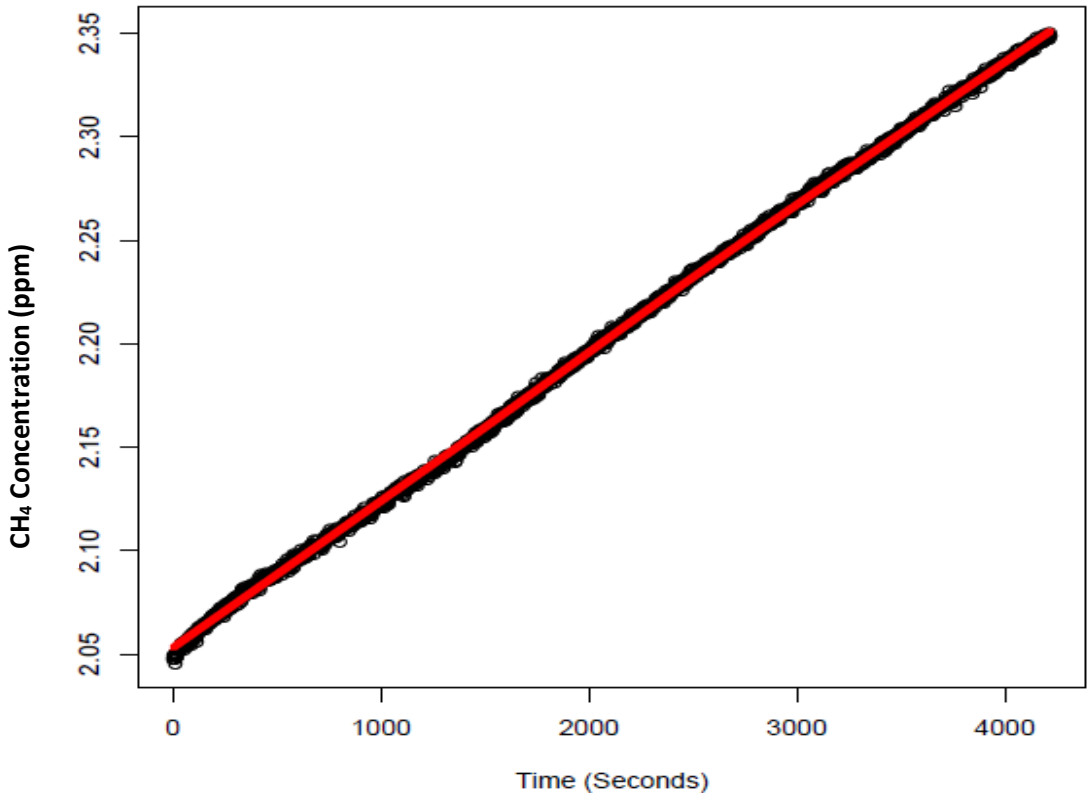

Figure 4.1.1.3 Negative control experiment 1. CH_4 measured from a negative control flask headspace (a 5 litre flask filled with 2.5L of sterile water) for a period of 1 hour. Measurements were made using the Picarro gas scout GHG analyser connected in a closed loop with the flask headspace. Flasks were incubated at 16°C for 24 hours prior to taking the measurement. n=1.

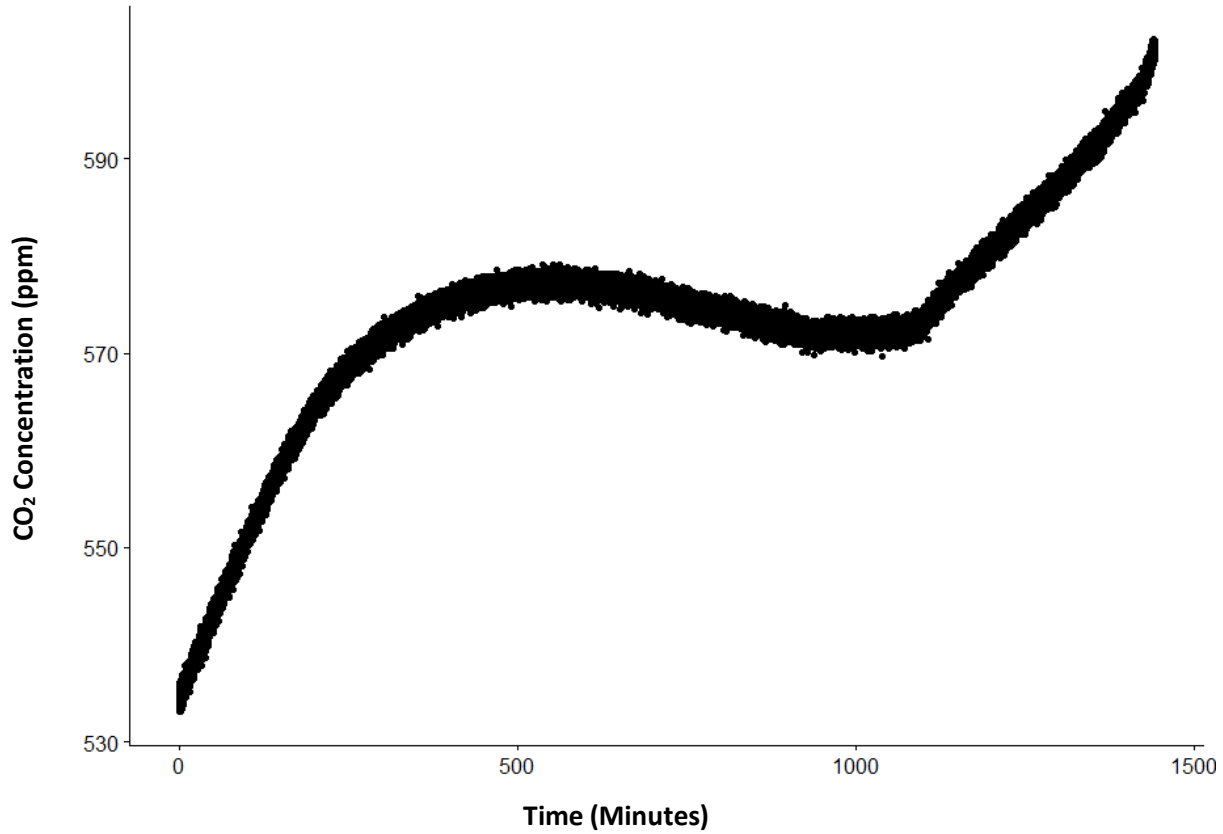

Figure 4.1.1.4 Negative control experiment 2. CO_2 measured from a negative control flask headspace (a 5 litre flask filled with 2.5L of sterile water) for a period of 24 hours. Measurements were made using the Picarro gas scout GHG analyser connected in a closed loop with the flask, outlet bubbling flask headspace through the sample water phase. Flasks were incubated at 16^{o}C for 24 hours prior to taking the measurement. n=1.

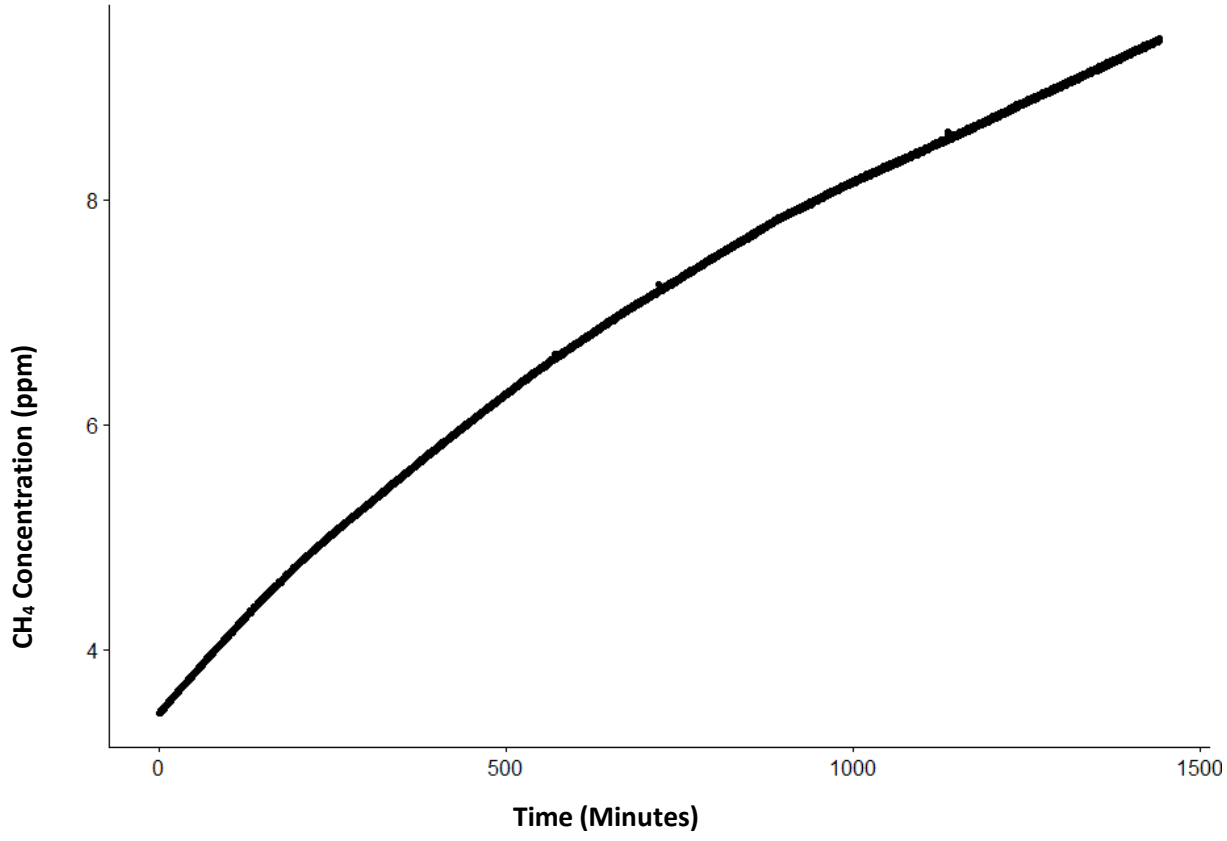

Figure 4.1.1.5 Negative control experiment 2. CH_4 measured from a negative control flask headspace (a 5 litre flask filled with 2.5L of sterile water) for a period of 25 hours. Measurements were made using the Picarro gas scout GHG analyser connected in a closed loop with the flask, outlet bubbling flask headspace through the sample water phase. Flasks were incubated at 16^{o}C for 24 hours prior to taking the measurement. n=1.

4.1.2 Cause of the False Positive

Potential causes of the false positive results from the Picarro GHG analyser were internal leaks (atmospheric air diffusing into the Picarro's CRDS absorption cavities), a computer system or calibration error or an internal source of CH_4 and CO_2. These scenarios were tested through a series of addition and removal experiments.

The functionality of the Picarro was tested to ensure that recorded measurements were in response to the input gas, and not spurious outputs as a result of computer error. Known concentrations of CH_4 and CO_2 were injected into the input of the Picarro, in an open loop with the lab environment. Concentrations measured by the Picarro matched the input concentrations.

Next the sensitivity of the Picarro (using negative control flask set-up two) was tested with a positive control. Stock *Synechocystis sp*. (a freshwater cyanobacterium) was cultured at 16°C, and 2.5 litres of culture transferred into 5 litre flasks. CO_2 and CH_4 headspace measurements were made for 1 hour periods, in light and dark conditions. Under light conditions, CO_2 is assimilated by cyanobacteria through photosynthesis, in contrast to CO_2 emission under dark conditions through respiration (Vermaas, 2001). From the headspace measurements, this was expected to be clearly observed due to the high cell count of the cyanobacteria stock, thus clearly detected by the Picarro. Results indeed displayed decreases in headspace CO_2 concentrations under light conditions and increases in headspace CO_2 concentrations under dark conditions (figure 4.1.2.2). The analyser was sensitive to more extreme changes in concentration, displaying the expected trends with time and light. This suggested that an internal source and build-up of gases, rather than a calibration drift, was causing the false positives in the negative control experiments; the leak rate was low enough that samples with high microbial activity could counteract the headspace build-up of CO_2 and CH_4. As such, the Picarro could be mistaken as functional.

To test for GHG production within the Picarro, CO_2, CH_4 and H_2O removal experiments were undertaken. The Picarro was run in an open loop. CO_2 and CH_4 were removed jointly from the input line through a series of activated carbon chambers, while H_2O was removed separately through a series of desiccant chambers (silica gel and Dryrite) in a separate run (figure 4.1.2.3). Results showed that despite carbon scrubbing, both CO_2 and CH_4 were still detected above the concentrations expected. In contrast, H_2O behaved as expected, remaining at a concentration of zero. These results suggested that the source of CO_2 and CH_4 detected was not from atmospheric diffusion through an internal interface with the atmosphere (for example a perforated pipe in the system), because atmospheric H_2O would have similarly been detectable. Instead CO_2 and CH_4 must originate from production within the analyser, the source of which was found to be the air intake pump, which had rubber moving parts releasing CO_2 and CH_4.

As compatible replacement pumps would still produce CO_2 and CH_4, and be beyond the available time frame, the best solution to this problem was to calculate and correct for the CO_2 and CH_4 production rate from the pump.

Correction Calculations

The air inlet of the Picarro was connected directly to its air outlet using gas tight tubing in a closed loop with itself (figure 4.1.2.1). Concentrations of CO_2 and CH_4 were then measured in this set-up for 12 hours. This was repeated 4 times (n=4). Gas concentrations were plotted against time in minutes and the gradient of each slope calculated (figure 4.1.2.4). Slope values were then averaged to give the correction values of -0.0375 ppm min^{-1} CO_2 and 0.00386 ppm min^{-1} CH_4. These values were removed from experimental rate measurements. As a result, false positives were accounted for and the Picarro gas analyser could be used in the subsequent closed loop experiments of this thesis.

A potential caveat of using a flux correction value is that GHG efflux from the pump may fluctuate. In investigations requiring closed loop sampling, it is advised that flux correction values should be calculated for experimental measurements individually, before and after sampling, to ensure precise readings and interpretation of data from the Picarro gas analyser.

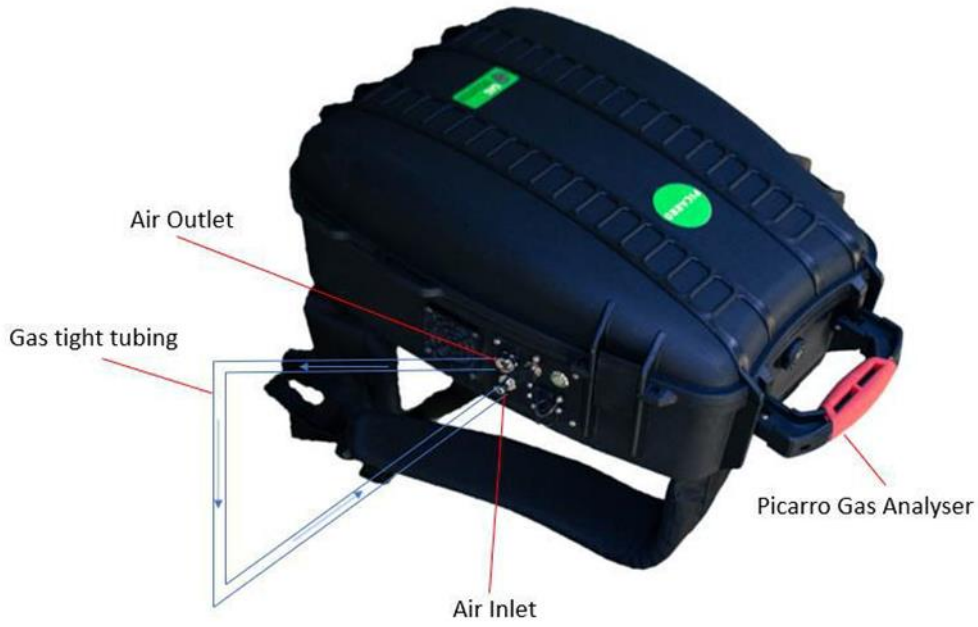

Figure 4.1.2.1 GHG analyser leak correction calculation using a closed loop set-up. Blue lines represent the gas tight tubing used in the experiment, connected directly from the analyser inlet to the analyser outlet. The gas analyser is the Picarro gas analyser model G4301.

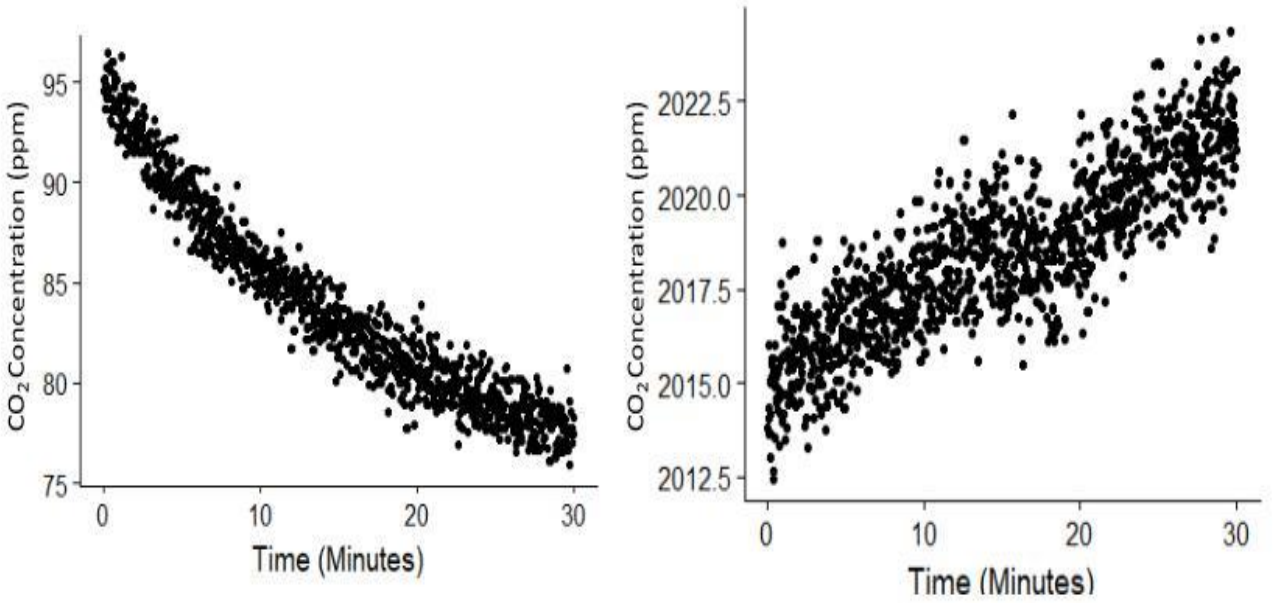

Figure 4.1.2.2 Example of the CO_2 results obtained during positive control testing; investigating the sensitivity and functionality of the Picarro gas analyser model G4301. 2.5 Litres of *Synechocystis sp.* stock was investigated in a 5-litre flask under light (left hand image) and dark (right hand image) conditions, for 1 hour, results show the final 30 minutes to avoid the equilibration period of the first 30 minutes. Dark conditions were applied using aluminium foil jacket. (This example n=1).

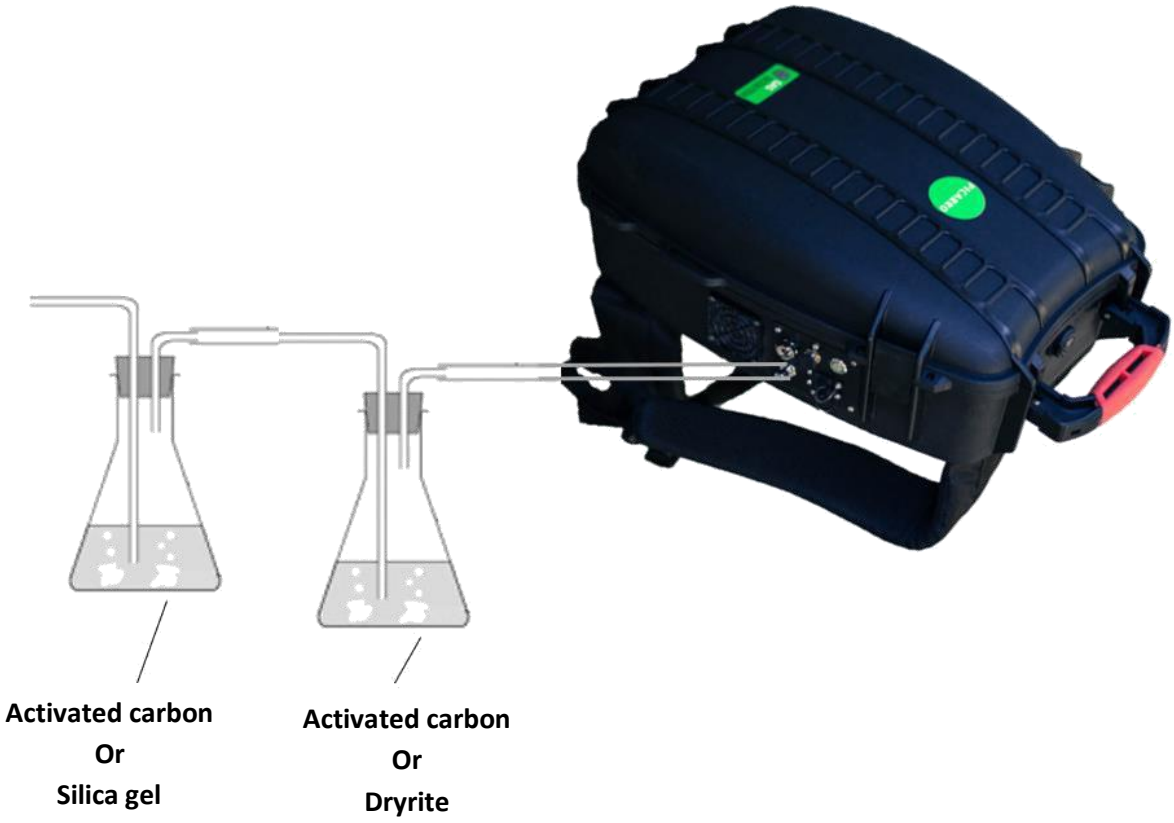

Figure 4.1.2.3 Removal of CO_2 and CH_4 or H_2O from the inlet of the gas to be analysed, as a part of removal experiments attempting to identify the source of CO_2 and CH_4 leaks from the Picarro G4301. Picarro gas analyser in an open loop with the lab environment.

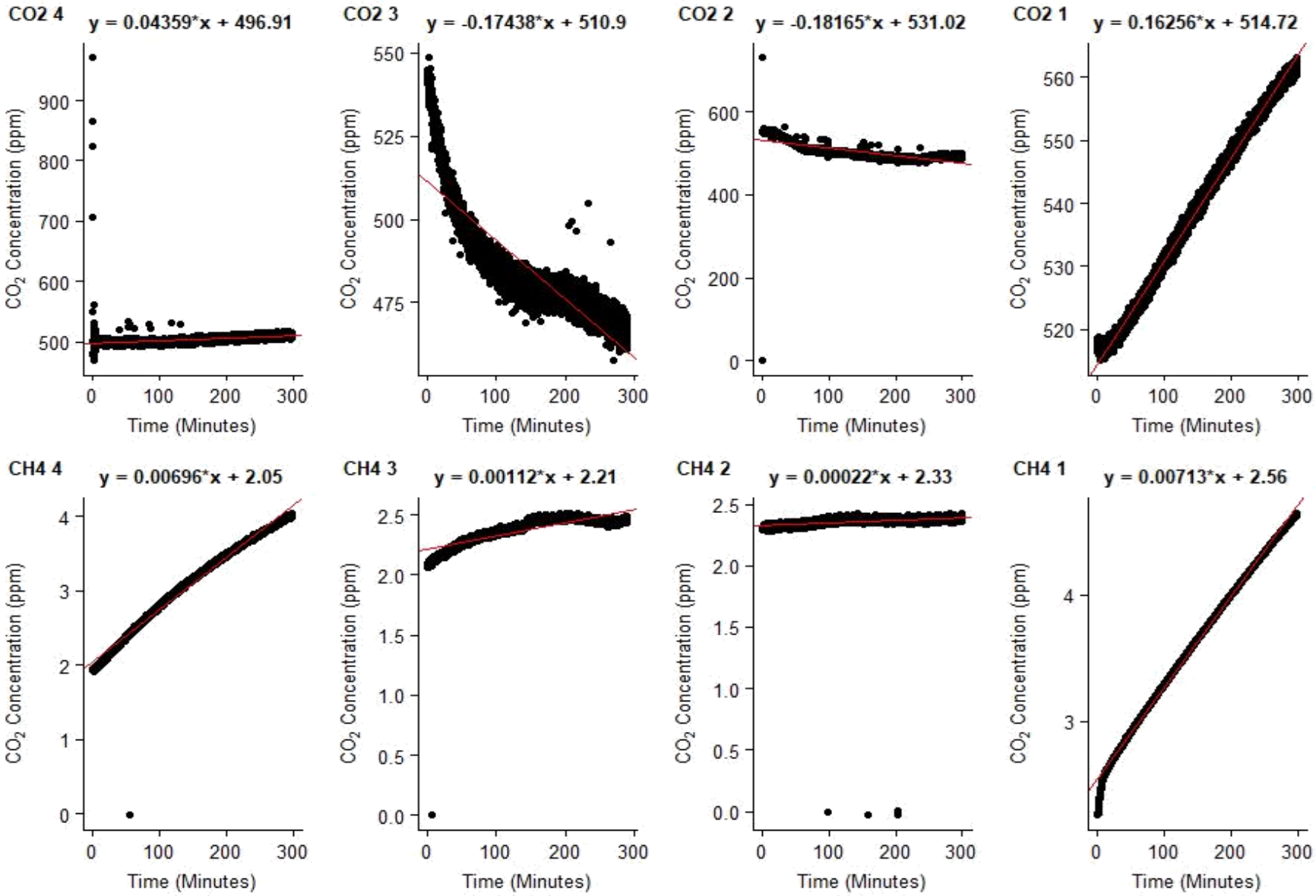

Figure 4.1.2.4 Calculating rates of CH_4 and CO_2 leak in Picarro G4301, for the purpose of calculating correction values to be applied to field and experimental measurements. Measurements taken with the Picarro in a closed loop with itself and measured for 5 hours. y = rate of flux, x = gradient intercept. n=4.

4.1.3 In-situ Reservoir Flux Investigation Methods Development

Reservoir CO_2 and CH_4 surface flux measurements in section 2 were collected using the closed dynamic chamber technique (described in section 1.5), which required the development and testing of a floating chamber experimental set-up. Testing was required to ensure the reliability of the chamber on the water surface, minimising its surface interference effect on turbulence (Kremer et al., 2003) and calculating its time of deployment. The time that chambers are deployed for is dependent on magnitude of gas flux, the volume of the floating chamber and the sensitivity of the GHG analyser used.

The chamber in this study was adapted from an inverted opaque white plastic bucket. This material reflected incident sunlight, minimising temperature increase and resultant rate of efflux increase within the chamber. The smooth interior shape prevented the formation of gas pockets and uneven mixing. The internal chamber volume was 22 litres and the contact surface area was 0.0962m^2. Concentrations within the floating chamber were measured using the Picarro G4301 portable greenhouse gas analyser (Picarro Inc), connected to the chamber head space in a closed loop using gas tight tubing (tubing volume was 78ml) (figure 4.1.3.1). Following suggestions from the literature (Cole et al., 2010; Matthews et al., 2003), a lip of 3cm penetrated the water to minimise artificial turbulence.

The optimal chamber deployment time for this set-up was determined by testing the chamber for durations of 10, 30 and 60 minutes; time ranges seen most frequently in the literature (Soumis et al., 2008; Guérin et al., 2007; Repo et al., 2007). Testing took place on the littoral zone of Ardleigh, Hanningfield and Alton reservoirs (section 2) during winter and spring 2018. Increases in CO_2 and CH_4 concentration were observed throughout each time scale with no sign of equilibrium (which could result when large magnitudes of gas collection relative to the chamber volume occur) or random measurements that could have resulted from a non-gastight seal (figures 4.1.3.2 and 4.1.3.3). The concentration of CH_4 accumulation was variable, sometimes not exceeding an increase of 0.4ppm over 60 minutes (figure 4.1.3.2 (run 2)), but in other cases up to 110ppm over 30 minutes (figure 4.1.3.4). Ebullition events were collected and detected in the chamber, observed as “spikes” in concentration

before returning to diffusion rates (figure 4.1.3.4), although these could be missed in shorter time frames. Longer chamber deployment times allow for more accurate detection of CH_4 during low flux rate events, and the quantification of sporadic ebullition pathways. As a result, 30 minutes was selected as the deployment time most suited to CH_4 measurements in this experimental set-up and considering the rates of efflux from reservoirs in this region.

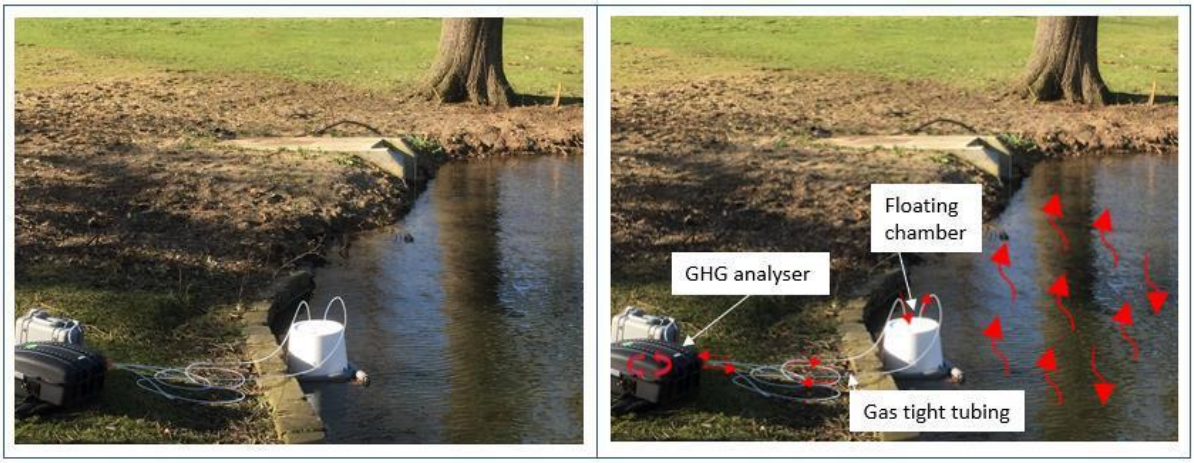

Figure 4.1.3.1 Dynamic floating chamber method in the field. Left hand image illustrates the chamber method 'in action'. The right hand image illustrates the movement for gases from the water (red arrows) collection in the chamber headspace, pumping to the GHG analyser (Picarro gas scouter (Picarro Inc)) where concentrations are determined, and pumping back to the chamber headspace.

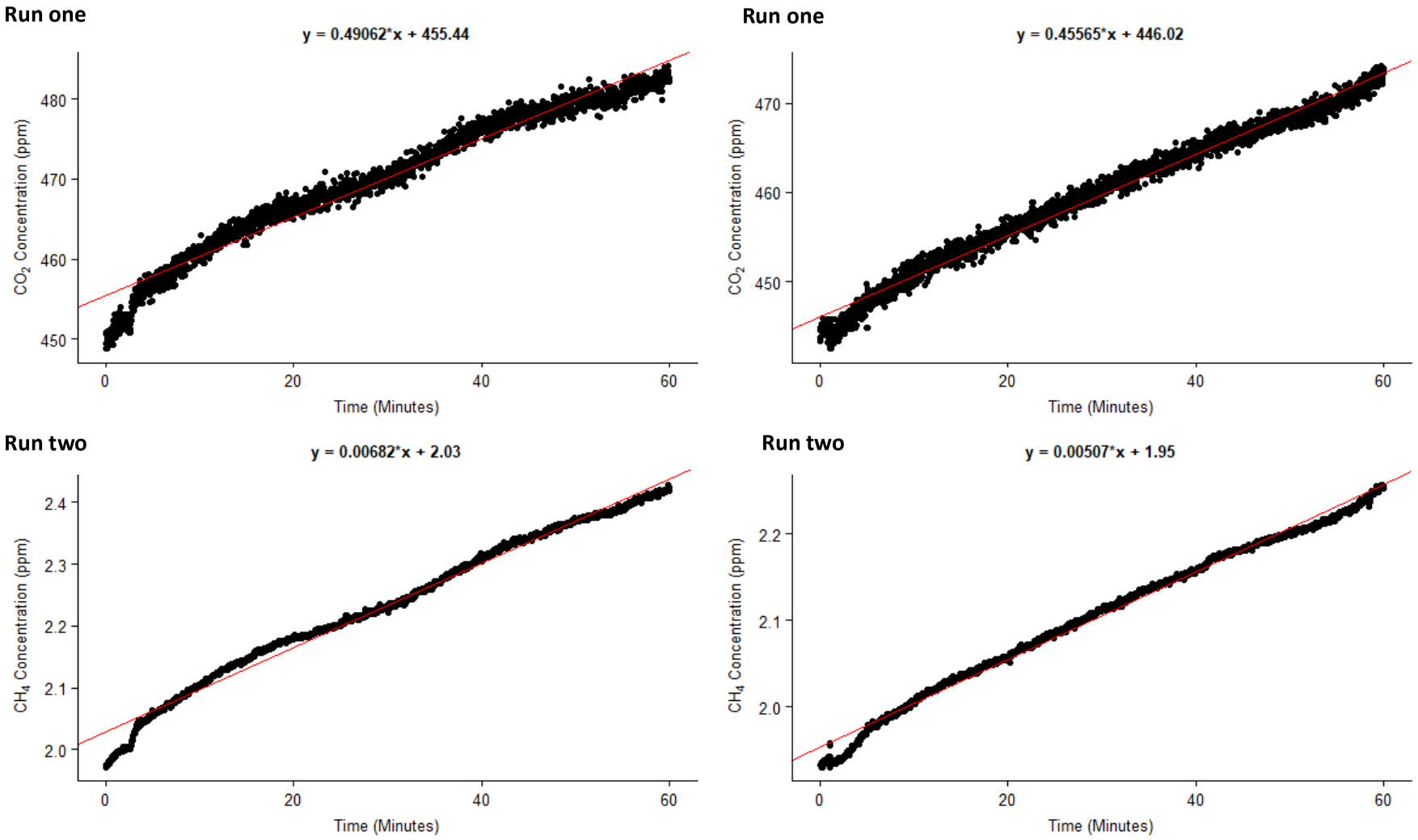

Figure 4.1.3.2 Dynamic floating chamber method trialling in the littoral zone of Ardleigh reservoir, March 2018. LNM = Littoral habitat with no emergent macrophytes. Y = gradient of the slope, x= intercept of the slope. Gases measured in parts per million (ppm) using a Picarro gas scout (picarro Inc). Chambers deployed for 60 minutes. n=2.

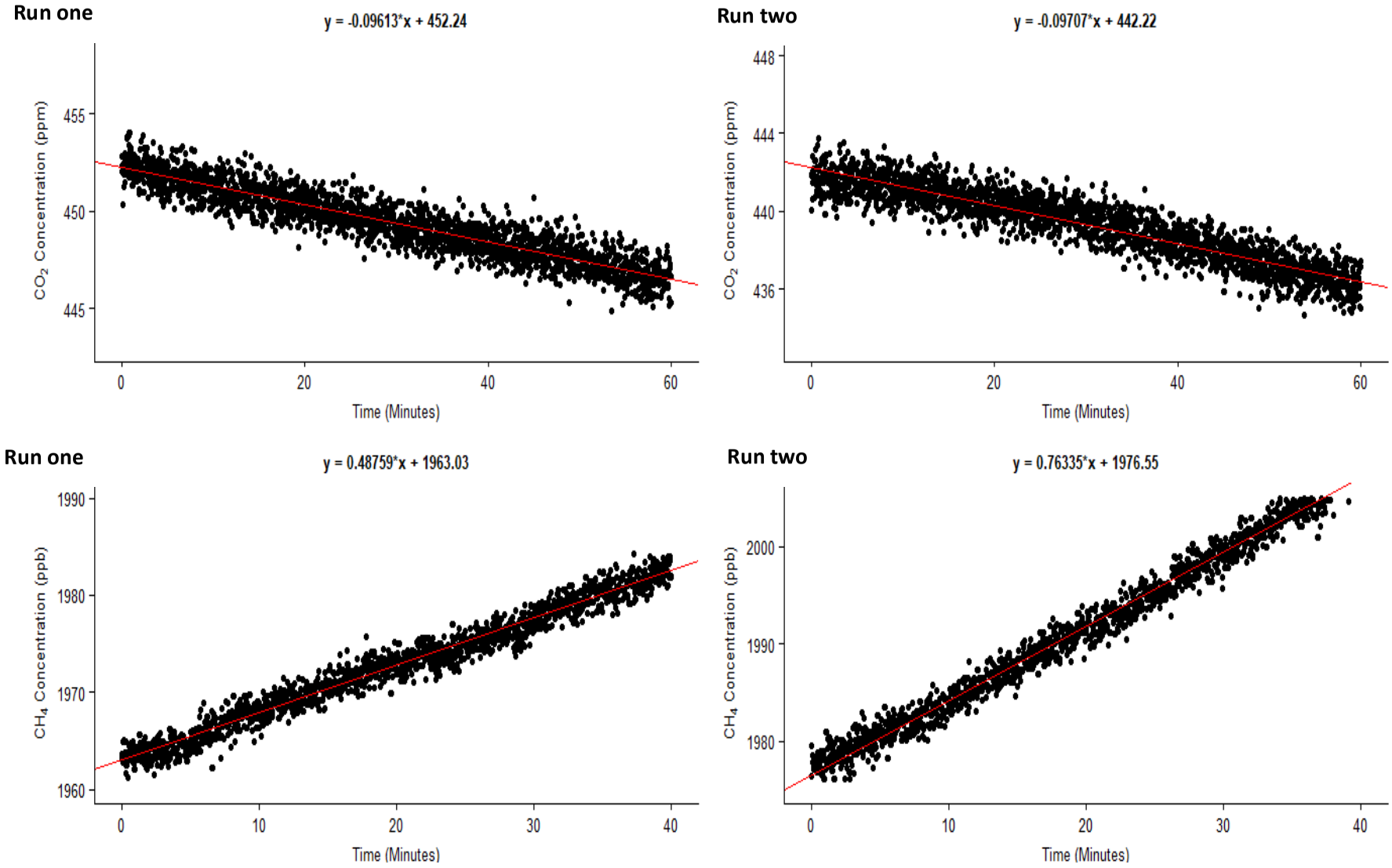

Figure 4.1.3.3 Floating chamber method trialling in the littoral zone of Alton reservoir, February 2018. Y = gradient of the slope, x= intercept of the slope. Gases measured in parts per million (ppm). Chambers deployed for 40 and 60 minutes. n=2.

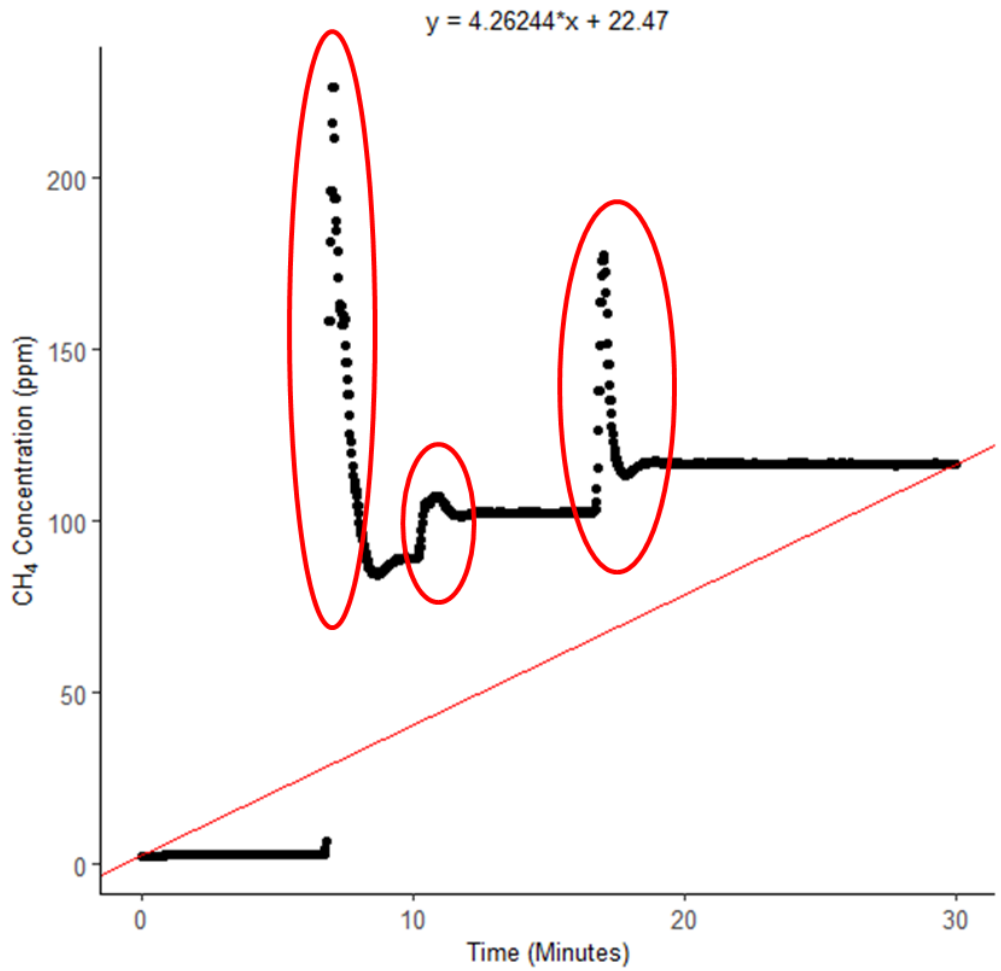

Figure 4.1.3.4 Example of ebullition visible when plotting headspace concentration with time. Spikes relating to bubbles are circled in red. Overall rate of flux is illustrated as the red line, the equation for which is at the top of the graph. Measurements taken as a part of dynamic floating chamber development and trialling from HanningField reservoir Spring 2018.

4.2 Lab-based Water Column Flux Investigation Methods Development

The environmental, biological and physicochemical constituents of freshwater bodies are complex and highly specific, each water body having its own 'fingerprint'. These fingerprints drive freshwater carbon fluxes, causing the variation seen between water bodies. However, the convoluted nature of these chemical and physical factors, and their interactions within the water body, make identifying or attributing patterns in carbon flux to individual factors difficult to distinguish. Investigating the contribution of an individual variable on gaseous carbon flux allows these interactions to be discerned. This can be done through addition or removal experiments, for example in mesocosms (Bogard et al., 2014) and full lake (Schindler et al., 1971) studies. However, these large-scale investigations can be expensive, invasive and maintain elements of convolution.

The following proposes a method of investigating individual physical/ chemical impacts on water column carbon flux, on a small laboratory scale. By creating a series of microcosms in a controlled laboratory environment, the impact of treatments upon carbon flux can be determined through headspace analysis. The benefit of this style of investigation is that any number of treatments and time scales can be applied to water samples, while eliminating the impacts of confounding variables such as temperature and other physical parameters, at little financial expense. Key results from these investigations can then be investigated more confidently in larger scale investigations.

4.2.1 Trial One

Experimental Design

Initial sampling was undertaken from Ardleigh reservoir in January 2018. A 15 litre water sample was collected from the top of the littoral water column in a 20 litre carboy. 2.5 litres of this sample were transferred to 5 litre conical flasks to form microcosms. The headspace of the microcosm flask was separated from the lab environment using a foam bung, while maintaining gas transfer between the water sample and the atmosphere. These microcosms were then incubated at 16°C (the average summer atmospheric temperature in England between 2016 and 2017 (Statista, 2018)) for 24 hours, removing the effect of temperature on gas transfer rates (Henry's Law constant (Fernández-Prini et al., 2003; Nicholson, 1984)).

After 24 hours of incubation, the rate of carbon flux from samples was determined by measuring the concentrations of CO_2 and CH_4 in the microcosm headspace. The Picarro GHG analyser (discussed in section 4.1) was connected to the headspace in a closed loop using a silicone bung with a gas tight inlet and outlet tubes passing through (figure 4.2.1.1). Head spaces were measured in this way for 1 hour. No treatments were applied at this point in the experimental development, though negative control microcosms containing milli-q water in place of reservoir water were run in tandem with reservoir microcosms.

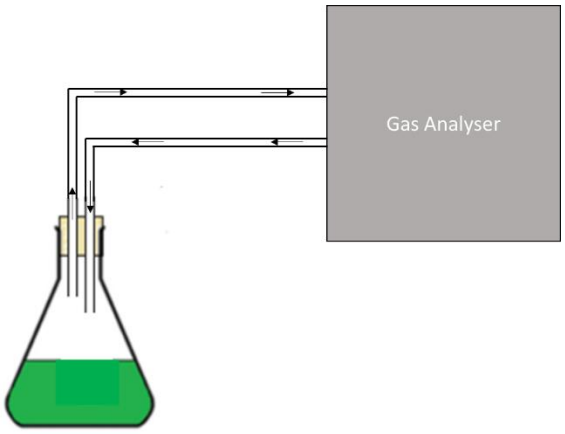

Figure 4.2.1.1 Diagram of microcosm trial 1 experimental set-up, measuring carbon fluxes from flask headspace.

Results and Discussion

Recorded gas concentrations were plotted against time in minutes for the 1 hour period, illustrated by figure 4.2.1.2 which shows a curved gradient throughout the time of the experiment. As observations were not linear, the reliable calculation of microcosm rate of flux could not be achieved.

The cause of these observations was the process of equilibration, as water sample gas concentrations and sealed microcosm headspace concentrations balanced. Equilibrium was not reached within the time frame of the trial experiment, after which the rate of flux would be linear and represent the production or assimilation of gases in the sample. As a result, the rate of gas concentration change taken from figure 4.2.1.2 would represent the rate of equilibration, not water sample gas production or assimilation rates. To reach the point past equilibrium, while allowing time for the rate of flux to be calculated, either the speed of equilibration or time of measurement had to be increased (alternatively equilibrium could be negated mathematically, though the variability exhibited between samples suggested this would yield inaccuracies). Due to the constraints of the investigation (having only one Picarro available and requiring the analysis of multiple microcosms in one day) a longer time of measurement was not feasible. The speed of equilibrium was by increased by pumping headspace air through the water sample, increasing the surface area for diffusion between free gas and dissolved gas.

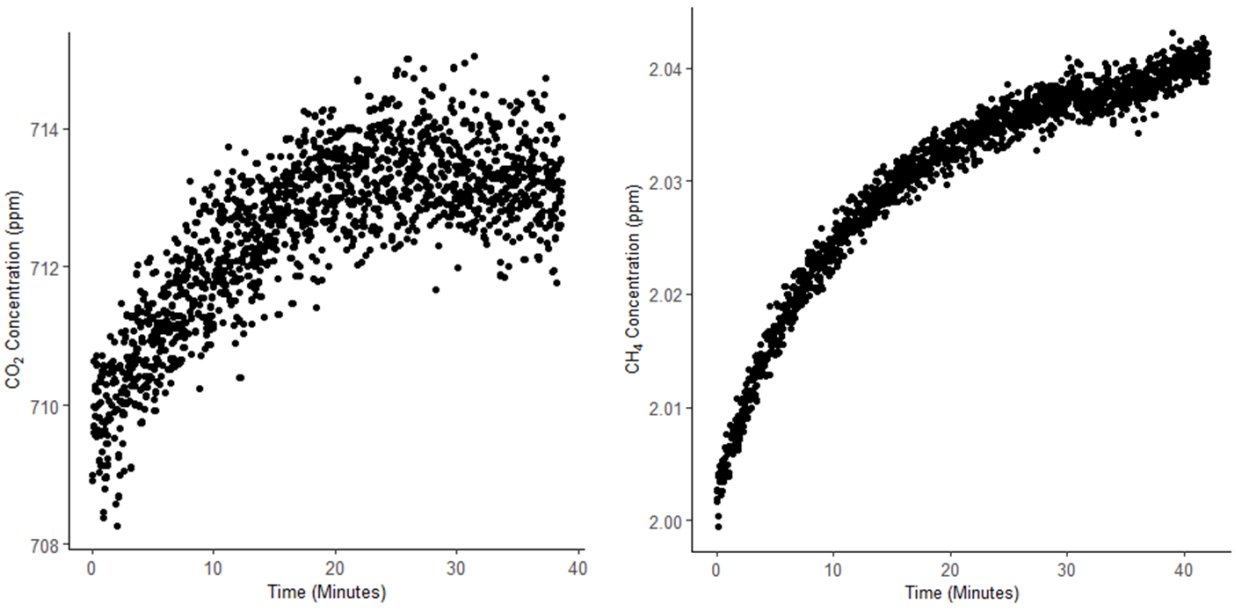

Figure 4.2.1.2 Results of microcosm trial one, concentration of CO_2 and CH_4 in parts per million plotted against time in seconds. Water sample taken from Ardleigh reservoir January 2018. Example n=1.

4.2.2 Trial Two

Experimental Design

Microcosms were set up in the same way as in section 4.2.1 and allowed to incubate for 24 hours at 16°C, however the method of measuring microcosm fluxes was changed. The microcosm was set up in a closed loop with the microcosm headspace, and the Picarro gas outlet was extended through the silicon bung into the sample water and bubbled through a diffuser to increase the gas exchange surface area (figure 4.2.2.1). From here, headspace gas concentrations were measured for 1 hour as previously.

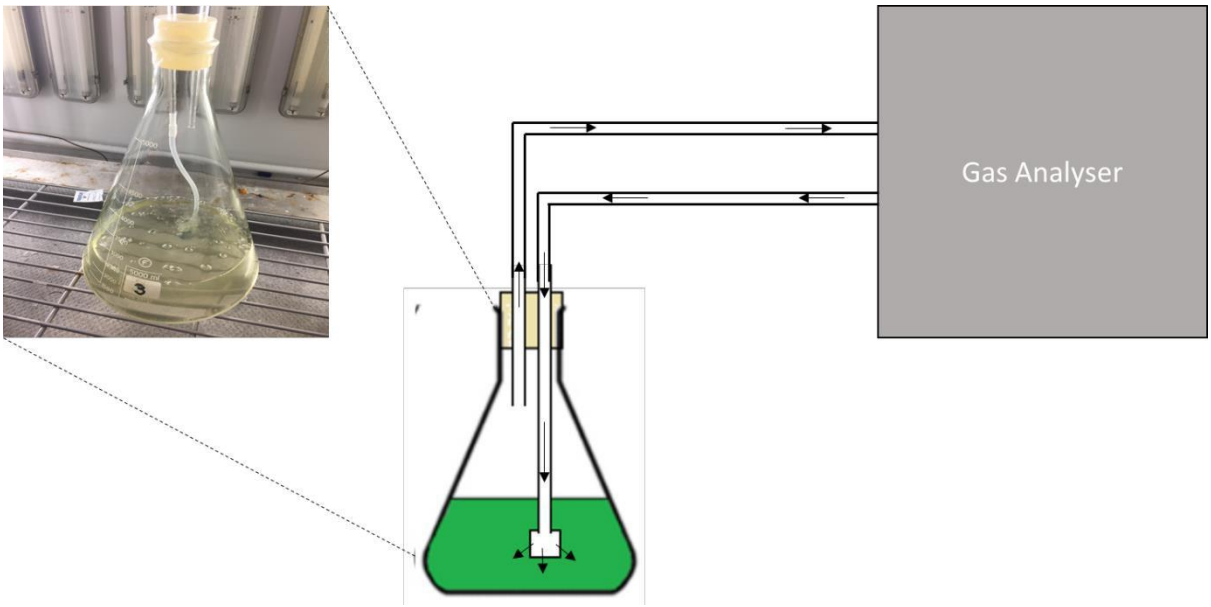

Figure 4.2.2.1 Diagram and photograph of microcosm trial 2 experimental set-up, measuring carbon flux from the flask headspace while pumping headspace air through the water sample to increase the speed of equilibration.

Results and Discussion

Figure 4.2.2.2 displays an annotated plot of microcosm headspace concentration against time. The initial stages of measurement illustrate the same process of equilibration observed in figure 4.2.1.2 (a curved increase or decrease (illustrated by the red circle in figure 4.2.2.2)) followed by a new steady linear trend (illustrated by the blue circle in figure 4.2.2.2) ~30-45 minutes into the measurement. This linear concentration increase is a result of gas production or assimilation within the water sample.

The protocol defined in trial two therefore solved the issues identified in trial one, by increasing the speed of equilibration and therefore allowing the identification and quantification of prolonged linear trends in CO_2 and CH_4 flux. This microcosm headspace method could then be used in subsequent treatment experiments, for example those used in section 3.

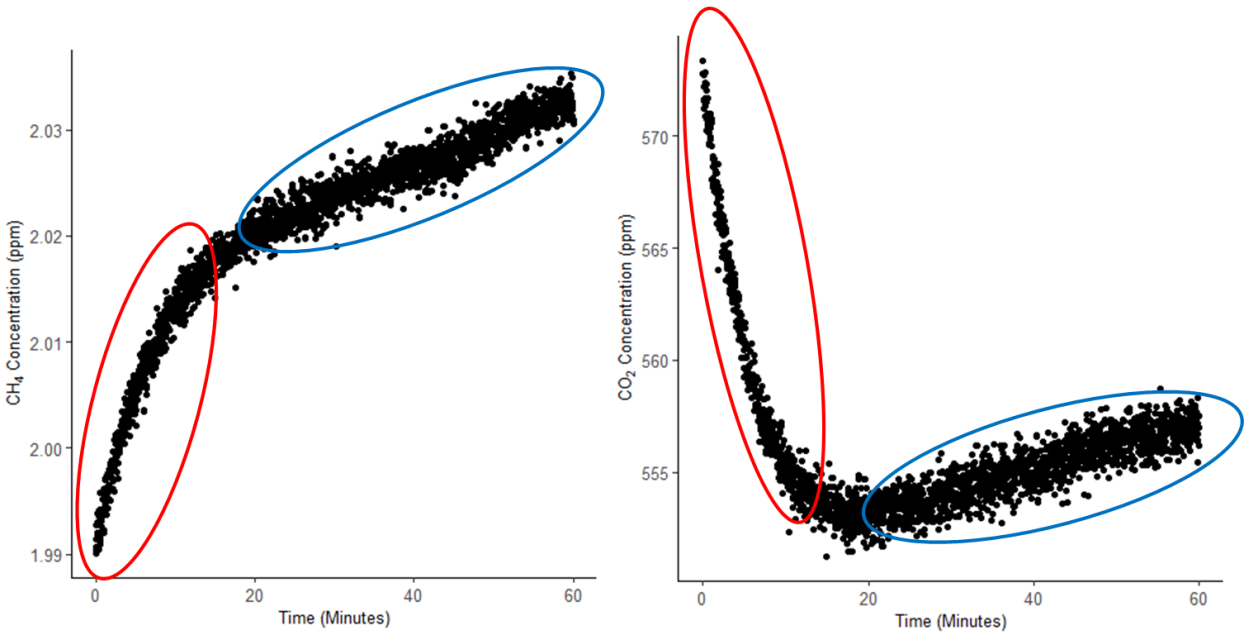

Figure 4.2.2.2 Annotated illustrations of CO_2 and CH_4 concentrations in parts per million (ppm) plotted against time in minutes. Red circles illustrate periods of equilibration between water sample and microcosm headspace. Blue circles illustrate linear rates of flux due to sample production or assimilation. Sample taken from Ardleigh reservoir littoral surface waters, March 2018. Example n=1.

Rate Extraction

Rates were taken from the last 15 minutes of the headspace measurement, showing the most consistent linear period from measurements required for accurate rate calculation. This was done by calculating the slope of the concentration change. Rates were corrected for the Picarro leak using the protocol described in section 4.1. To ensure leak rates had not changed, negative control measurements were repeated 8 times in light and dark conditions (section 4.2.3 figures 4.2.3.1 to 4.2.3.5). Rates of CH_4 and CO_2 production were averaged, and this value removed from experimental flux measurements, to ensure that the rates of production measured were biogenic, and not from the machine (CO_2= -0.0418 ppm, CH_4= 0.000179ppm).

Further Notes

A caveat of the microcosm bubbling method is that bubbling increases the dissimilarity between microcosms and actual water body environments, which are only bubbled in such a way at reservoir bubble curtains. Measuring the dissolved O_2 concentrations of microcosms before and after bubbling using a Vernier optical dissolved oxygen probe, found high O_2 concentrations were maintained throughout the sampling period, mean= 10.08 ± 0.74 mg/L (n=6). These high concentrations are similar to those observed in the reservoir epilimnions investigated in section 2; measurements using a miniDO2T giving a mean of 9.6 ± 1.31 mg/L. As a result, this method is appropriate for experiments investigating oxic water environments or applying oxic treatments. To investigate anoxic environments, such as benthic or hypolimnetic zones, it is likely that an alternative anoxic method would have to be developed, perhaps using a controlled atmosphere in the microcosm's headspace with O_2 absent. However, for the purposes of investigations such as section 3, bubbling methods are appropriate. Other changes to the methodology could include experimentation with larger flasks thus creating micro/mesocosms of larger volume to increase the accuracy and parallels with reservoir environments,

but for the lab space available and aims of the investigation, the methods described were most appropriate. Future investigations, where more gas analysers are available, could remove the need for bubbling through longer microcosm headspace measurements, giving longer for equilibration and subsequent linear fluxes to be observed. Alternatively, the bubbling period could be maintained to reach equilibrium more rapidly, after which bubbling could be stopped to minimise sample integrity damage. The Picarro outlet could then be transferred to the flask headspace using a valve (section 4.2.3 figure 4.2.3.6), after which rates of flux would be determined. However, the effort involved in such a method alteration is arguably futile, considering bubble treatment must still be applied to the sample; the treatment this method would attempt to negate.

4.2.3 Methods Development Supplementary Materials

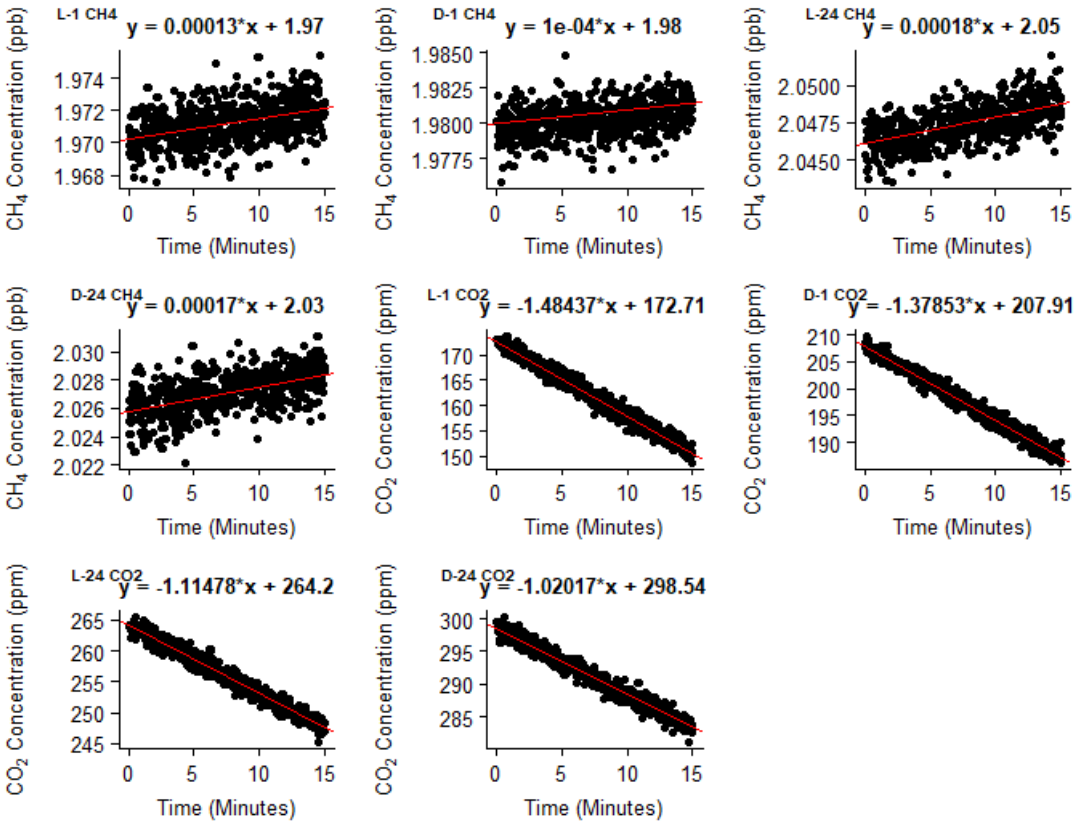

Figure 4.2.3.1 Negative control run 5. Values used to calculate flask experiment correction values. "L" = Light, "D"= Dark, "1" = 1 hour into run, "24" = twenty four hours after 1 hour run.

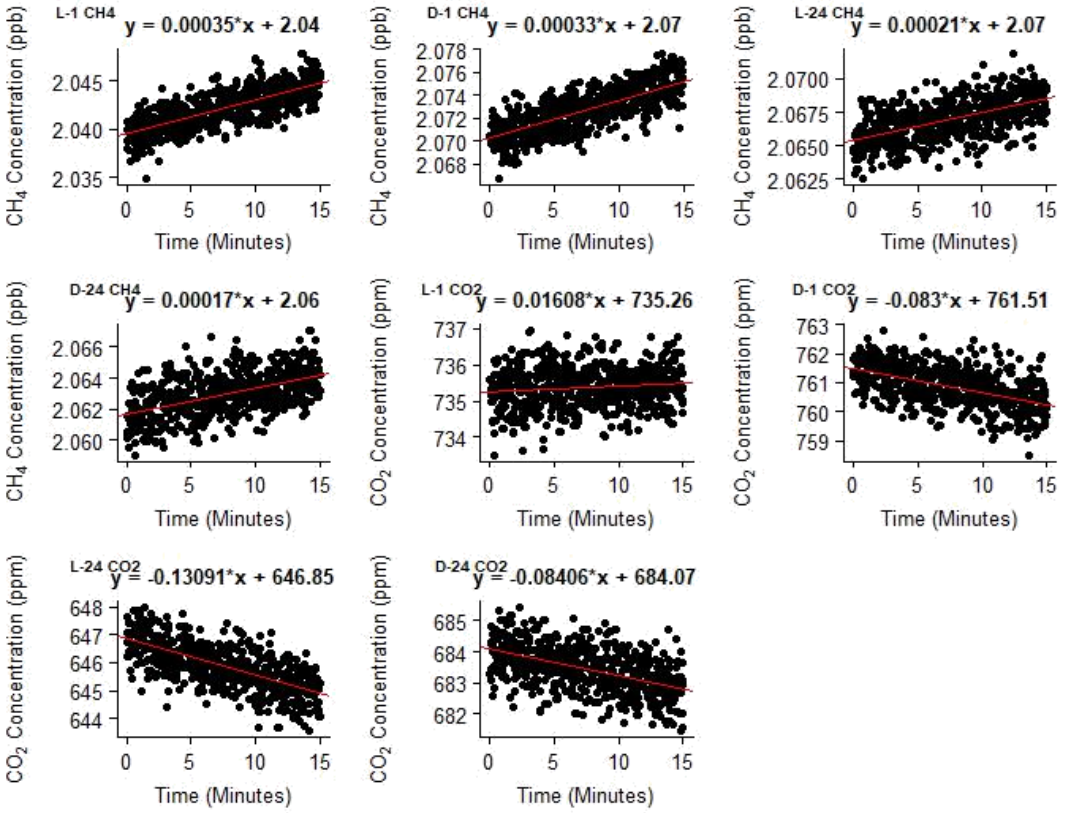

Figure 4.2.3.2 Negative control microcosm flask run 1. Values used to calculate flask experiment correction values. "L" = Light, "D"= Dark, "1" = one hour into run, "24" = twenty four hours after one hour run.

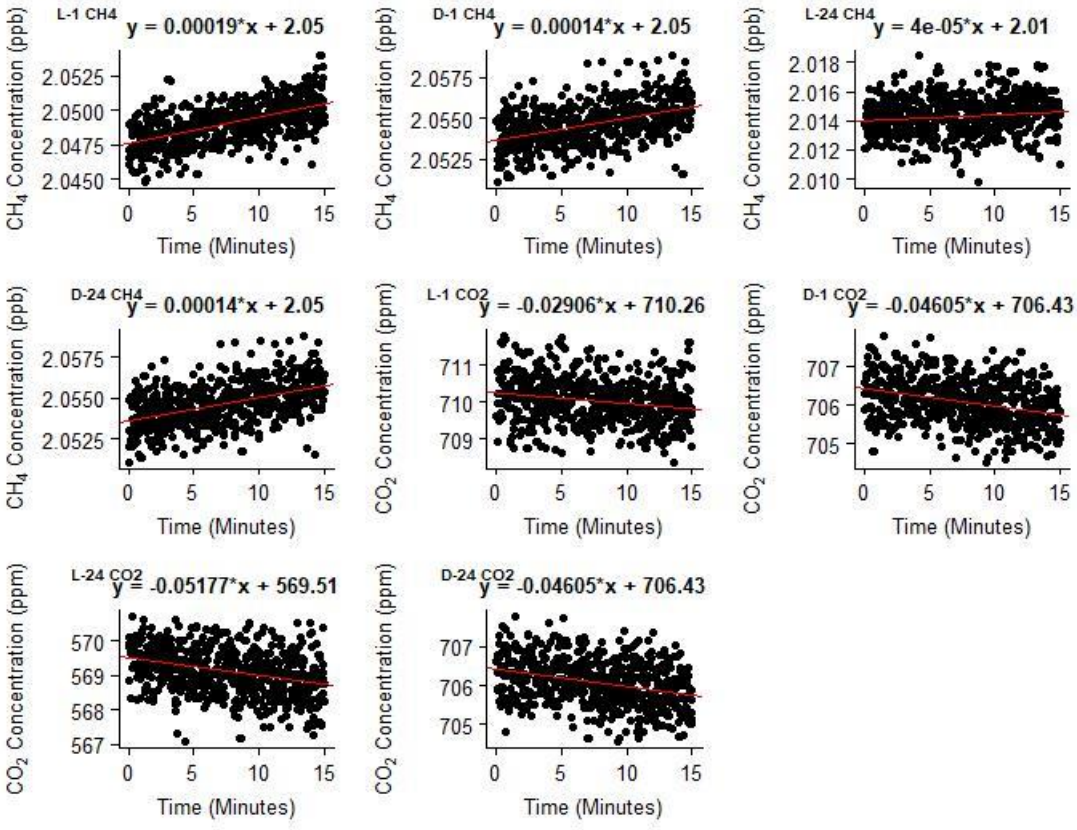

Figure 4.2.3.3 Negative control microcosm flask run 2. Values used to calculate flask experiment correction values. "L" = Light, "D"= Dark, "1" = 1 hour into run, "24" = twenty four hours after 1 hour run.

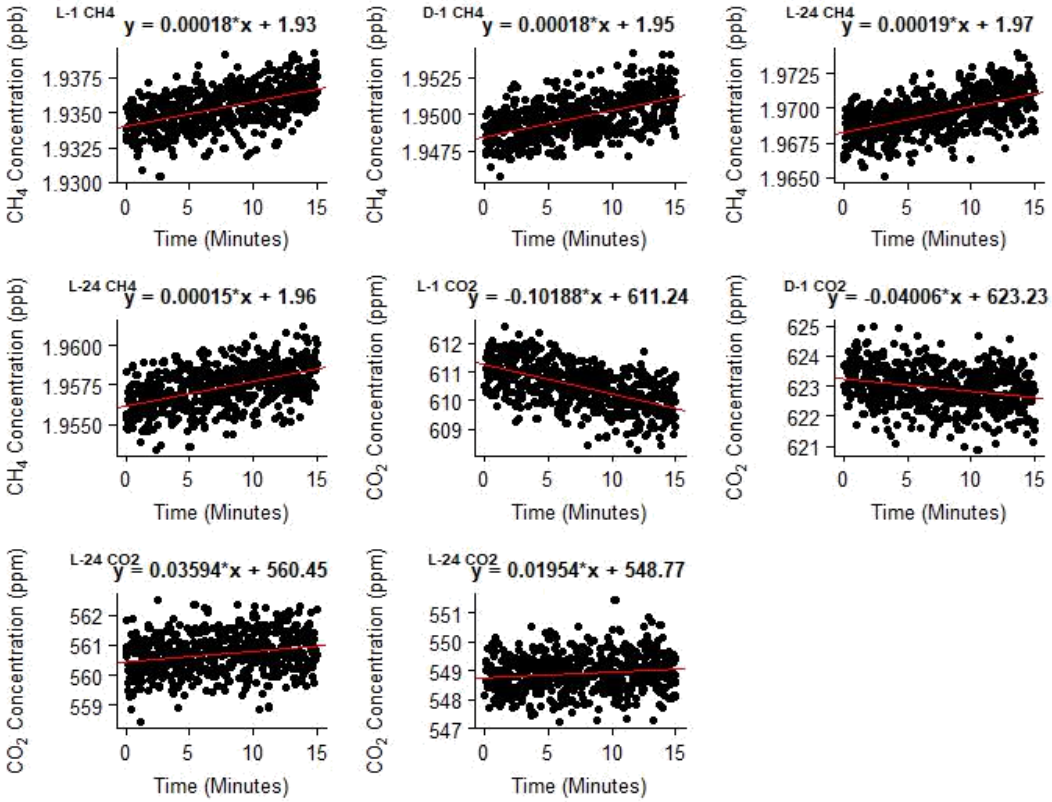

Figure 4.2.3.4 Negative control microcosm flask run 3. Values used to calculate flask experiment correction values. "L" = Light, "D"= Dark, "1" = 1 hour into run, "24" = twenty four hours after 1 hour run.

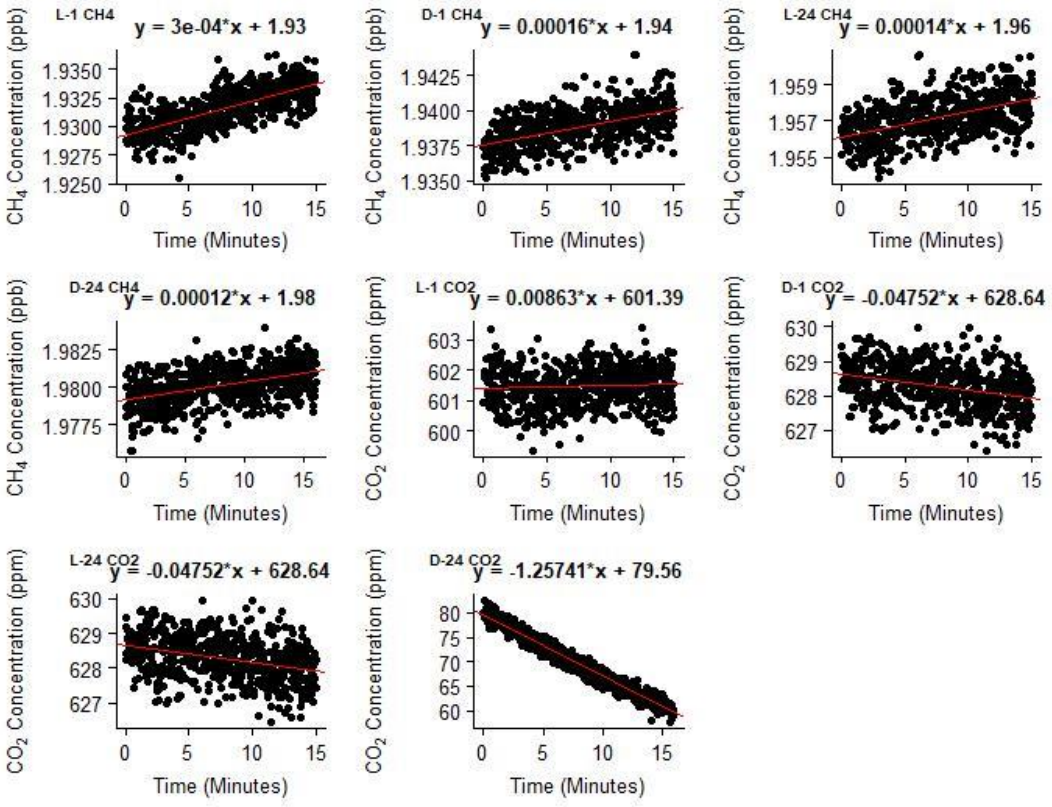

Figure 4.2.3.5 Negative control microcosm flask run 4**.** Values used to calculate flask experiment correction values. "L" = Light, "D"= Dark, "1" = 1 hour into run, "24" = twenty four hours after 1 hour run.

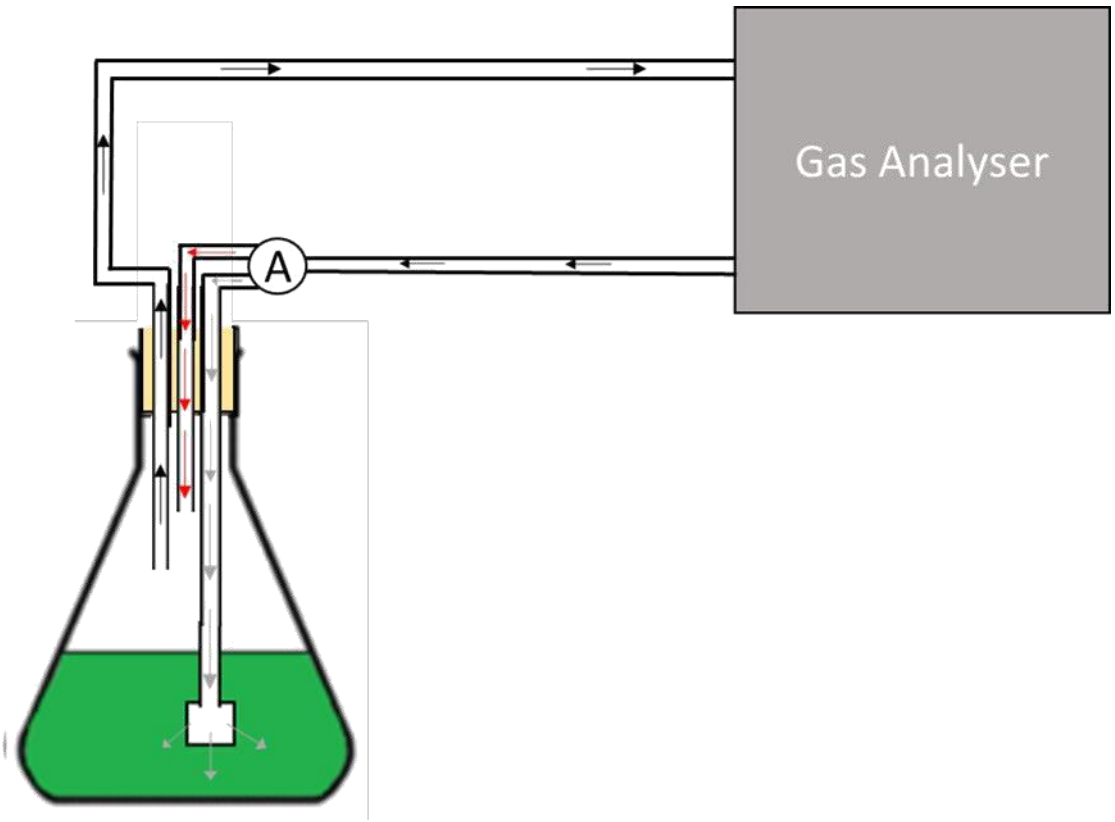

Figure 4.2.3.6 Diagram illustrating an alternative method of microcosm headspace analysis using valve 'A' to divert gas analyser output from bubbling the water column (grey arrows) to the microcosm headspace (red arrows). As a result, rates of flux from the sample can be recorded without the immediate effect of bubbling, which is still used for gas concentrations in the sample to equilibrate with the headspace beforehand.

4.3 Field Campaign Supplementary Materials

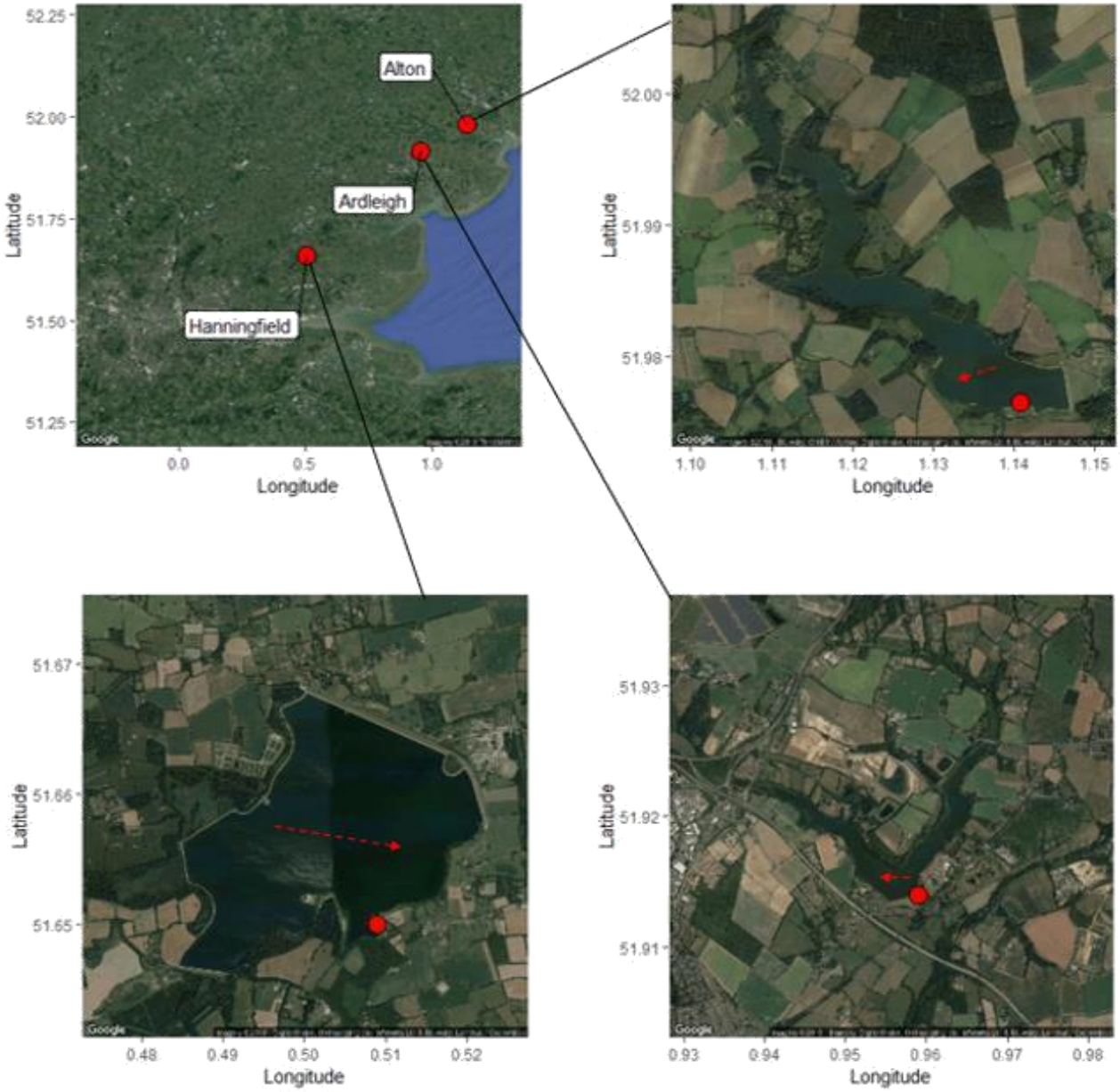

Figure 4.3.1 Satellite illustration of reservoirs and sample sites. Red points on the top left image depict the reservoirs sampled. Red points on the bottom left, right and to right images shows the littoral sample sites. Dashed arrows on these images show the course and direction of pelagic drift samples. Maps were created in R version 3.4.2 using ggmaps.

Figure 4.3.2 photographic illustrations of carbon flux sampling. Pictures in section 'a.)' display floating chamber pelagic drift deployed from the side of a boat. Picture in section 'b.)' display floating chamber littoral loosely tethered sampling deployed from the side of a pontoon.

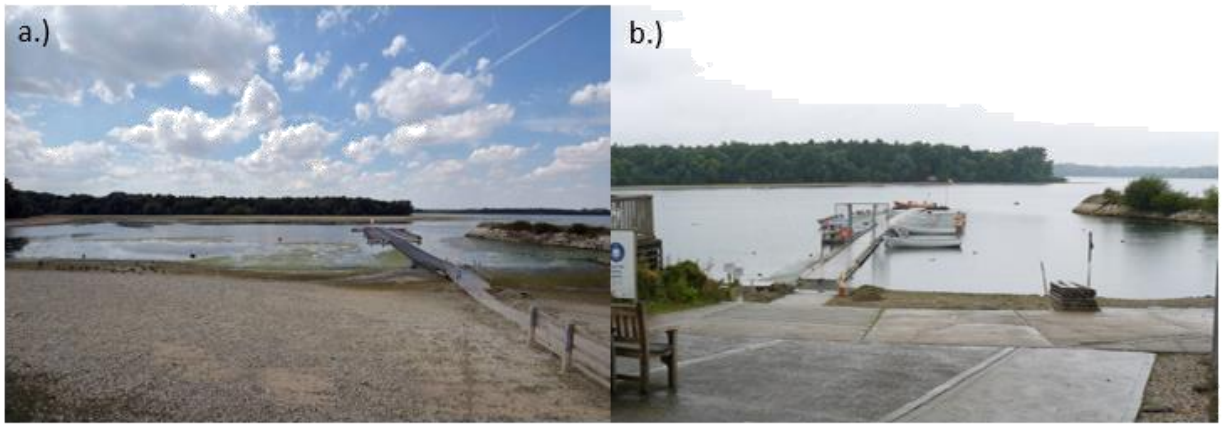

Figure 4.3.3 Photographs of Hanningfield reservoir illustrating reduced shorelines of ~15 to 20m during the summer of 2018 (a.) compared to high water in the winter (b.). Images of the Jetty in lodge bay facing west.

Figure 4.3.4 Photographs of Ladybower reservoir illustrating drastically reduced shorelines during the summer (a.) compared to high water in the winter (b.) of 2018. Images taken from the Derby Telegraph (Reid., 2018).

Table 4.3.1 Mean physicochemical conditions sampled from each reservoir summer 2018. n=16 for each reservoir.

	Whole Reservoir		
Condition	**Hanningfield**	**Alton**	**Ardleigh**
POC (mg/L)	9.156	5.711	0.062
DOC (mg/L)	12.376	11.699	11.054
DIC (mg/L)	31.169	25.481	32.130
TC (ug/L)	54.547	45.283	47.286
DIN (ug/L)	2524.460	2471.600	2593.395
Dissolved Ammonium (ug/L)	569.508	56.007	168.392
Nitrogen Dioxide (ug/L)	458.004	179.220	310.548
Dissolved Nitrate (ug/L)	1496.949	2236.300	2114.456
Dissolved Silicate (ug/L)	7749.376	7234.800	6000.825
Dissolved Phosphate (ug/L)	285.772	22.436	34.198
Particulate Phosphate (ug/L)	7216.576	4155.200	3384.178
Chlorophyll-a (ug/L)	50.654	30.877	15.233
Phaeopigments (ug/L)	-0.016	-0.031	-0.052
pH	8.779	8.234	7.772
Secchi depth (m)	1.141	0.525	1.340
Water temperature (^{O}C)	22.429	25.013	20.244

Table 4.3.2 Mean atmospheric conditions of each reservoir throughout sampling summer 2018. Data taken from nearby weather stations taking part in the wunderground.com weather project.

Condition	**Hanningfield** (Tattingstone WS)	**Alton** (Wickford WS)	**Ardleigh** (St. Johns WS)
Atmospheric Temperature (^{O}C)	23.863	20.7	21.811
Wind speed (Km/h)	2.511	12.7625	2.4
Wind direction	W	SE	E
Pressure (hPa)	1017.142	1015.913	1017.444
Weather Station (WS) Coordinates	51.624, 0.519714	51.988, 1.114	51.908, 0.928738

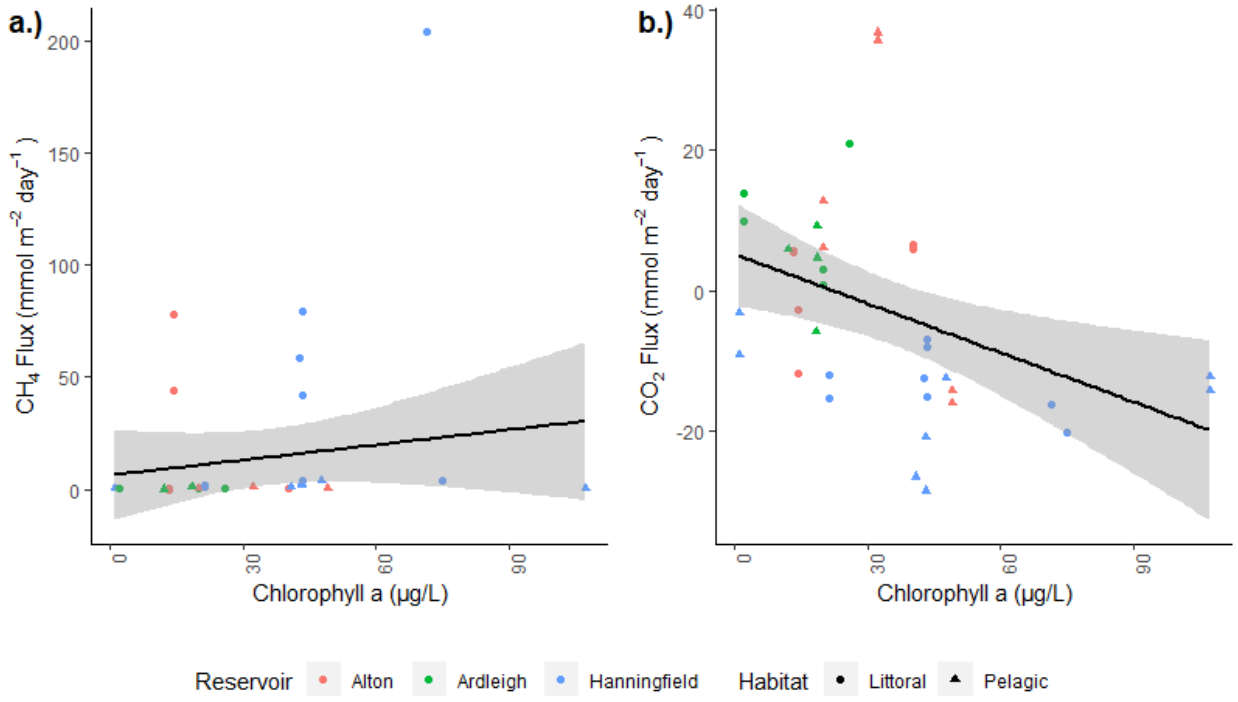

Figure 4.3.5 Illustration of CH_4 and CO_2 rate of flux (mmol m^{-2} day^{-1}) against Chlorophyll concentration. Points display pelagic and littoral habitats and reservoir investigated. Measurements were taken from May to September 2018. CH_4 fluxes have been temperature corrected to 16ºC. Error bars represent standard error. n=8.

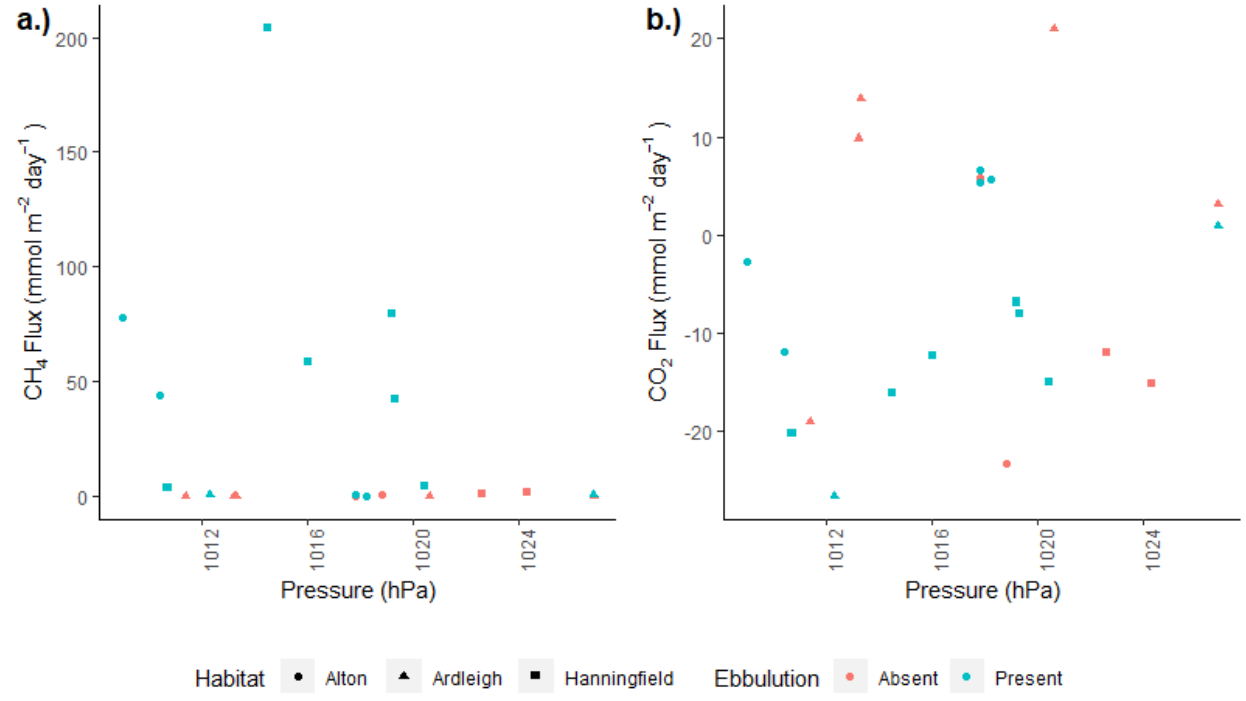

Figure 4.3.6 Illustration of CH_4 and CO_4 rate of flux (mmol m^{-2} day^{-1}) against atmospheric pressure and the presence of ebullition. Points display pelagic and littoral habitats and reservoir investigated. Measurements were taken from May to September 2018. CH_4 fluxes have been temperature corrected to 16ºC. Error bars represent standard error. n=8.

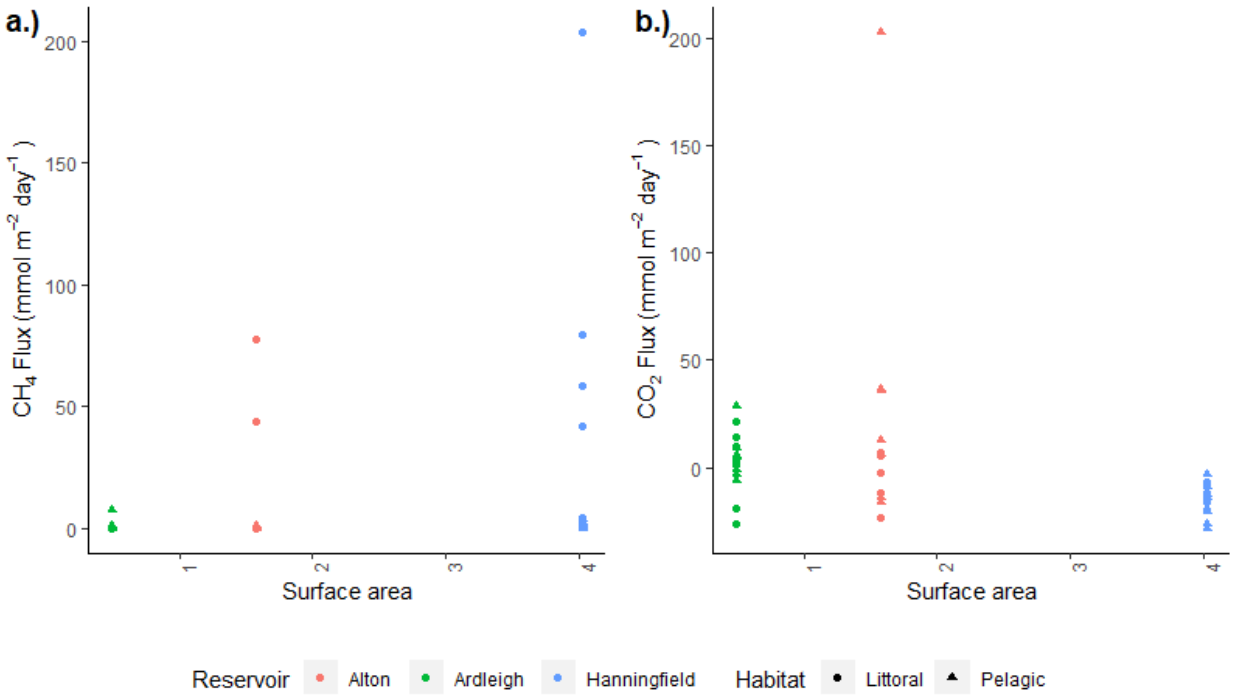

Figure 4.3.7 Illustration of CH_4 and CO_4 rate of flux (mmol m^2 day^{-1}) against reservoir surface area. Points display pelagic and littoral habitats and reservoir investigated. Measurements were taken from May to September 2018. CH_4 fluxes have been temperature corrected to 16°C. Error bars represent standard error. n=8.

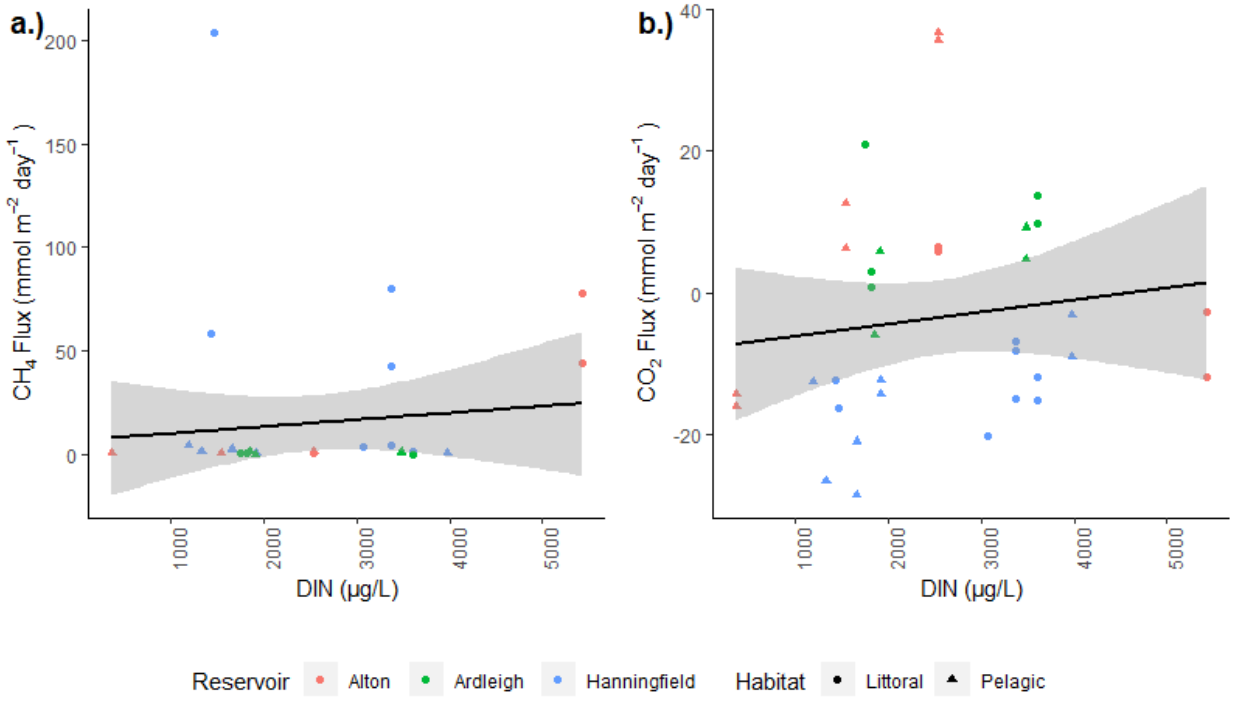

Figure 4.3.8 Illustration of CH_4 and CO_2 rate of flux (mmol m^{-2} day^{-1}) against dissolved inorganic nitrogen (DIN). Points display pelagic and littoral habitats and reservoir investigated. Measurements were taken from May to September 2018. CH_4 fluxes have been temperature corrected to 16°C. Error bars represent standard error. n=8

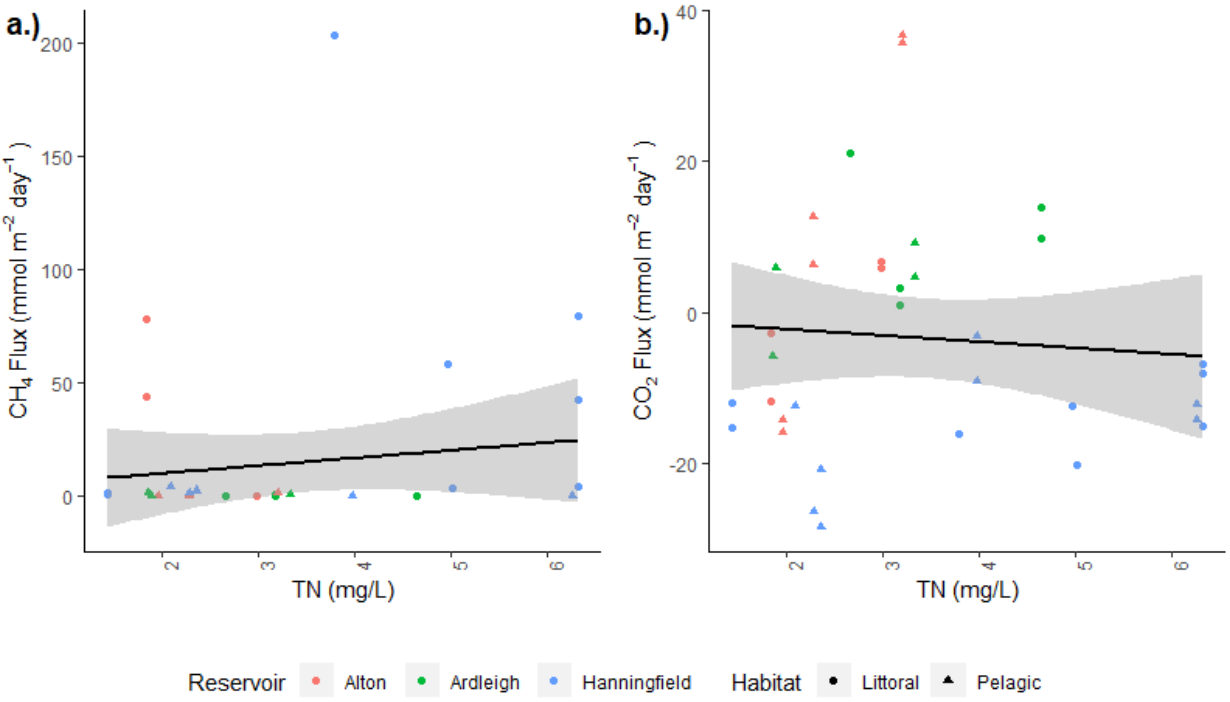

Figure 4.3.9 Illustration of CH_4 and CO_2 rate of flux (mmol m^{-2} day^{-1}) against total nitrogen (TN). Points display pelagic and littoral habitats and reservoir investigated. Measurements were taken from May to September 2018. CH_4 fluxes have been temperature corrected to 16ºC. Error bars represent standard error TN may have been affected by storage time. n=8.

4.4 Microcosm Experiment Supplementary Materials

Figure 4.4.1 a.) Photograph of 20 litre carboy with sample taken from the littoral zone of reservoirs for microcosm flask experiments. Carboy is filled to 10 litres to allow headspace for gas exchange with the water sample. b.) Photograph of the conical flasks forming the microcosms for the experiment, incubating at 16^{o}C before the application of treatments and ensuing headspace gas analyses.

4.4.1 Cellobiose Treatment Results

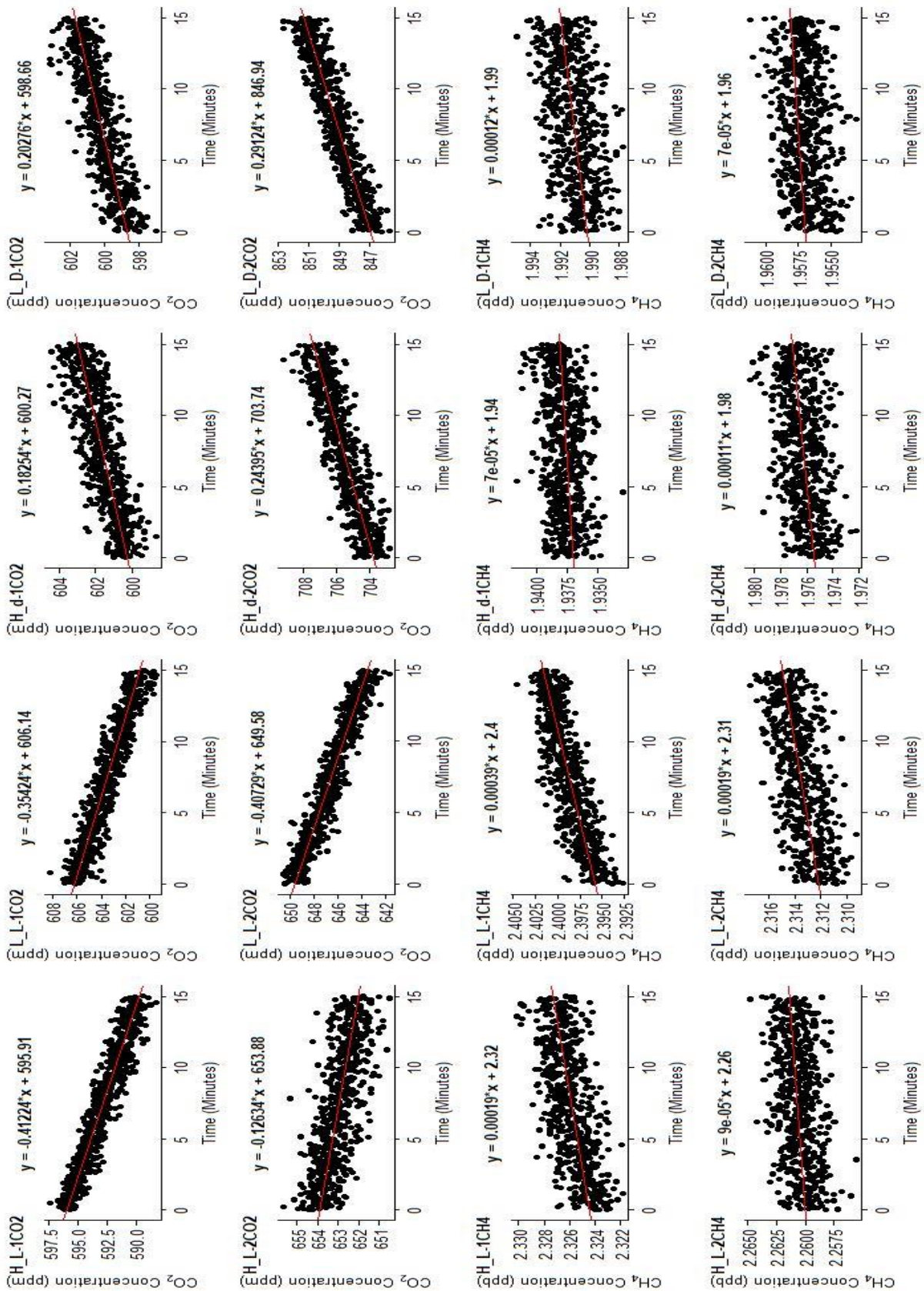

Figure 4.4.1.1 Alton sample microcosm rate extraction graphs. Cellobiose treatment 1 hour after treatment addition.

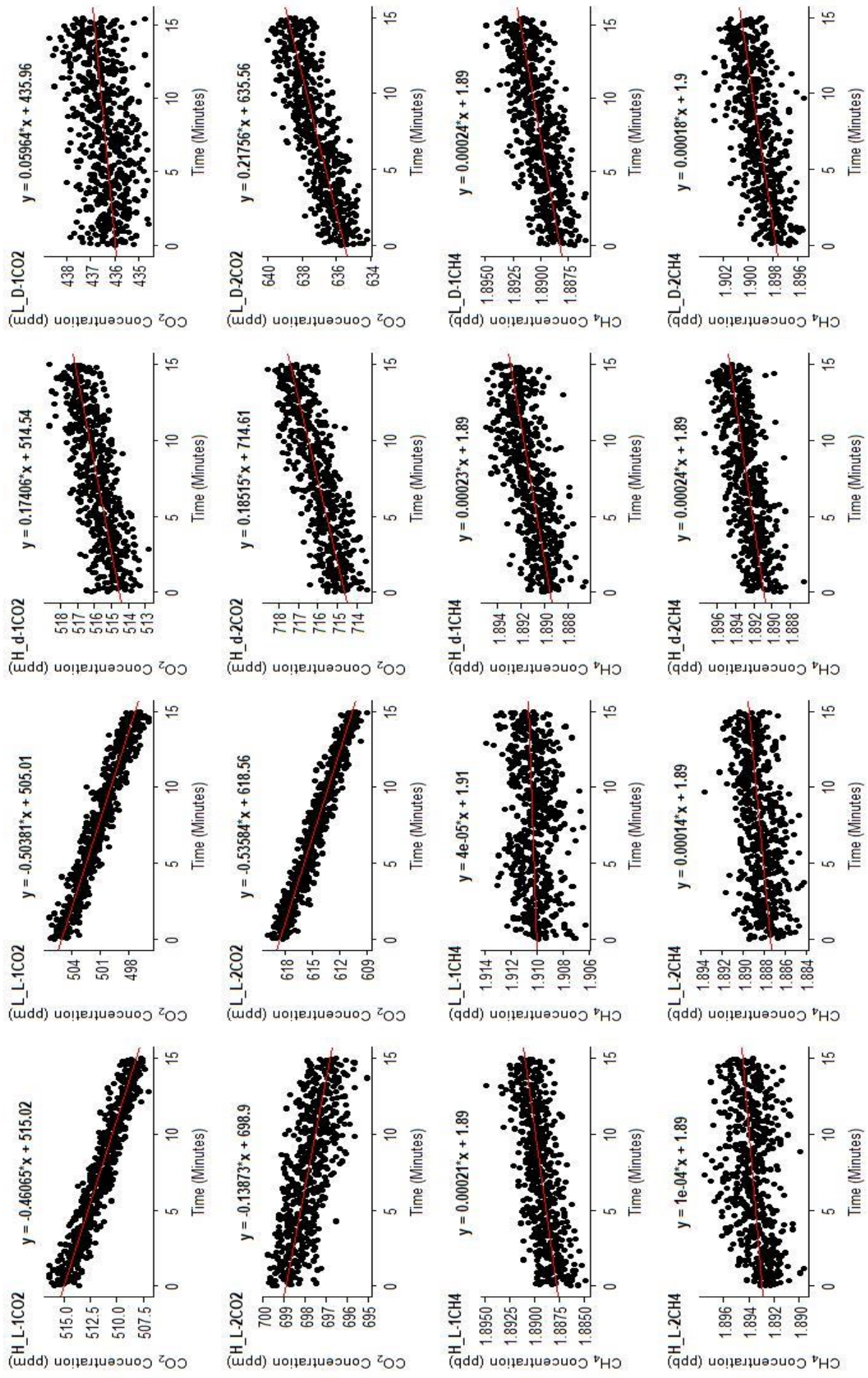

Figure 4.4.1.2 Alton sample microcosm rate extraction graphs. Cellobiose treatment twenty-four hours after treatment addition.

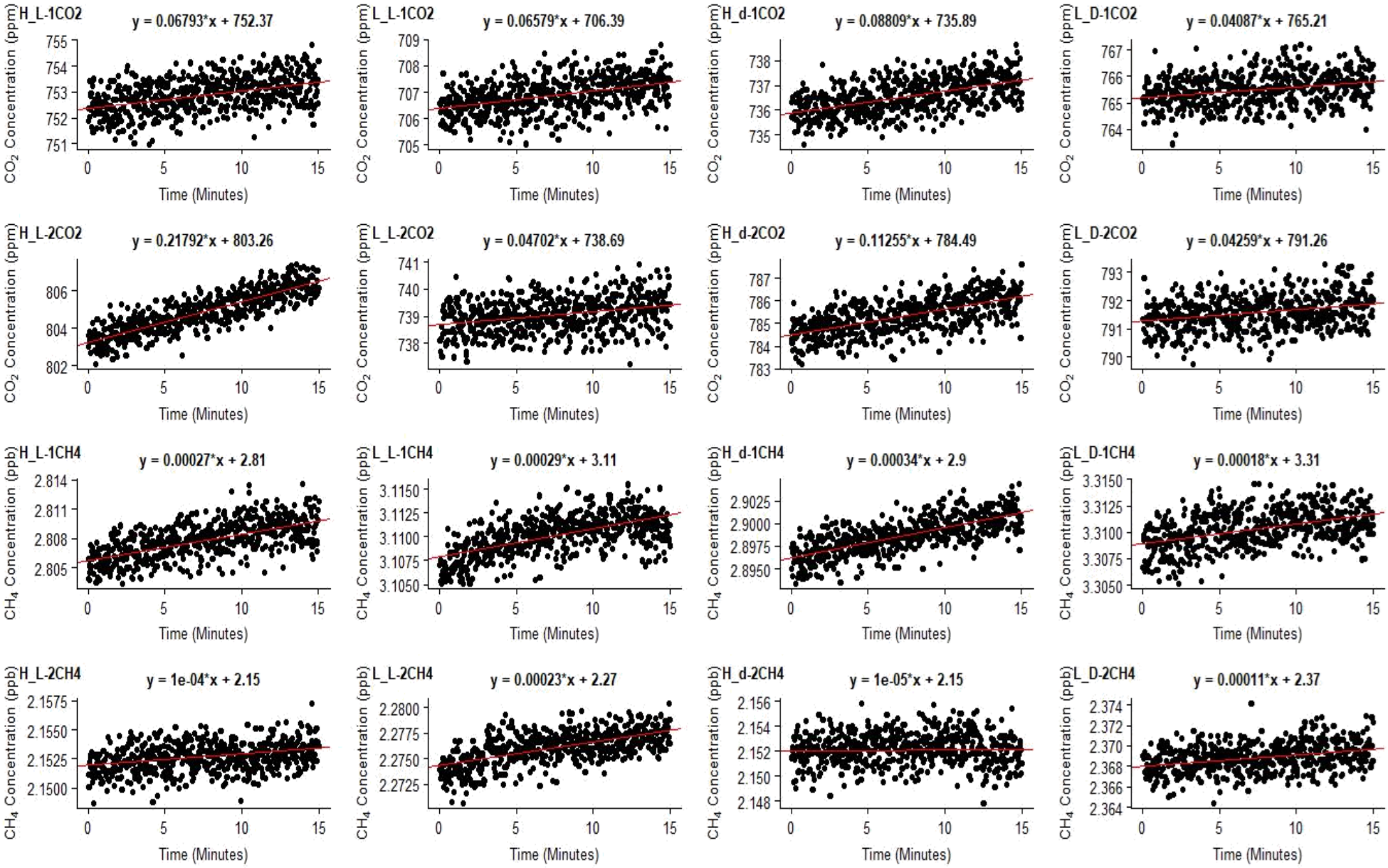

Figure 4.4.1.3 Ardleigh sample microcosm rate extraction graphs. Cellobiose treatment one hour after treatment addition.

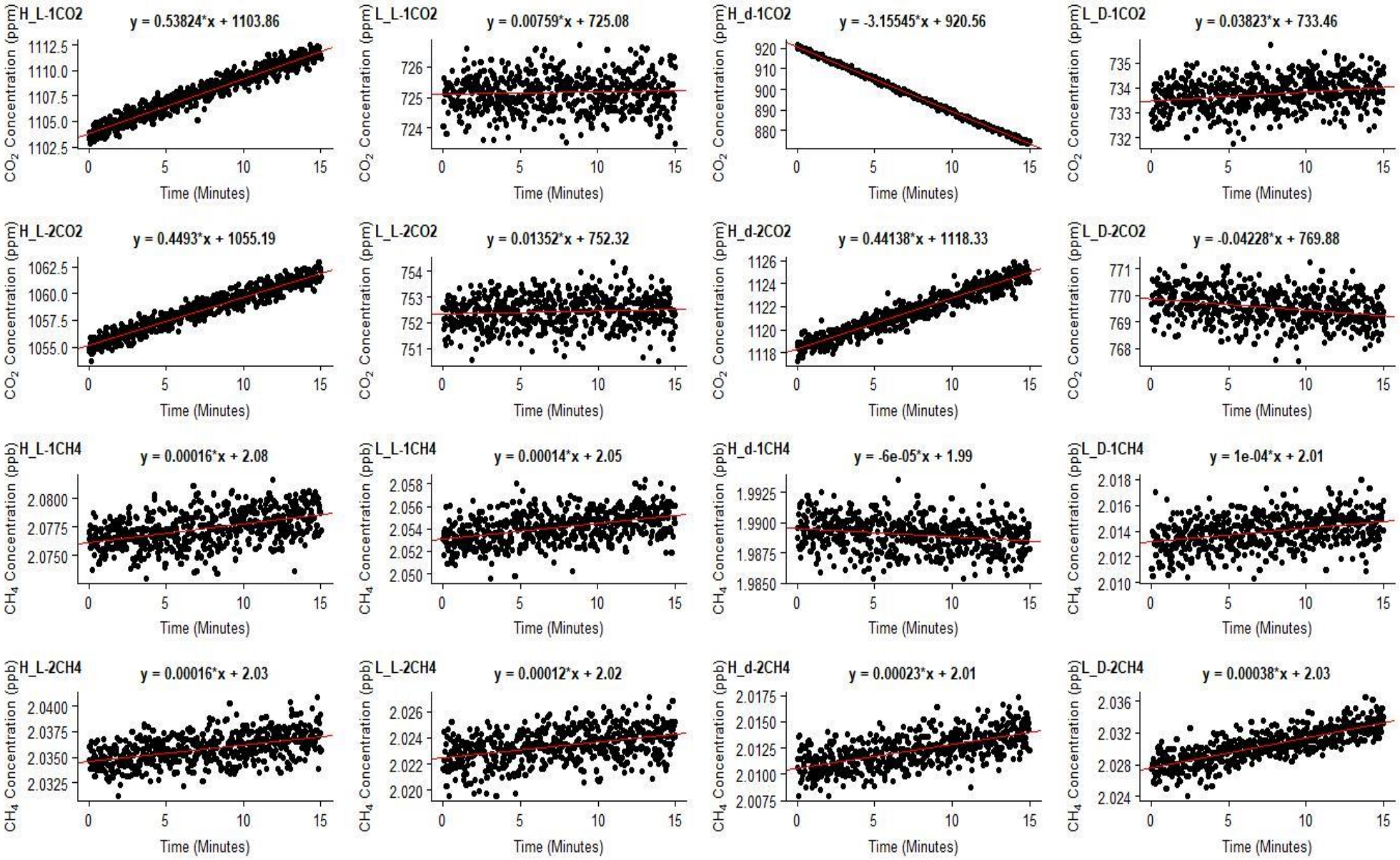

Figure 4.4.1.4 Ardleigh sample microcosm rate extraction graphs. Cellobiose treatment twenty-four hours after treatment

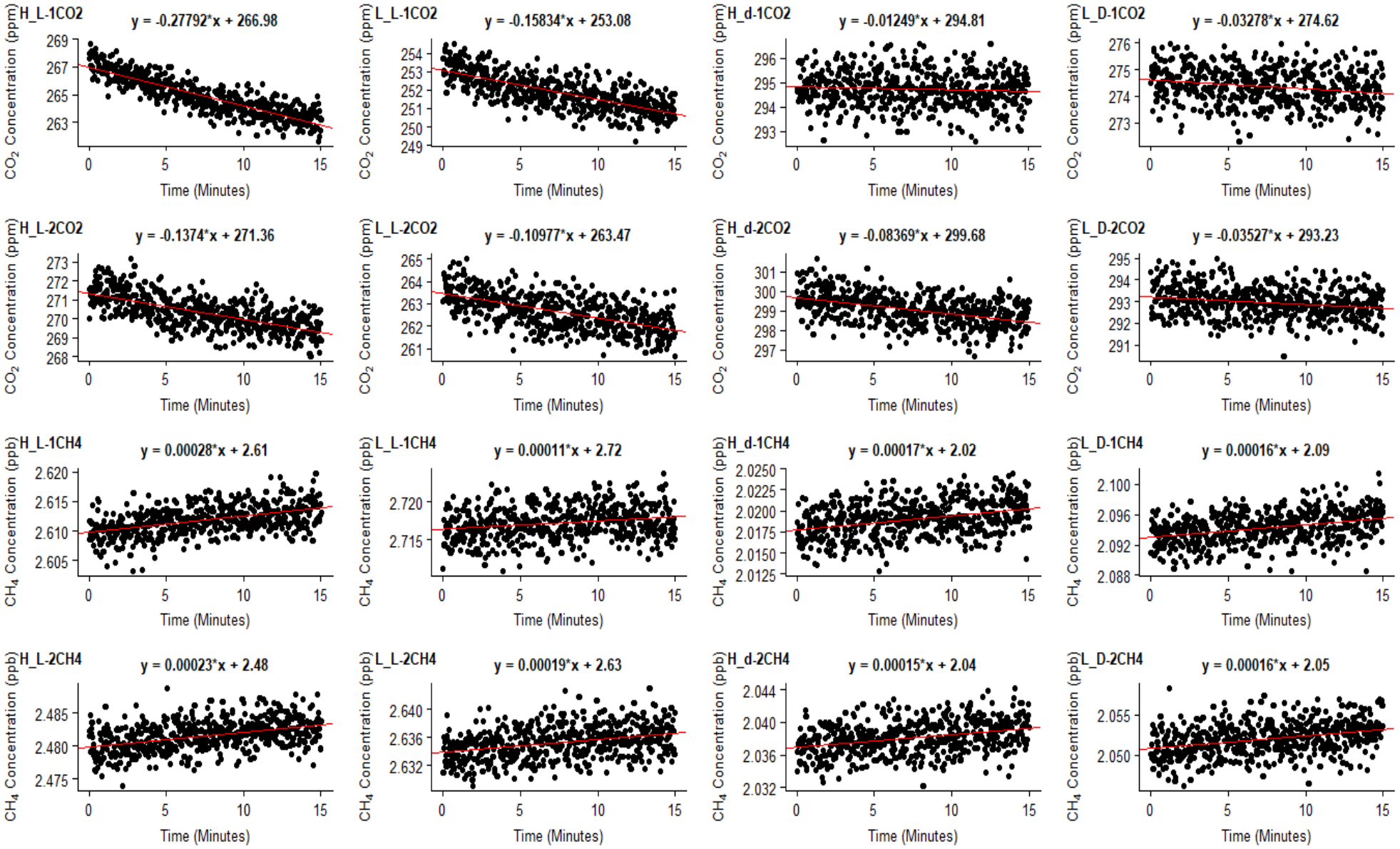

Figure 4.4.1.5 Hanningfield sample microcosm rate extraction graphs. Cellobiose treatment one hour after treatment addition.

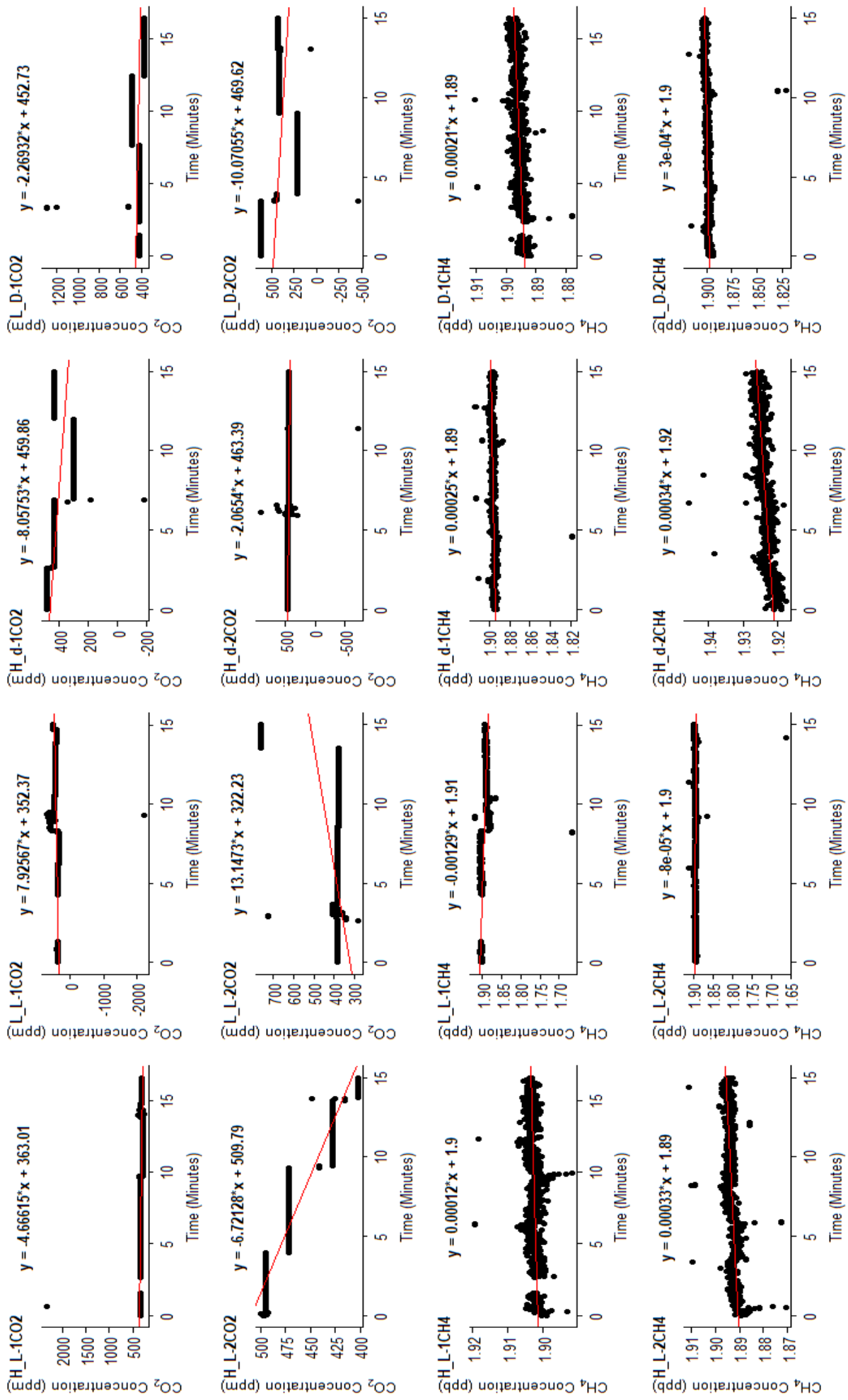

Figure 4.4.1.6 Hannningfield sample microcosm rate extraction graphs. Cellobiose treatment twenty-four hours after treatment addition.

4.4.2 Acetate Treatment Results

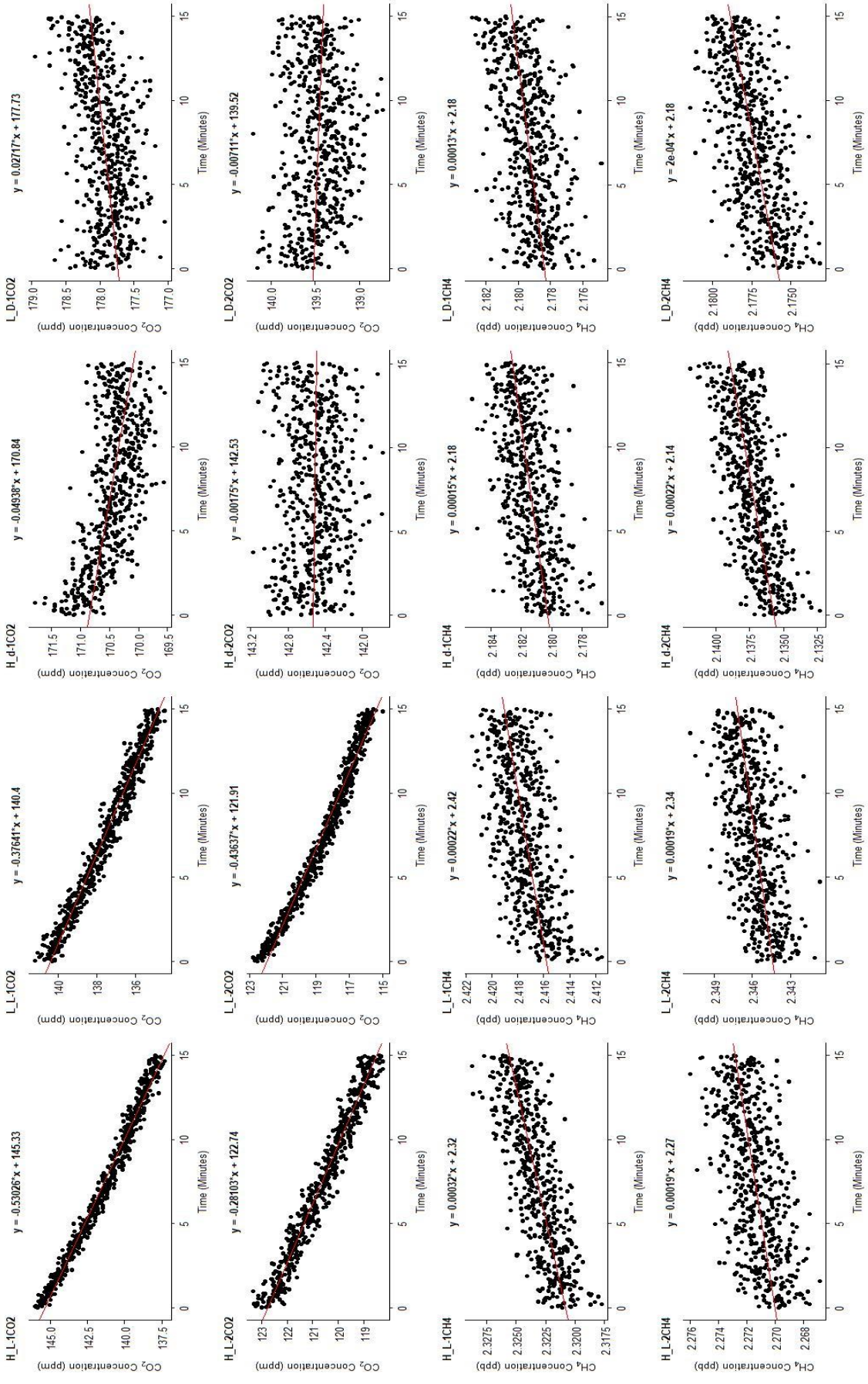

Figure 4.4.2.1 Alton sample microcosm rate extraction graphs. Acetate treatment one hour after treatment addition.

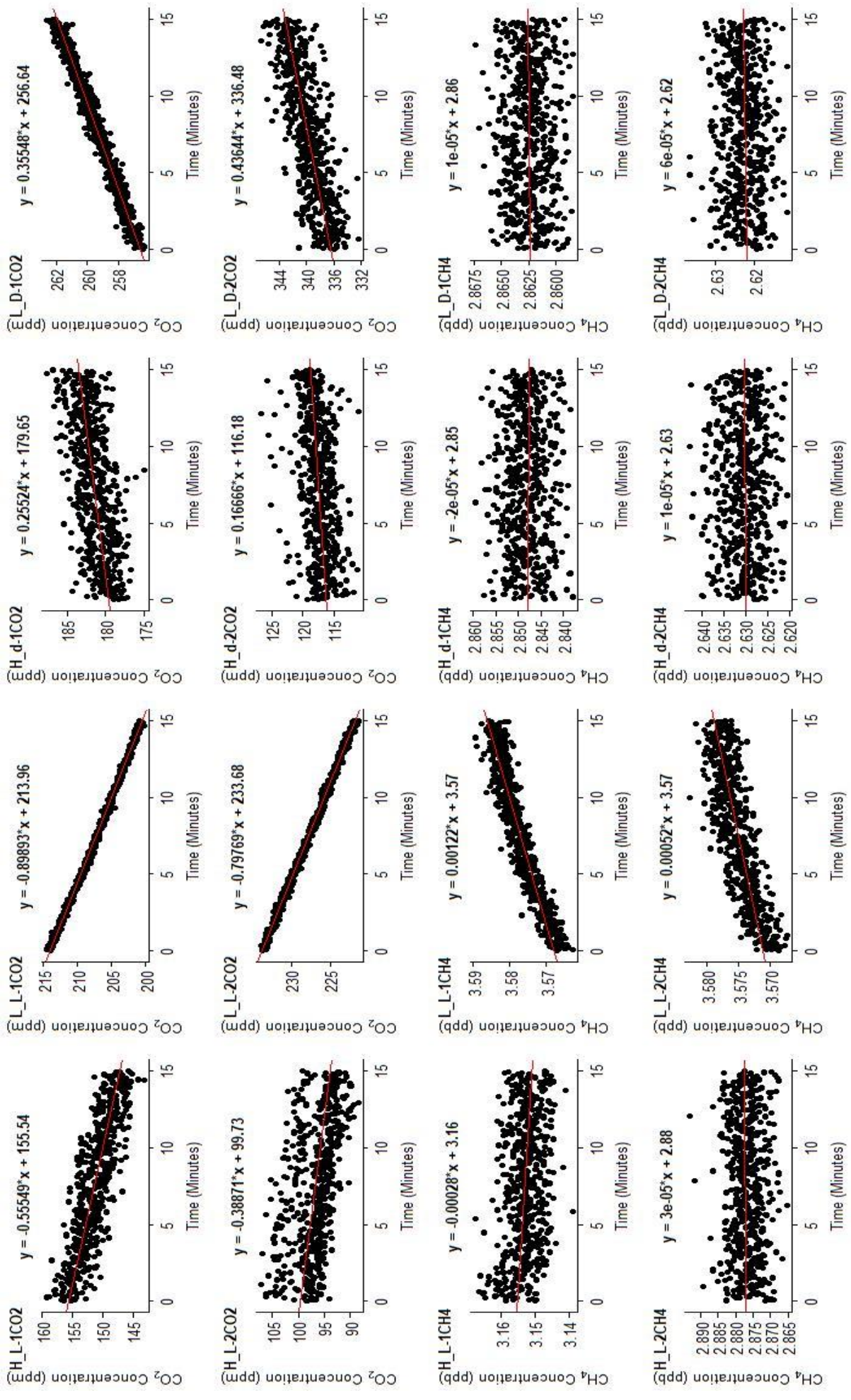

Figure 4.4.2.2 Alton sample microcosm rate extraction graphs. Acetate treatment twenty-four hours after treatment addition.

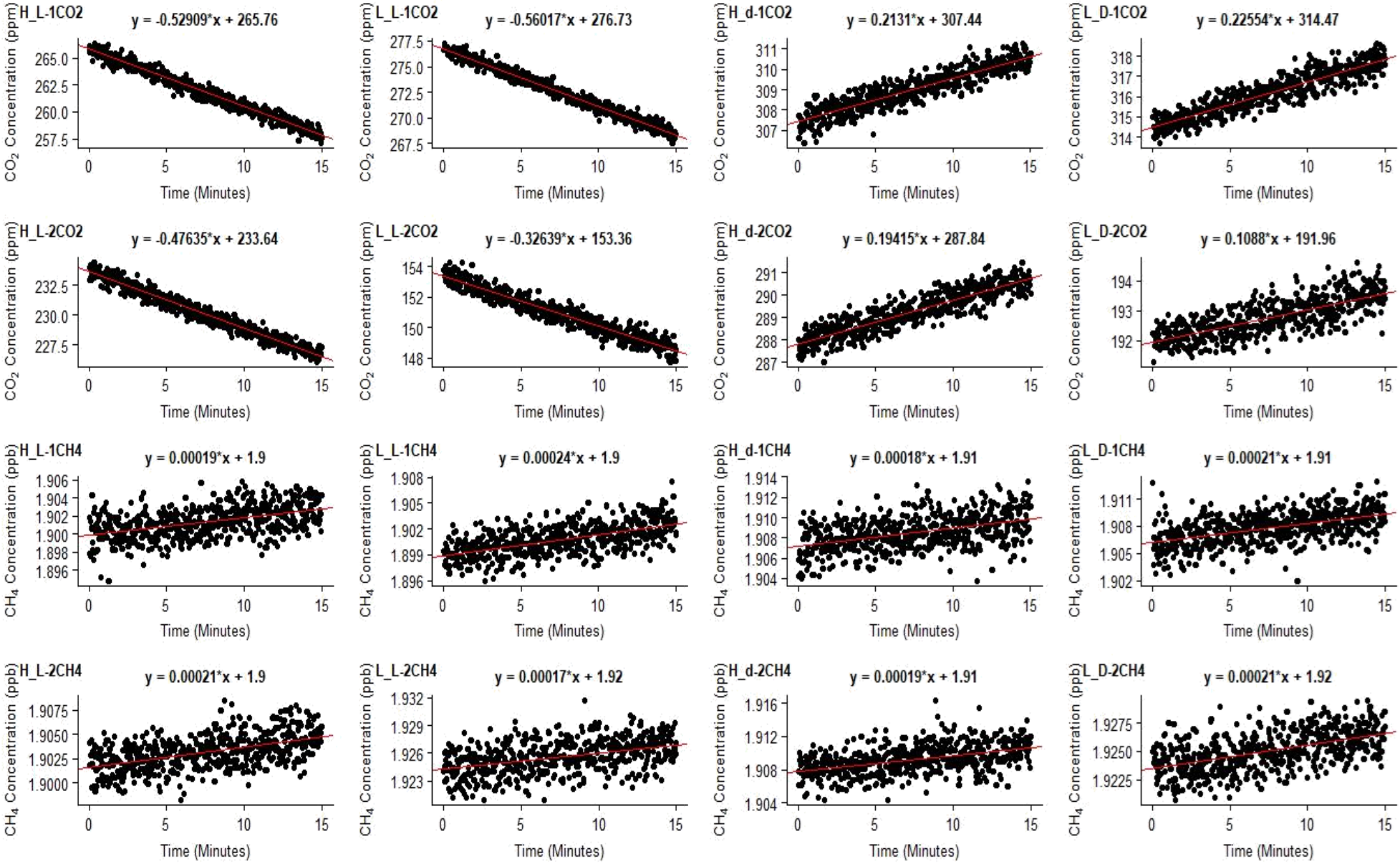

Figure 4.4.2.3 Ardleigh sample microcosm rate extraction graphs. Acetate treatment one hour after treatment addition.

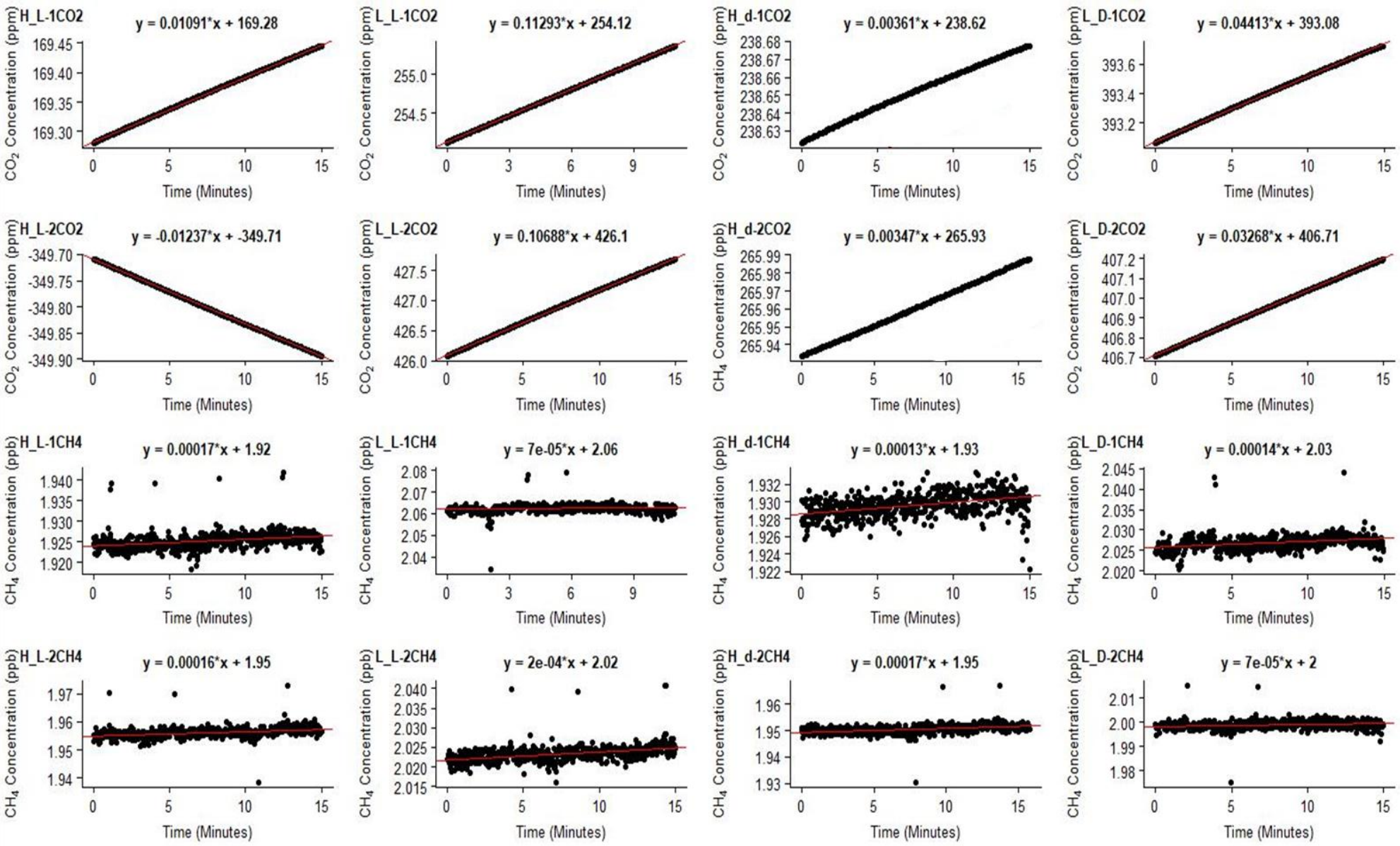

Figure 4.4.2.4 Ardleigh sample microcosm rate extraction graphs. Acetate treatment twenty-four hours after treatment addition.

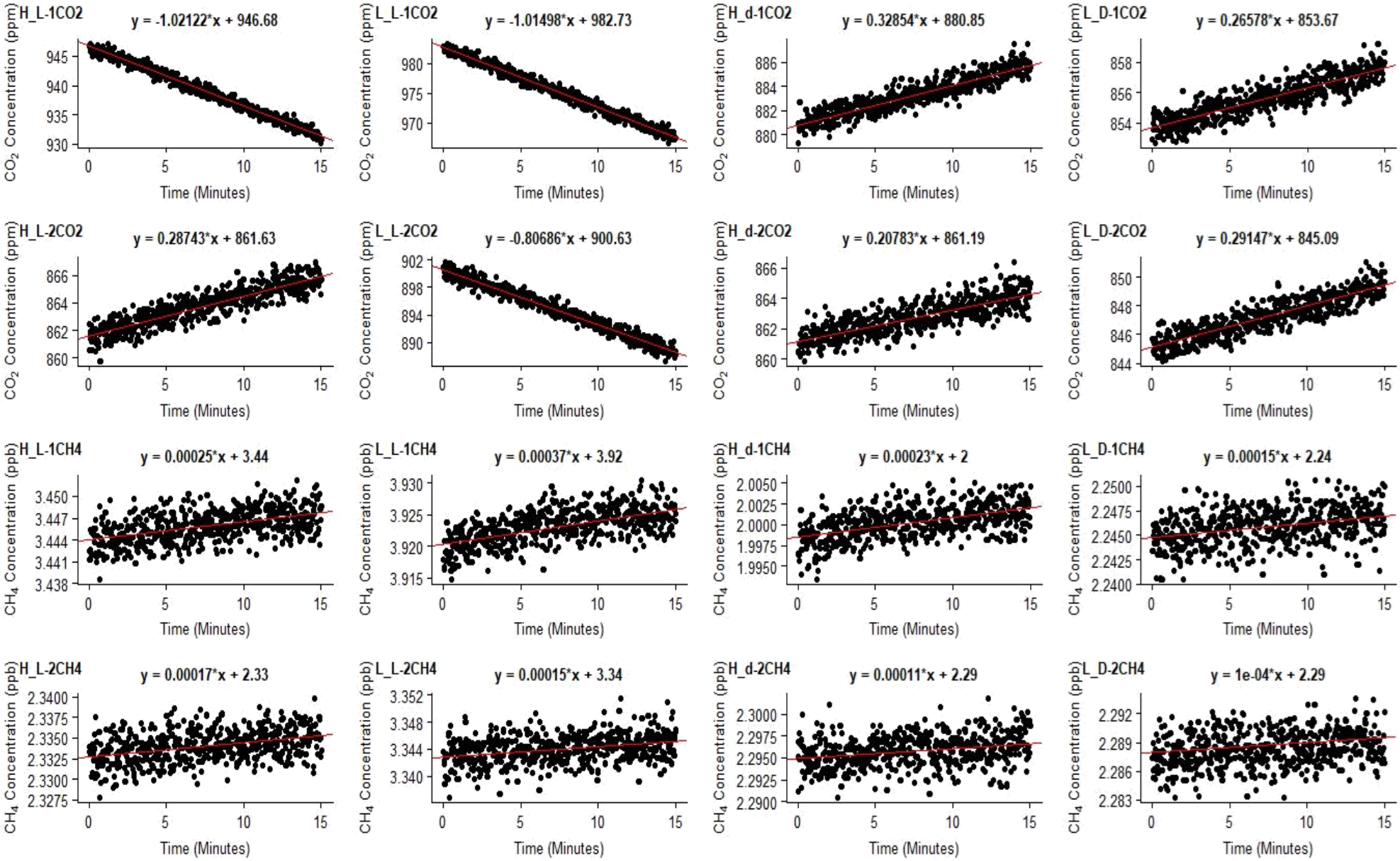

Figure 4.4.2.5 Hanningfield sample microcosm rate extraction graphs. Acetate treatment one hour after treatment addition.

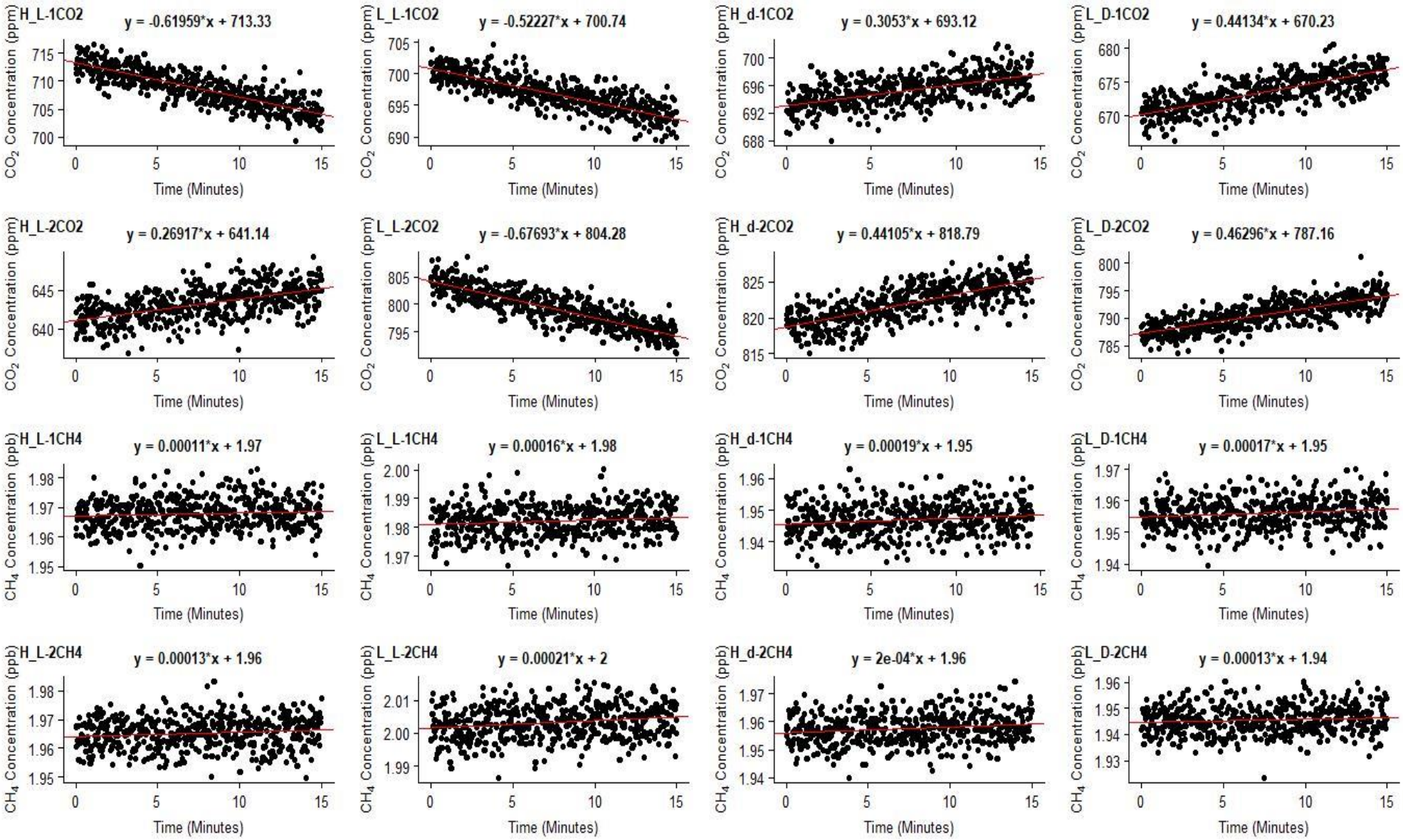

Figure 4.4.2.6 Hanningfield sample microcosm rate extraction graphs. Acetate treatment twenty-four hours after treatment addition.

4.4.3 Phosphate Treatment Results

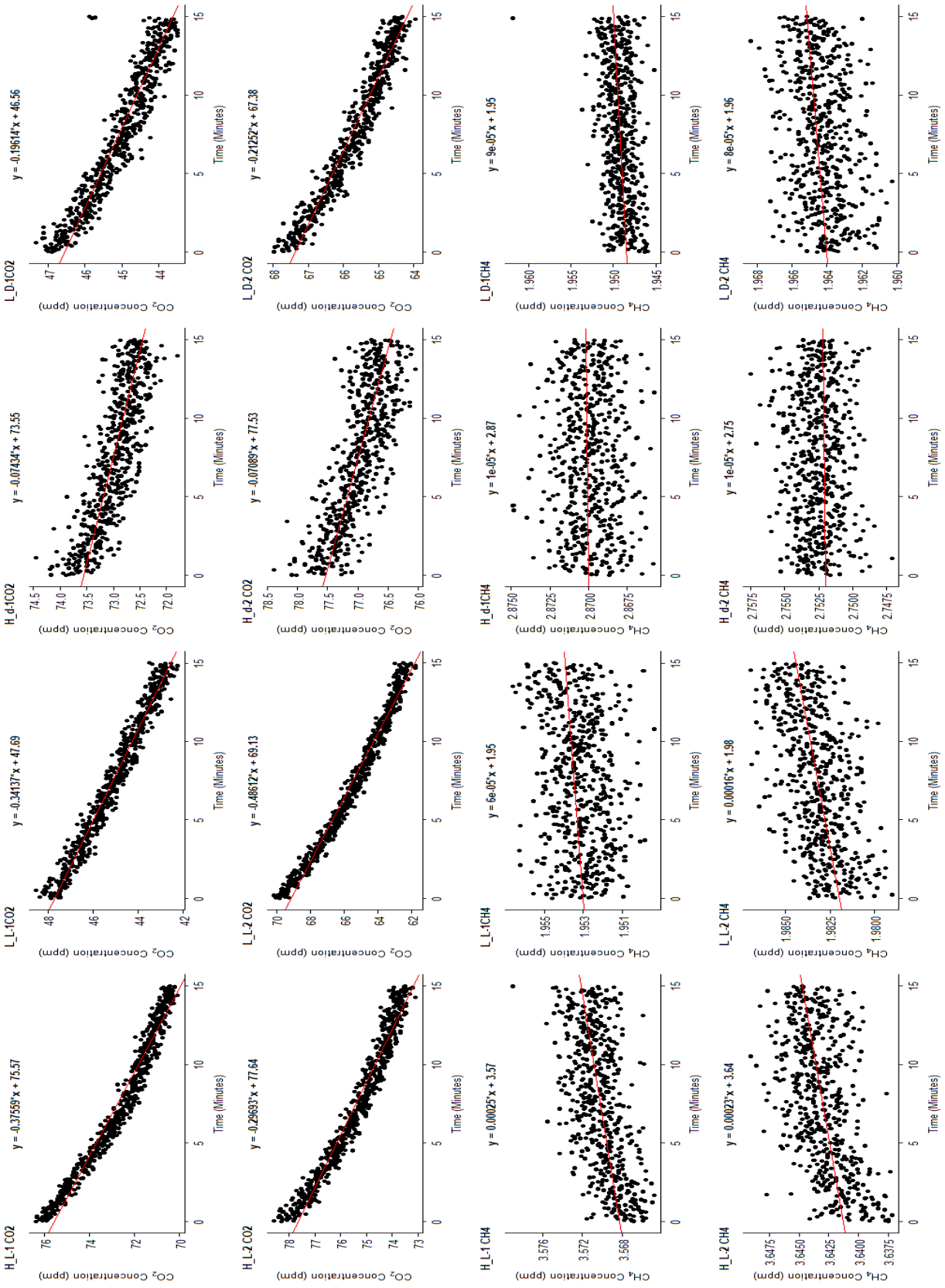

Figure 4.4.3.1 Hanningfield sample microcosm rate extraction graphs. Phosphate treatment one hour after treatment addition.

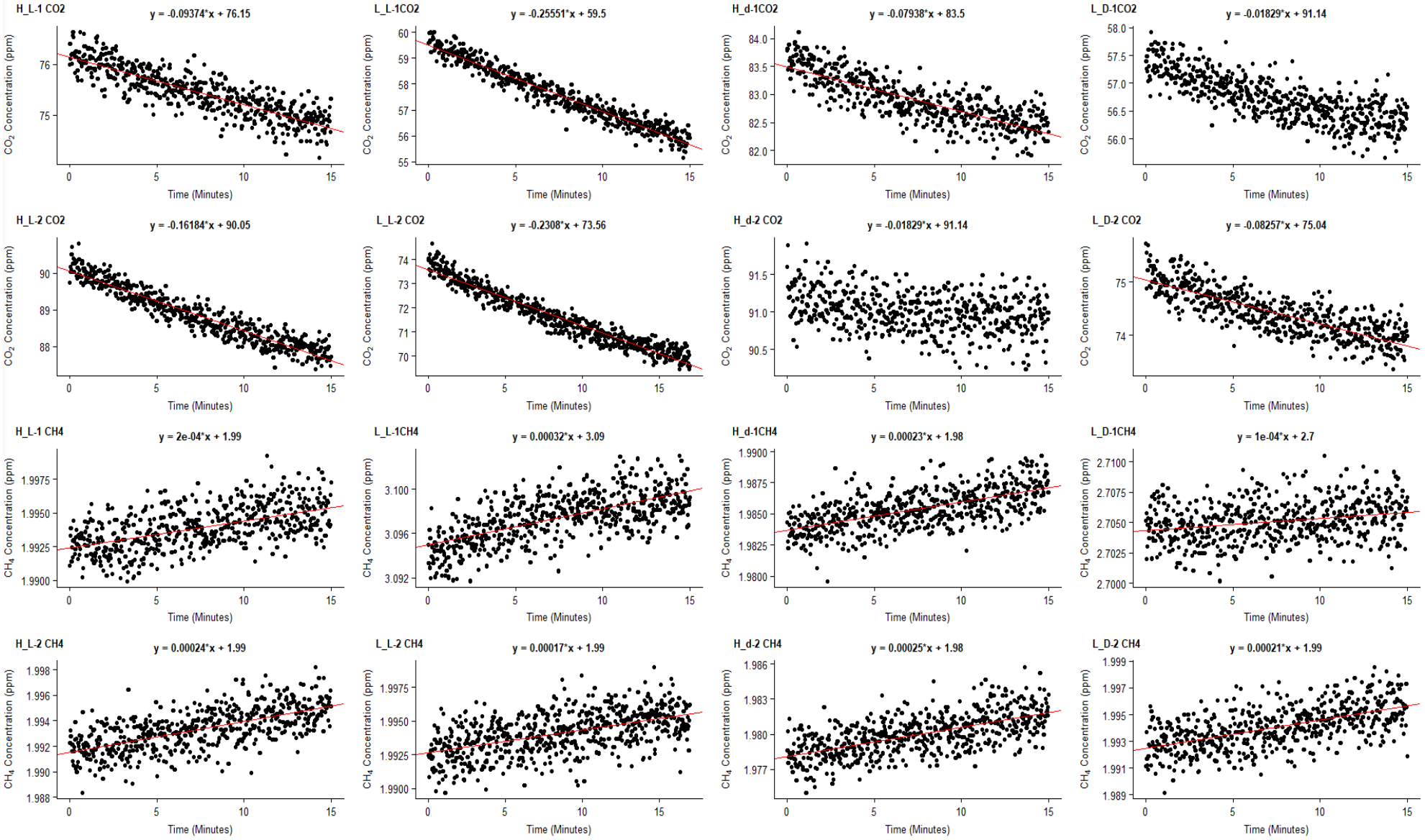

Figure 4.4.3.2 Hanningfield sample microcosm rate extraction graphs. Phosphate treatment twenty-four hours after treatment addition.

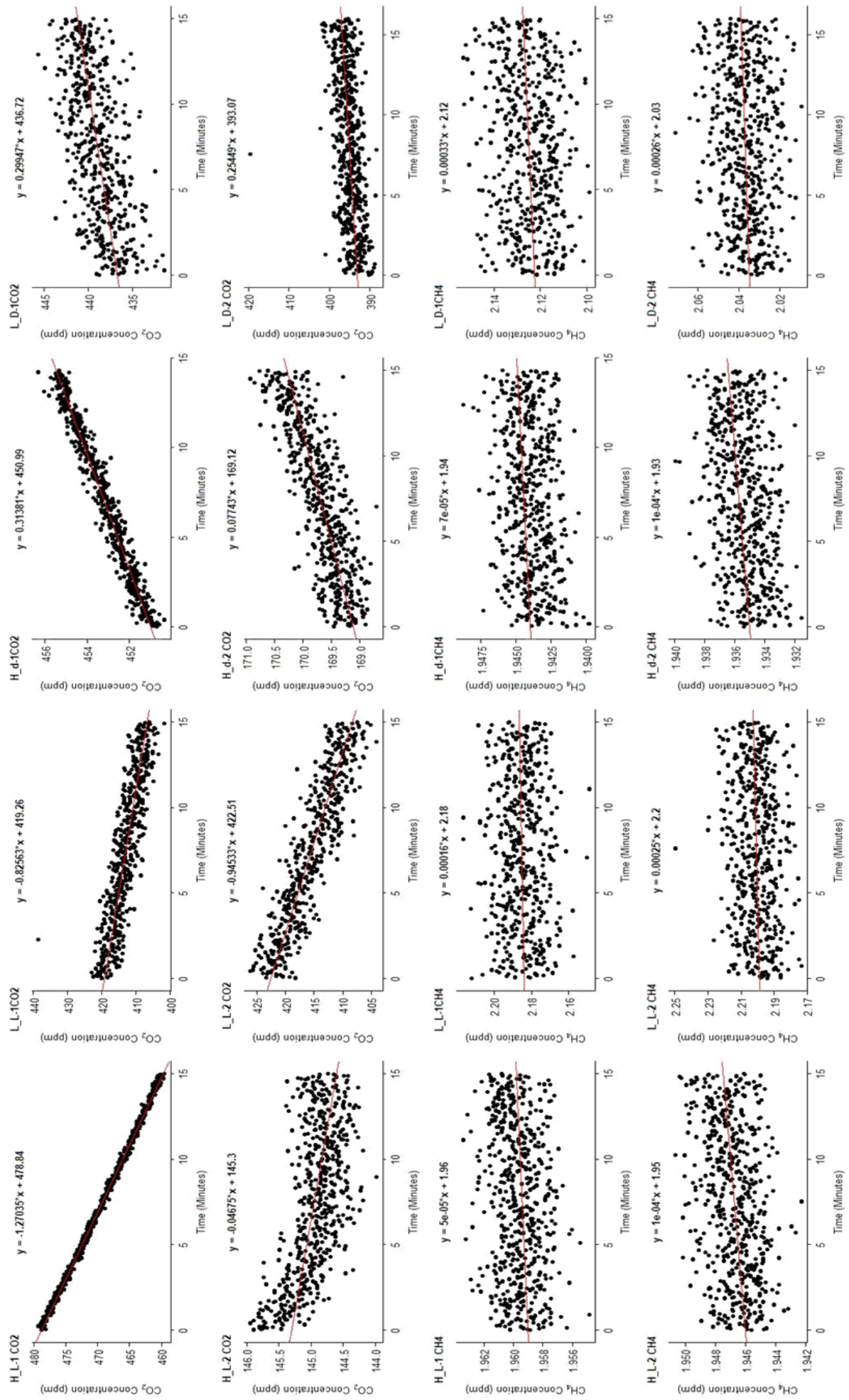

Figure 4.4.3.3 Ardleigh sample microcosm rate extraction graphs. Phosphate treatment one hour after treatment addition.

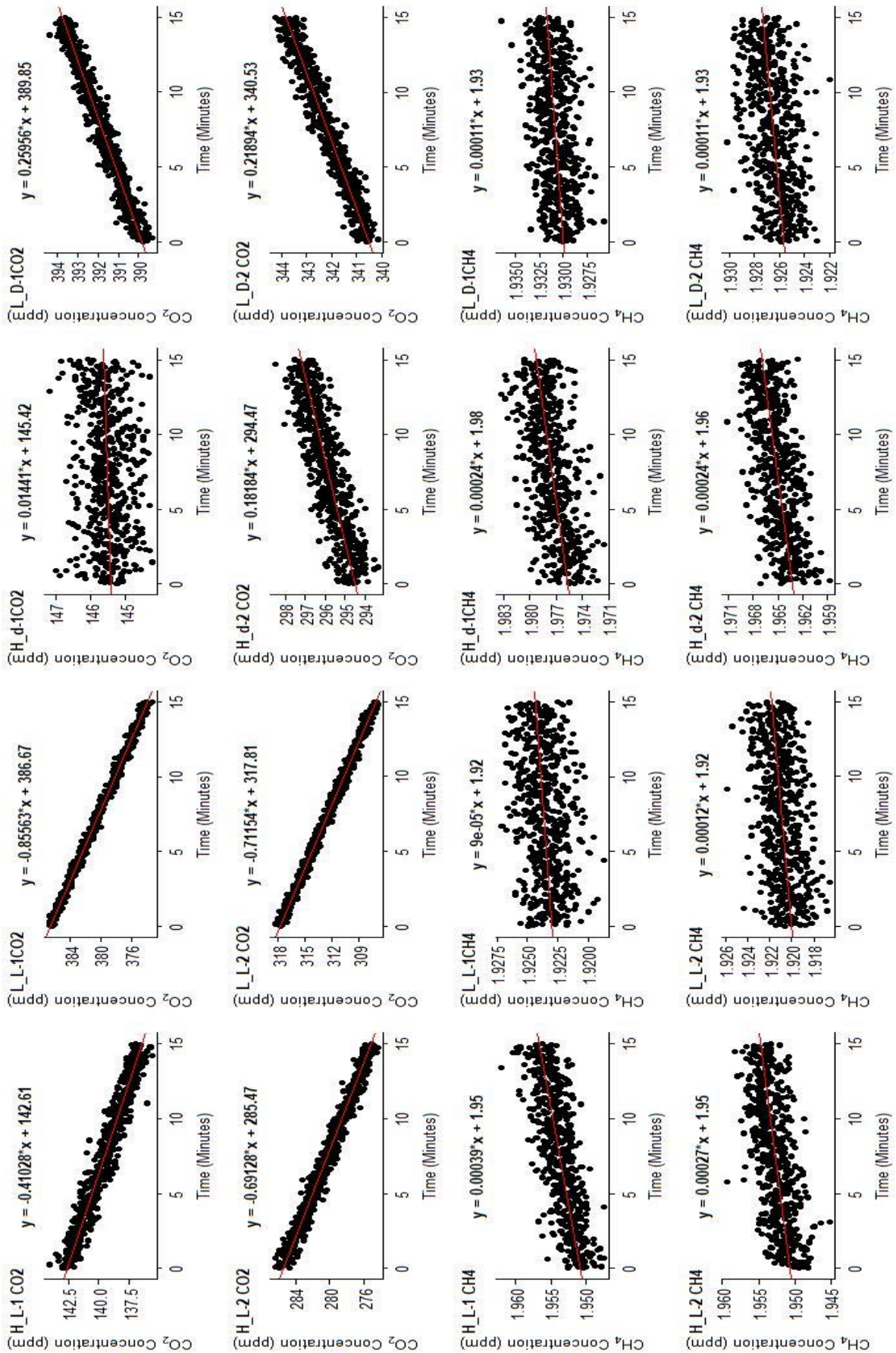

Figure 4.4.3.4 Ardleigh sample microcosm rate extraction graphs. Phosphate treatment twenty-four hours after treatment addition.

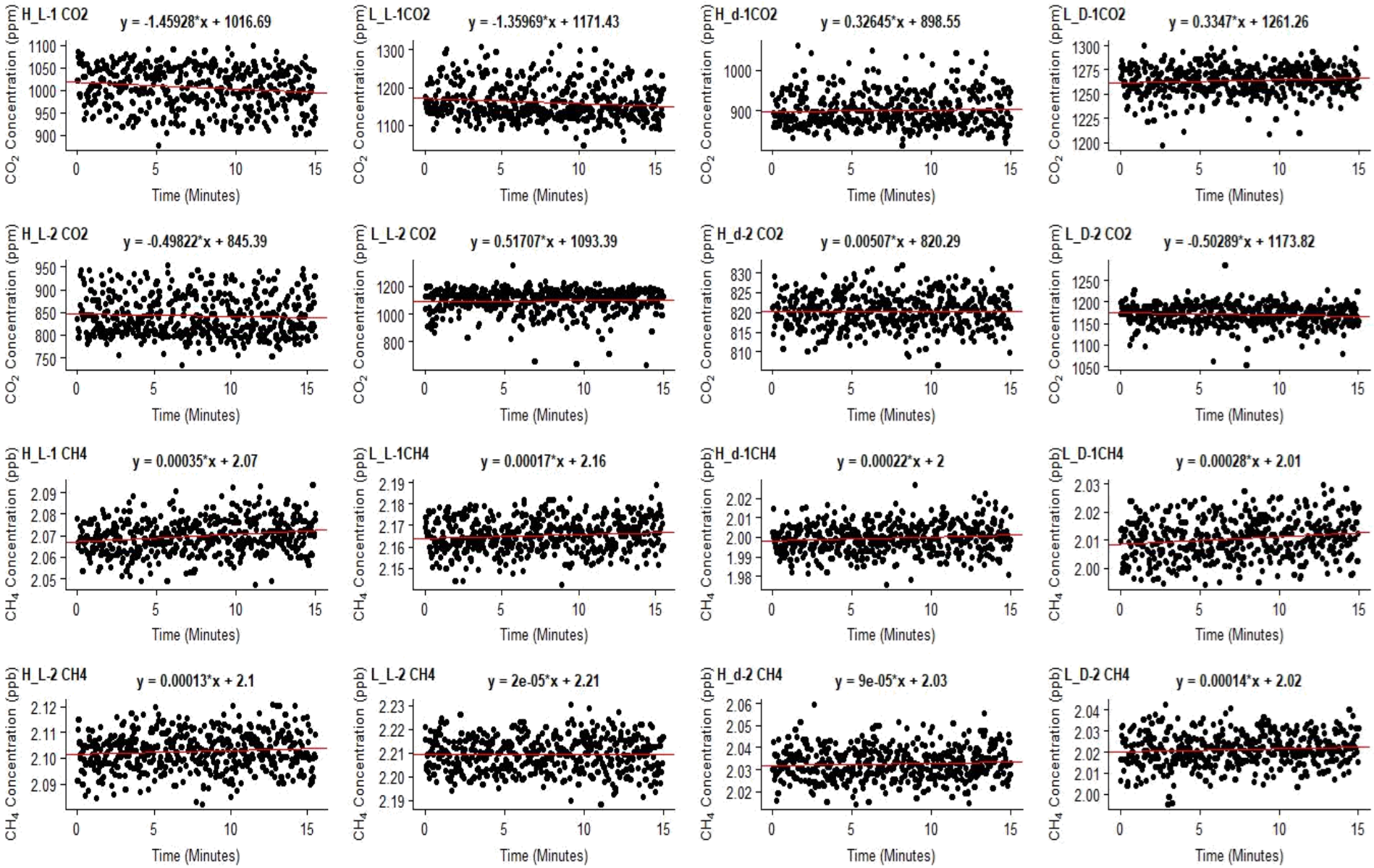

Figure 4.4.3.5 Alton sample microcosm rate extraction graphs. Phosphate treatment one hour after treatment addition.

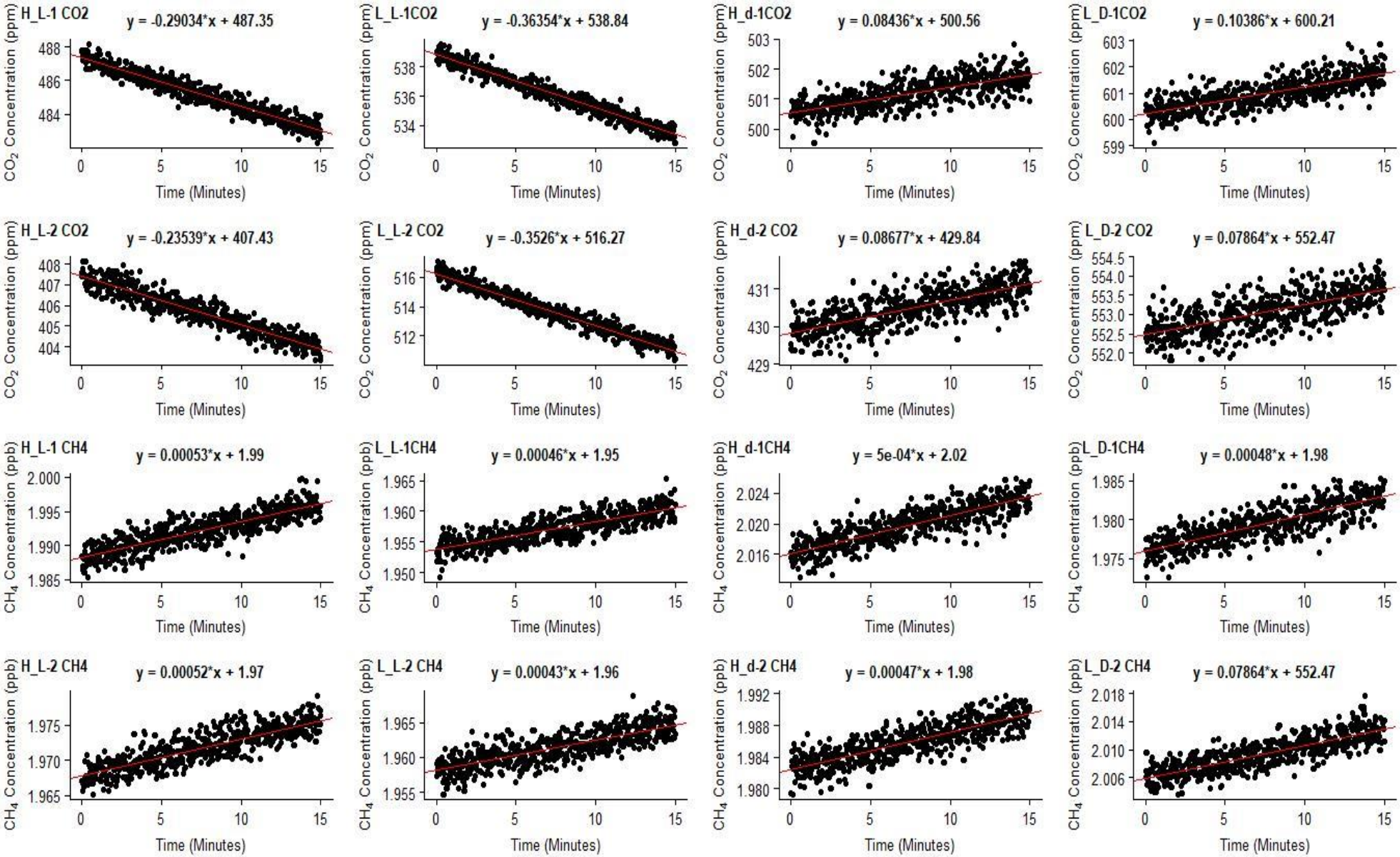

Figure 4.4.3.6 Alton sample microcosm rate extraction graphs. Phosphate treatment twenty-four hours after treatment addition.

5.0 References

Abdul-Hussein, M.M. and Mason, C.F. (1988). The phytoplankton community of a eutrophic reservoir. *Hydrobiologia*, 169(3), pp.265–277.

Abril, G., Guérin, F., Richard, S., Delmas, R., Galy-Lacaux, C., Gosse, P., Tremblay, A., Varfalvy, L., Dos Santos, M.A. and Matvienko, B. (2005). Carbon dioxide and methane emissions and the carbon budget of a 10-year old tropical reservoir (Petit Saut, French Guiana). *Global Biogeochemical Cycles*, 19(4), p.n/a-n/a.

Admiraal, W., Breugem, P., Jacobs, D.M.L.H.A. and De Ruyter Van Steveninck, E.D. (1990). Fixation of dissolved silicate and sedimentation of biogenic silicate in the lower river Rhine during diatom blooms. *Biogeochemistry*, 9(2), pp.175–185.

Adrian, R., O'Reilly, C.M., Zagarese, H., Baines, S.B., Hessen, D.O., Keller, W., Livingstone, D.M., Sommaruga, R., Straile, D., Van Donk, E., Weyhenmeyer, G.A. and Winder, M. (2009). Lakes as sentinels of climate change. *Limnology and Oceanography*, 54(6part2), pp.2283–2297.

askabiologist. 2018. biomes. [ONLINE] Available at: https://askabiologist.asu.edu/sites/default/files/resources/articles/biomes/world-biomes-map.gif. [Accessed 1 December 2018].

Balcombe, P., Speirs, J.F., Brandon, N.P. and Hawkes, A.D. (2018). Methane emissions: choosing the right climate metric and time horizon. *Environmental Science: Processes & Impacts*, 20(10), pp.1323–1339.

Barica, J., Kling, H. and Gibson, J. (1980). Experimental Manipulation of Algal Bloom Composition by Nitrogen Addition. *Canadian Journal of Fisheries and Aquatic Sciences*, 37(7), pp.1175–1183.

Bartosiewicz, M., Laurion, I. and MacIntyre, S., 2015. Greenhouse gas emission and storage in a small shallow lake. *Hydrobiologia*, *757*(1), pp.101-115.

Bastviken, D., Cole, J., Pace, M. and Tranvik, L. (2004). Methane emissions from lakes: Dependence of lake characteristics, two regional assessments, and a global estimate. *Global Biogeochemical Cycles*, 18(4), p.n/a-n/a.

Bastviken, D., Cole, J.J., Pace, M.L. and Van de Bogert, M.C. (2008). Fates of methane from different lake habitats: Connecting whole-lake budgets and CH4 emissions. *Journal of Geophysical Research: Biogeosciences*, 113(G2), p.n/a-n/a.

Bastviken, D., Tranvik, L.J., Downing, J.A., Crill, P.M. and Enrich-Prast, A. (2011). Freshwater Methane Emissions Offset the Continental Carbon Sink. *Science*, 331(6013), pp.50–50.

Bédard, C. and Knowles, R. (1989). Physiology, biochemistry, and specific inhibitors of CH4, NH4+, and CO oxidation by methanotrophs and nitrifiers. *Microbiology and Molecular Biology Reviews*, 53(1), pp.68–84.

Beerling, D.J. and Royer, D.L. (2011). Convergent Cenozoic CO2 history. *Nature Geoscience*, 4(7), pp.418–420.

Berden, G. and Engeln, R. eds., 2009. *Cavity ring-down spectroscopy: techniques and applications*. John Wiley & Sons.

Bergström, I., Kortelainen, P., Sarvala, J. and Salonen, K., 2010. Effects of temperature and sediment properties on benthic CO2 production in an oligotrophic boreal lake. *Freshwater Biology*, *55*(8), pp.1747-1757.

Birk, S., Bonne, W., Borja, A., Brucet, S., Courrat, A., Poikane, S., Solimini, A., van de Bund, W., Zampoukas, N. and Hering, D. (2012). Three hundred ways to assess Europe's surface waters: An almost complete overview of biological methods to implement the Water Framework Directive. *Ecological Indicators*, 18, pp.31–41.

Bižić-Ionescu, M., Klintzsch, T., Ionescu, D., Hindiyeh, M.Y., Günthel, M., Muro-Pastor, A.M., Keppler, F. and Grossart, H.P., 2018. Widespread formation of methane by Cyanobacteria in aquatic and terrestrial environments. *bioRxiv*, p.398958.

Bogard, M.J., Del Giorgio, P.A., Boutet, L., Chaves, M.C.G., Prairie, Y.T., Merante, A. and Derry, A.M., 2014. Oxic water column methanogenesis as a major component of aquatic CH 4 fluxes. *Nature Communications*, *5*, p.5350.

Borrel, G., Jézéquel, D., Biderre-Petit, C., Morel-Desrosiers, N., Morel, J.P., Peyret, P., Fonty, G. and Lehours, A.C., 2011. Production and consumption of methane in freshwater lake ecosystems. *Research in Microbiology*, *162*(9), pp.832-847.

Broecker, W.S., Peng, T.-H., Mathieu, G., Hesslein, R. and Torgersen, T. (1980). Gas Exchange Rate Measurements in Natural Systems. *Radiocarbon*, 22(3), pp.676–683.

Carey, C.C., McClure, R.P., Doubek, J.P., Lofton, M.E., Ward, N.K. and Scott, D.T., 2018. Chaoborus spp. transport CH4 from the sediments to the surface waters of a eutrophic reservoir, but their contribution to water column CH4 concentrations and diffusive efflux is minor. *Environmental Science & Technology*, *52*(3), pp.1165-1173.

Casper, P., Maberly, S.C., Hall, G.H. and Finlay, B.J., 2000. Fluxes of methane and carbon dioxide from a small productive lake to the atmosphere. *Biogeochemistry*, *49*(1), pp.1-19.

Chin, K.J. and Conrad, R., 1995. Intermediary metabolism in methanogenic paddy soil and the influence of temperature. *FEMS Microbiology Ecology*, *18*(2), pp.85-102.

Cole, J.J., Bade, D.L., Bastviken, D., Pace, M.L. and Van de Bogert, M., 2010. Multiple approaches to estimating air-water gas exchange in small lakes. *Limnology and Oceanography: Methods*, *8*(6), pp.285-293.

Conrad, R., 1999. Contribution of hydrogen to methane production and control of hydrogen concentrations in methanogenic soils and sediments. *FEMS Microbiology Ecology*, *28*(3), pp.193-202.

Costello, A.M., Auman, A.J., Macalady, J.L., Scow, K.M. and Lidstrom, M.E., 2002. Estimation of methanotroph abundance in a freshwater lake sediment. *Environmental Microbiology*, *4*(8), pp.443-450.

Crowley, T.J., 1983. The geologic record of climatic change. *Reviews of Geophysics*, *21*(4), pp.828-877.

Damm, E., Helmke, E., Thoms, S., Schauer, U., Nöthig, E., Bakker, K. and Kiene, R.P., 2010. Methane production in aerobic oligotrophic surface water in the central Arctic Ocean. *Biogeosciences*, *7*(3), pp.1099-1108.

Davidson, T.A., Audet, J., Jeppesen, E., Landkildehus, F., Lauridsen, T.L., Søndergaard, M. and Syväranta, J., 2018. Synergy between nutrients and warming enhances methane ebullition from experimental lakes. *Nature Climate Change*, *8*(2), p.156.

Deemer, B.R., Harrison, J.A., Li, S., Beaulieu, J.J., DelSontro, T., Barros, N., Bezerra-Neto, J.F., Powers, S.M., Dos Santos, M.A. and Vonk, J.A., 2016. Greenhouse gas emissions from reservoir water surfaces: a new global synthesis. *BioScience*, *66*(11), pp.949-964.

Del Giorgio, P.A. and Peters, R.H., 1994. Patterns in planktonic P: R ratios in lakes: influence of lake trophy and dissolved organic carbon. *Limnology and Oceanography*, *39*(4), pp.772-787.

Del Sontro, T., Boutet, L., St-Pierre, A., del Giorgio, P.A. and Prairie, Y.T., 2016. Methane ebullition and diffusion from northern ponds and lakes regulated by the interaction between temperature and system productivity. *Limnology and Oceanography*, *61*(S1), pp.S62-S77.

De Gruijl, F.R., Longstreth, J., Norval, M., Cullen, A.P., Slaper, H., Kripke, M.L., Takizawa, Y. and van der Leun, J.C., 2003. Health effects from stratospheric ozone depletion and interactions with climate change. *Photochemical & Photobiological Sciences*, *2*(1), pp.16-28.

De Vicente, I., Cruz-Pizarro, L. and Rueda, F.J., 2010. Sediment resuspension in two adjacent shallow coastal lakes: controlling factors and consequences on phosphate dynamics. *Aquatic Sciences*, *72*(1), pp.21-31.

Donis, D., Flury, S., Stöckli, A., Spangenberg, J.E., Vachon, D. and McGinnis, D.F., 2017. Full-scale evaluation of methane production under oxic conditions in a mesotrophic lake. *Nature Communications*, *8*(1), p.1661.

Downing, J.A., Prairie, Y.T., Cole, J.J., Duarte, C.M., Tranvik, L.J., Striegl, R.G., McDowell, W.H., Kortelainen, P., Caraco, N.F., Melack, J.M. and Middelburg, J.J., 2006. The global abundance and size distribution of lakes, ponds, and impoundments. *Limnology and Oceanography*, *51*(5), pp.2388-2397.

Duc, N.T., Crill, P. and Bastviken, D., 2010. Implications of temperature and sediment characteristics on methane formation and oxidation in lake sediments. *Biogeochemistry*, *100*(1-3), pp.185-196.

Duc, N.T., Silverstein, S., Lundmark, L., Reyier, H., Crill, P. and Bastviken, D., 2012. Automated flux chamber for investigating gas flux at water–air interfaces. *Environmental Science & Technology*, *47*(2), pp.968-975.

Duchemin, É., Lucotte, M., Canuel, R. and Soumis, N., 2006. First assessment of methane and carbon dioxide emissions from shallow and deep zones of boreal reservoirs upon ice break-up. *Lakes & Reservoirs: Research & Management*, *11*(1), pp.9-19.

Duchemin, E., 2000. Hydroelectricity and greenhouse gases: Emission evaluation and identification of biogeochemical processes responsible for their production. *Disseration, Université du Québec à Montréal, Montréal (Québec), Canada*, *321*.

Duchemin, E., Lucotte, M. and Canuel, R., 1999. Comparison of static chamber and thin boundary layer equation methods for measuring greenhouse gas emissions from large water bodies §. *Environmental Science & Technology*, *33*(2), pp.350-357.

Duchemin, E., Lucotte, M., Canuel, R. and Chamberland, A., 1995. Production of the greenhouse gases CH4 and CO2 by hydroelectric reservoirs of the boreal region. *Global Biogeochemical Cycles*, *9*(4), pp.529-540.

Eaton, A.D., Clesceri, L.S., Greenberg, A.E. and Franson, M.A.H., 2005. Standard methods for the examination of water and wastewater. *American Public Health Association*, 1015, pp.49-51.

Ehhalt, D.H., 1974. The atmospheric cycle of methane. *Tellus*, *26*(1-2), pp.58-70.

Etiope, G., 2009. Natural emissions of methane from geological seepage in Europe. *Atmospheric Environment*, *43*(7), pp.1430-1443.

Eugster, W., Kling, G., Jonas, T., McFadden, J.P., Wüest, A., MacIntyre, S. and Chapin III, F.S., 2003. CO2 exchange between air and water in an Arctic Alaskan and midlatitude Swiss lake: Importance of convective mixing. *Journal of Geophysical Research: Atmospheres*, *108*(D12), pp. 4362.

Falkowski, P., Scholes, R.J., Boyle, E.E.A., Canadell, J., Canfield, D., Elser, J., Gruber, N., Hibbard, K., Högberg, P., Linder, S. and Mackenzie, F.T., 2000. The global carbon cycle: a test of our knowledge of earth as a system. *Science*, *290*(5490), pp.291-296.

Fahrner, S., Radke, M., Karger, D. and Blodau, C., 2008. Organic matter mineralisation in the hypolimnion of an eutrophic Maar lake. *Aquatic Sciences*, *70*(3), pp.225-237.

Fernández-Prini, R., Alvarez, J.L. and Harvey, A.H., 2003. Henry's constants and vapor–liquid distribution constants for gaseous solutes in H2O and D2O at high temperatures. *Journal of Physical and Chemical Reference Data*, *32*(2), pp.903-916.

Filstrup, C.T. and Downing, J.A., 2017. Relationship of chlorophyll to phosphorus and nitrogen in nutrient-rich lakes. *Inland Waters*, *7*(4), pp.385-400.

Flynn, K.J., Clark, D.R. and Xue, Y., 2008. Modelling the release of dissolved organic matter by phytoplankton 1. *Journal of Phycology*, *44*(5), pp.1171-1187.

Franzmann, P.D., Roberts, N.J., Mancuso, C.A., Burton, H.R. and McMeekin, T.A., 1991. Methane production in meromictic ace lake, Antarctica. *Hydrobiologia*, *210*(3), pp.191-201.

Fuchs, A., Lyautey, E., Montuelle, B. and Casper, P., 2016. Effects of increasing temperatures on methane concentrations and methanogenesis during experimental incubation of sediments from oligotrophic and mesotrophic lakes. *Journal of Geophysical Research: Biogeosciences*, *121*(5), pp.1394-1406.

Garnett, M.H., Hardie, S.M.L., Murray, C. and Billett, M.F., 2013. Radiocarbon dating of methane and carbon dioxide evaded from a temperate peatland stream. *Biogeochemistry*, *114*(1-3), pp.213-223.

Gerardo-Nieto, O., Vega-Peñaranda, A., Gonzalez-Valencia, R., Alfano-Ojeda, Y. and Thalasso, F., 2019. Continuous Measurement of Diffusive and Ebullitive Fluxes of Methane in Aquatic Ecosystems by an Open Dynamic Chamber Method. *Environmental Science & Technology*, *53*(9), pp.5159-5167.

Glissman, K., Chin, K.J., Casper, P. and Conrad, R., 2004. Methanogenic pathway and archaeal community structure in the sediment of eutrophic Lake Dagow: effect of temperature. *Microbial Ecology*, *48*(3), pp.389-399.

Grossart, H.P. and Simon, M., 1993. Limnetic macroscopic organic aggregates (lake snow): Occurrence, characteristics, and microbial dynamics in Lake Constance. *Limnology and Oceanography*, *38*(3), pp.532-546.

Grossart, H.P., Frindte, K., Dziallas, C., Eckert, W. and Tang, K.W., 2011. Microbial methane production in oxygenated water column of an oligotrophic lake. *Proceedings of the National Academy of Sciences*, *108*(49), pp.19657-19661.

Guérin, F., Abril, G., Serça, D., Delon, C., Richard, S., Delmas, R., Tremblay, A. and Varfalvy, L., 2007. Gas transfer velocities of CO2 and CH4 in a tropical reservoir and its river downstream. *Journal of Marine Systems*, *66*(1-4), pp.161-172.

Hanson, P.C., Carpenter, S.R., Cardille, J.A., Coe, M.T. and Winslow, L.A., 2007. Small lakes dominate a random sample of regional lake characteristics. *Freshwater Biology*, *52*(5), pp.814-822.

Harrison, J.A., Deemer, B.R., Birchfield, M.K. and O'Malley, M.T., 2017. Reservoir water-level drawdowns accelerate and amplify methane emission. *Environmental Science & Technology*, *51*(3), pp.1267-1277.

Heinemeyer, A. and McNamara, N.P., 2011. Comparing the closed static versus the closed dynamic chamber flux methodology: Implications for soil respiration studies. *Plant and Soil*, *346*(1-2), pp.145-151.

Hellsten, S.K., Martikainen, P., Väisänen, T.S., Niskanen, A., Huttunen, J., Heiskanen, M., Nenonen, O., 1996. Measured Greenhouse Gas Emissions from Two Hydropower Reservoirs in Northern Finland. *IAEA Advisory Group Meeting on Assessment of Greenhouse Gas Emissions from the Full Energy Chain for Hydropower, Nuclear Power and Other Energy Sources*. Montréal (Québec): Hydro-Québec Headquarters.

Houghton, J.T., Ding, Y.D.J.G., Griggs, D.J., Noguer, M., van der Linden, P.J., Dai, X., Maskell, K. and Johnson, C.A., 2001. Climate change 2001: the scientific basis. *The Press Syndicate of the University of Cambridge.*

Hudson, J.J., Dillon, P.J. and Somers, K.M. (2003). Long-term patterns in dissolved organic carbon in boreal lakes: the role of incident radiation, precipitation, air temperature, southern oscillation and acid deposition. *Hydrology and Earth System Sciences*, 7(3), pp.390–398.

Huotari, J., Ojala, A., Peltomaa, E., Pumpanen, J., Hari, P. and Vesala, T., 2009. Temporal variations in surface water CO2 concentration in a boreal humic lake based on high-frequency measurements. *Boreal Environment Research,* 14(A), pp.48-60.

Huttunen, J.T., Alm, J., Liikanen, A., Juutinen, S., Larmola, T., Hammar, T., Silvola, J. and Martikainen, P.J., 2003. Fluxes of methane, carbon dioxide and nitrous oxide in boreal lakes and potential anthropogenic effects on the aquatic greenhouse gas emissions. *Chemosphere*, *52*(3), pp.609-621.

IPCC, 2013: Climate Change 2013: The Physical Science Basis. Contribution of Working Group I to the Fifth Assessment Report of the Intergovernmental Panel on Climate Change [Stocker, T.F., D. Qin, G.-K. Plattner, M. Tignor, S.K. Allen, J. Boschung, A. Nauels, Y. Xia, V. Bex and P.M. Midgley (eds.)]. *Cambridge University Press*, Cambridge, United Kingdom and New York, NY, USA, pp.1535.

Johnson, K.A. and Johnson, D.E., 1995. Methane emissions from cattle. *Journal of Animal Science*, *73*(8), pp.2483-2492.

Joyce, J. and Jewell, P.W., 2003. Physical controls on methane ebullition from reservoirs and lakes. *Environmental & Engineering Geoscience*, *9*(2), pp.167-178.

Käki, T., Ojala, A. and Kankaala, P., 2001. Diel variation in methane emissions from stands of Phragmites australis (Cav.) Trin. ex Steud. and Typha latifolia L. in a boreal lake. *Aquatic Botany*, *71*(4), pp.259-271.

Kankaala, P., Huotari, J., Peltomaa, E., Saloranta, T. and Ojala, A., 2006. Methanotrophic activity in relation to methane efflux and total heterotrophic bacterial production in a stratified, humic, boreal lake. *Limnology and Oceanography*, *51*(2), pp.1195-1204.

Kohnert, K., Serafimovich, A., Hartmann, J. and Sachs, T., 2014. Airborne measurements of methane fluxes in Alaskan and Canadian tundra with the research aircraft Polar 5. *Berichte zur Polar-und Meeresforschung: Reports on Polar and Marine Research*, *673*.

Kelly, C.A., Rudd, J.W.M., Bodaly, R.A., Roulet, N.P., St. Louis, V.L., Heyes, A., Moore, T.R., Schiff, S., Aravena, R., Scott, K.J. and Dyck, B., 1997. Increases in fluxes of greenhouse gases and methyl mercury following flooding of an experimental reservoir. *Environmental Science & Technology*, *31*(5), pp.1334-1344.

Kelly, C.A., Rudd, J.W., St. Louis, V.L. and Moore, T., 1994. Turning attention to reservoir surfaces, a neglected area in greenhouse studies. *Eos, Transactions American Geophysical Union*, *75*(29), pp.332-333.

Kremer, J.N., Nixon, S.W., Buckley, B. and Roques, P., 2003. Conditions for using the floating chamber method to estimate air-water gas exchange. *Estuaries and Coasts*, *26*(4), pp.985-990.

Krevš, A. and Kučinskienė, A., 2018. Microbial decomposition of sedimentary organic matter in small temperate lakes. *Fundamental and Applied Limnology/Archiv für Hydrobiologie*, *191*(3), pp.239-251.

Lai, D.Y.F., 2009. Methane dynamics in northern peatlands: a review. *Pedosphere*, *19*(4), pp.409-421.

Lambert, M. and Fréchette, J.L., 2005. Analytical techniques for measuring fluxes of CO2 and CH4 from hydroelectric reservoirs and natural water bodies. *Greenhouse gas emissions—fluxes and processes* (pp. 37-60). Springer, Berlin, Heidelberg.

Larmola, T., Alm, J., Juutinen, S., Huttunen, J.T., Martikainen, P.J. and Silvola, J., 2004. Contribution of vegetated littoral zone to winter fluxes of carbon dioxide and methane from boreal lakes. *Journal of Geophysical Research: Atmospheres*, *109*(D19).

Leschine, S.B., 1995. Cellulose degradation in anaerobic environments. *Annual Review of Microbiology*, 49(1), pp.399-426.

Liu, H., Zhang, Q., Katul, G.G., Cole, J.J., Chapin III, F.S. and MacIntyre, S., 2016. Large CO2 effluxes at night and during synoptic weather events significantly contribute to CO2 emissions from a reservoir. *Environmental Research Letters*, *11*(6), p.064001.

Lomans, B.P., Luderer, R., Steenbakkers, P., Pol, A., van der Drift, C., Vogels, G.D. and den Camp, H.J.O., 2001. Microbial populations involved in cycling of dimethyl sulfide and methanethiol in freshwater sediments. *Applied and Environmental Microbiology*, *67*(3), pp.1044-1051.

Maberly, S.C., 1996. Diel, episodic and seasonal changes in pH and concentrations of inorganic carbon in a productive lake. *Freshwater Biology*, *35*(3), pp.579-598.

Matthews, C.J., St. Louis, V.L. and Hesslein, R.H., 2003. Comparison of three techniques used to measure diffusive gas exchange from sheltered aquatic surfaces. *Environmental Science & Technology*, *37*(4), pp.772-780.

Mau, S., Gentz, T., Körber, J.-H., Torres, M.E., Römer, M., Sahling, H., Wintersteller, P., Martinez, R., Schlüter, M. and Helmke, E. (2015). Seasonal methane accumulation and release from a gas emission site in the central North Sea. *Biogeosciences*, 12(18), pp.5261–5276.

McDonald, J.E., de Menezes, A.B., Allison, H.E. and McCarthy, A.J., 2009. Molecular biological detection and quantification of novel Fibrobacter populations in freshwater lakes. *Applied and Environmental Microbiology.*, *75*(15), pp.5148-5152.

McGinnis, D.F., Greinert, J., Artemov, Y., Beaubien, S.E. and Wüest, A., 2006. Fate of rising methane bubbles in stratified waters: How much methane reaches the atmosphere?. *Journal of Geophysical Research: Oceans*, *111*(C9), p. C09007.

McGinnis, D.F., Kirillin, G., Tang, K.W., Flury, S., Bodmer, P., Engelhardt, C., Casper, P. and Grossart, H.P., 2015. Enhancing surface methane fluxes from an oligotrophic lake: exploring the microbubble hypothesis. *Environmental Science & Technology*, *49*(2), pp.873-880.

Megonigal, J.P., Hines, M.E. and Visscher, P.T., 2004. Anaerobic metabolism: linkages to trace gases and aerobic processes. *Biogeochemistry*, 8, pp.317-424

Metoffice. 2018. Was summer 2018 the hottest on record? [ONLINE] Available at: https://www.metoffice.gov.uk/news/releases/2018/end-of-summer-stats. [Accessed 1 December 2018].

Minnesota Department of Natural Resources. 2018. Fisheries Lake Surveys. [ONLINE] Available at: https://www.dnr.state.mn.us/lakefind/surveys.html. [Accessed 1 December 2018].

Murase, J. and Sugimoto, A., 2005. Inhibitory effect of light on methane oxidation in the pelagic water column of a mesotrophic lake (Lake Biwa, Japan). *Limnology and Oceanography*, *50*(4), pp.1339-1343.

Murase, J., Sakai, Y., Kametani, A. and Sugimoto, A., 2005. Dynamics of methane in mesotrophic Lake Biwa, Japan. In *Forest Ecosystems and Environments,* Springer, Tokyo. pp. 143-151.

Musti V. Krishna Sastry, Diane E. Robertson, James A. Moynihan, and M. F. R., 1992. Enzymatic Degradation of Cyclic 2, 3-Diphosphoglycerate to 2, 3-Diphosphoglycerate in Methanobacterium thermoautotrophicum, *American Chemical Society*, 2, pp. 2926–2935.

Musti, V. Sastry, K., Robertson, E., Moynihan, J. and Roberts, M. 1992. Enzymatic degradation of cyclic 2,3-diphosphoglycerate to 2,3-diphosphoglycerate in Methanobacterium thermoautotrophicum. *Biochemistry*, 31(11), pp.2926–2935.

Neubauer, S.C. and Megonigal, J.P., 2015. Moving beyond global warming potentials to quantify the climatic role of ecosystems. *Ecosystems*, *18*(6), pp.1000-1013.

Ng, T.K. and Zeikus, J.G., 1982. Differential metabolism of cellobiose and glucose by Clostridium thermocellum and Clostridium thermohydrosulfuricum. *Journal of Bacteriology*, *150*(3), pp.1391-1399.

Nicholson, B., Maguire, B.P. and Bursill, D.B., 1984. Henry's law constants for the trihalomethanes: effects of water composition and temperature. *Environmental Science & Technology*, *18*(7), pp.518-521.

Nijnik, M., 2010. Carbon capture and storage in forests. *Issues in Environmental Science and Technology*, *29*, p.203.

NOAA. 2019. State of the Climate in 2016. [ONLINE] Available at: https://journals.ametsoc.org/doi/pdf/10.1175/2017BAMSStateoftheClimate.1. [Accessed 30 December 2017].

Pace, M.L. and Prairie, Y.T., 2005. Respiration in lakes. *Respiration in Aquatic Ecosystems*, *1*, pp.103-122.

Ptacnik, R., Andersen, T. and Tamminen, T., 2010. Performance of the Redfield ratio and a family of nutrient limitation indicators as thresholds for phytoplankton N vs. P limitation. *Ecosystems*, *13*(8), pp.1201-1214.

Pavel, A., Durisch-Kaiser, E., Balan, S., Radan, S., Sobek, S. and Wehrli, B., 2009. Sources and emission of greenhouse gases in Danube Delta lakes. *Environmental Science and Pollution Research*, *16*(1), pp.86-91.

Peeters, F., Fernandez, J.E. and Hofmann, H., 2019. Sediment fluxes rather than oxic methanogenesis explain diffusive CH4 emissions from lakes and reservoirs. *Scientific Reports*, *9*.

Perkins, R.G. and Underwood, G.J.C., 2001. The potential for phosphorus release across the sediment–water interface in an eutrophic reservoir dosed with ferric sulphate. *Water Research*, *35*(6), pp.1399-1406.

Phelps, A.R., Peterson, K.M. and Jeffries, M.O., 1998. Methane efflux from high-latitude lakes during spring ice melt. *Journal of Geophysical Research: Atmospheres*, *103*(D22), pp.29029-29036.

Pihlatie, M.K., Christiansen, J.R., Aaltonen, H., Korhonen, J.F., Nordbo, A., Rasilo, T., Benanti, G., Giebels, M., Helmy, M., Sheehy, J. and Jones, S., 2013. Comparison of static chambers to measure CH4 emissions from soils. *Agricultural and Forest Meteorology*, *171*, pp.124-136.

R Core Team. 2017. R: A language and environment for statistical computing. R Foundation for Statistical Computing, Vienna, Austria. URL https://www.R-project.org/.

Raskin, L., Rittmann, B.E. and Stahl, D.A., 1996. Competition and coexistence of sulfate-reducing and methanogenic populations in anaerobic biofilms. *Applied and Environmental Microbiology*, *62*(10), pp.3847-3857.

Raymond, P.A., Hartmann, J., Lauerwald, R., Sobek, S., McDonald, C., Hoover, M., Butman, D., Striegl, R., Mayorga, E., Humborg, C. and Kortelainen, P., 2013. Global carbon dioxide emissions from inland waters. *Nature*, *503*(7476), p.355.

Redshaw, C.J., Mason, C.F., Hayes, C.R. and Roberts, R.D., 1990. Factors influencing phosphate exchange across the sediment-water interface of eutrophic reservoirs. *Hydrobiologia*, *192*(2-3), pp.233-245.

Repo, E., Huttunen, J.T., Naumov, A.V., Chichulin, A.V., Lapshina, E.D., Bleuten, W. and Martikainen, P.J., 2007. Release of CO2 and CH4 from small wetland lakes in western Siberia. *Tellus B: Chemical and Physical Meteorology*, *59*(5), pp.788-796.

Roden, E.E. and Wetzel, R.G., 2003. Competition between Fe (III)-reducing and methanogenic bacteria for acetate in iron-rich freshwater sediments. *Microbial Ecology*, *45*(3), pp.252-258.

Roehm, C.L., Prairie, Y.T. and Del Giorgio, P.A., 2009. The pCO2 dynamics in lakes in the boreal region of northern Québec, Canada. *Global Biogeochemical Cycles*, *23*(3).

Sanches, L.F., Guenet, B., Marinho, C.C., Barros, N. and de Assis Esteves, F., 2019. Global regulation of methane emission from natural lakes. *Scientific Reports*, *9*(1), p.255.

Saunois, M., Bousquet, P., Poulter, B., Peregon, A., Ciais, P., Canadell, J.G., Dlugokencky, E.J., Etiope, G., Bastviken, D., Houweling, S. and Janssens-Maenhout, G., 2016. The global methane budget 2000–2012. *Earth System Science Data*, *8*(2), pp.697-751.

Saarnio, S., Winiwarter, W. and Leitao, J., 2009. Methane release from wetlands and watercourses in Europe. *Atmospheric Environment*, *43*(7), pp.1421-1429.

Schmidt, A., Müller, N., Schink, B. and Schleheck, D., 2013. A proteomic view at the biochemistry of syntrophic butyrate oxidation in Syntrophomonas wolfei. *PloS one*, *8*(2), p.e56905.

Schutz, H., 1991. Role of plants in regulating the methane flux to the atmosphere. *Trace Gas Emission by Plants*, pp.29-63.

Schindler, D.W., Armstrong, F.A.J., Holmgren, S.K. and Brunskill, G.J., 1971. Eutrophication of Lake 227, Experimental Lakes Area, northwestern Ontario, by addition of phosphate and nitrate. *Journal of the Fisheries Board of Canada*, *28*(11), pp.1763-1782.

Simmons, J., 1998. Algal control and destratification at Hanningfield Reservoir. *Water Science and Technology*, *37*(2), pp.309-316.

Smith, K.A., Dobbie, K.E., Ball, B.C., Bakken, L.R., Sitaula, B.K., Hansen, S., Brumme, R., Borken, W., Christensen, S., Priemé, A. and Fowler, D., 2000. Oxidation of atmospheric methane in Northern European soils, comparison with other ecosystems, and uncertainties in the global terrestrial sink. *Global Change Biology*, *6*(7), pp.791-803.

Smith, S.V., Renwick, W.H., Bartley, J.D. and Buddemeier, R.W., 2002. Distribution and significance of small, artificial water bodies across the United States landscape. *Science of the Total Environment*, *299*(1-3), pp.21-36.

Sobek, S., Tranvik, L.J., Prairie, Y.T., Kortelainen, P. and Cole, J.J., 2007. Patterns and regulation of dissolved organic carbon: An analysis of 7,500 widely distributed lakes. *Limnology and Oceanography*, *52*(3), pp.1208-1219.

Soumis, N., Canuel, R. and Lucotte, M., 2008. Evaluation of two current approaches for the measurement of carbon dioxide diffusive fluxes from lentic ecosystems. *Environmental Science & Technology*, *42*(8), pp.2964-2969.

Stams, A.J.M. (1994). Metabolic interactions between anaerobic bacteria in methanogenic environments. *Antonie van Leeuwenhoek*, 66(1–3), pp.271–294.

Sterner, R.W., Elser, J.J., Fee, E.J., Guildford, S.J. and Chrzanowski, T.H., 1997. The light: nutrient ratio in lakes: the balance of energy and materials affects ecosystem structure and process. *The American Naturalist*, *150*(6), pp.663-684.

Stewart, C. and Hessami, M.A., 2005. A study of methods of carbon dioxide capture and sequestration-the sustainability of a photosynthetic bioreactor approach. *Energy Conversion and Management*, *46*(3), pp.403-420.

St. Louis, Vincent L., Carol A. Kelly, Éric Duchemin, John WM Rudd, and David M. Rosenberg., 2000. Reservoir Surfaces as Sources of Greenhouse Gases to the Atmosphere: A Global Estimate: Reservoirs are sources of greenhouse gases to the atmosphere, and their surface areas have increased to the point where they should be included in global inventories of anthropogenic emissions of greenhouse gases. *BioScience,* 50(9), pp. 766-775.

Statista. 2018. Monthly mean temperature in England from 2014 to 2018. [ONLINE] Available at: https://www.statista.com/statistics/585133/monthly-mean-temperature-in-england-uk/. [Accessed 30 September 2018].

Talling, J.F., 2010. pH, the CO2 system and freshwater science. *Freshwater Reviews*, *3*(2), pp.133-146.

Tang, K.W., McGinnis, D.F., Frindte, K., Brüchert, V. and Grossart, H.P., 2014. Paradox reconsidered: Methane oversaturation in well-oxygenated lake waters. *Limnology and Oceanography*, *59*(1), pp.275-284.

They, N.H., Amado, A.M. and Cotner, J.B., 2017. Redfield ratios in inland waters: higher biological control of C: N: P ratios in tropical semi-arid high water residence time lakes. *Frontiers in Microbiology*, *8*, p.1505.

Tranvik, L.J., Downing, J.A., Cotner, J.B., Loiselle, S.A., Striegl, R.G., Ballatore, T.J., Dillon, P., Finlay, K., Fortino, K., Knoll, L.B. and Kortelainen, P.L., 2009. Lakes and reservoirs as regulators of carbon cycling and climate. *Limnology and Oceanography*, *54*(6part2), pp.2298-2314.

Travis, J.M.J., 2003. Climate change and habitat destruction: a deadly anthropogenic cocktail. *Proceedings of the Royal Society of London. Series B: Biological Sciences*, *270*(1514), pp.467-473.

Trout Fisherman. 2018. Stillwater and reservoir fly fishing guide: Hanningfield Reservoir. [ONLINE] Available at: https://www.troutfisherman.co.uk/fishing-tips/stillwater-guides/articles/stillwater-and-reservoir-fly-fishing-guide-hanningfield-reservoir. [Accessed 1 December 2018].

Tušer, M., Picek, T., Sajdlová, Z., Jůza, T., Muška, M. and Frouzová, J., 2017. Seasonal and Spatial Dynamics of Gas Ebullition in a Temperate Water-Storage Reservoir. *Water Resources Research*, *53*(10), pp.8266-8276.

Upstill-Goddard, R.C., Watson, A.J., Liss, P.S. and Liddicoat, M.I., 1990. Gas transfer velocities in lakes measured with SF6. *Tellus B*, *42*(4), pp.364-377.

Vachon, D., Prairie, Y.T. and Cole, J.J., 2010. The relationship between near-surface turbulence and gas transfer velocity in freshwater systems and its implications for floating chamber measurements of gas exchange. *Limnology and Oceanography*, *55*(4), pp.1723-1732.

Vermaas, W.F., 2001. Photosynthesis and Respiration in Cyanobacteria. *Encyclopedia of Life Sciences*. [online] Available at: https://onlinelibrary.wiley.com/doi/abs/10.1038/npg.els.0001670 [Accessed 22 Nov. 2019].

Verpoorter, C., Kutser, T., Seekell, D.A. and Tranvik, L.J., 2014. A global inventory of lakes based on high-resolution satellite imagery. *Geophysical Research Letters*, *41*(18), pp.6396-6402.

Visnovitz, F., Bodnár, T., Tóth, Z., Spiess, V., Kudó, I., Timár, G. and Horváth, F., 2015. Seismic expressions of shallow gas in the lacustrine deposits of Lake Balaton, Hungary. *Near Surface Geophysics*, *13*(5), pp.433-446.

Walther, G.R., Hughes, L., Vitousek, P. and Stenseth, N.C., 2005. Consensus on climate change. *Trends in Ecology & Evolution*, *20*(12), pp.648-649.

Wanninkhof, R., Ledwell, J.R., Broecker, W.S. and Hamilton, M., 1987. Gas exchange on Mono lake and Crowley lake, California. *Journal of Geophysical Research: Oceans*, *92*(C13), pp.14567-14580.

West, W.E., Coloso, J.J. and Jones, S.E., 2012. Effects of algal and terrestrial carbon on methane production rates and methanogen community structure in a temperate lake sediment. *Freshwater Biology*, *57*(5), pp.949-955.

West, J.J. and Fiore, A.M., 2005. Management of Tropospheric Ozone by Reducing Methane Emissions. *Environmental Science & Technology*, 39(13), pp.4685–4691.

Williamson, C.E., Saros, J.E., Vincent, W.F. and Smol, J.P., 2009. Lakes and reservoirs as sentinels, integrators, and regulators of climate change. *Limnology and Oceanography*, *54*(6), pp.2273-2282.

WMO., 2017. The State of Greenhouse Gases in the Atmosphere Based on Global Observations through 2015. *Greenhouse Gas Bulletin (GHG Bulletin),* 12.

Wootten, R., 1973. The metazoan parasite-fauna of fish from Hanningfield Reservoir, Essex in relation to features of the habitat and host populations. *Journal of Zoology*, *171*(3), pp.323-331.

Wu, M.L., Ettwig, K.F., Jetten, M.S.M., Strous, M., Keltjens, J.T. and Niftrik, L. van (2011). A new intra-aerobic metabolism in the nitrite-dependent anaerobic methane-oxidizing bacterium Candidatus 'Methylomirabilis oxyfera.' *Biochemical Society Transactions*, 39(1), pp.243–248.

Xing, Y., Xie, P., Yang, H., Ni, L., Wang, Y. and Rong, K., 2005. Methane and carbon dioxide fluxes from a shallow hypereutrophic subtropical Lake in China. *Atmospheric Environment*, *39*(30), pp.5532-5540.

Yan, X., Xu, X., Ji, M., Zhang, Z., Wang, M., Wu, S., Wang, G., Zhang, C. and Liu, H., 2019. Cyanobacteria blooms: A neglected facilitator of CH4 production in eutrophic lakes. *Science of the Total Environment*, *651*, pp.466-474.

Yao, M., Henny, C. and Maresca, J.A., 2016. Freshwater bacteria release methane as a by-product of phosphorus acquisition. *Applied and Environmental Microbiology*, *82*(23), pp.6994-7003.

Zinder, S.H. (1990). Conversion of acetic acid to methane by thermophiles. *FEMS Microbiology Letters*, 75(2–3), pp.125–137.